

**REPUBLIC OF TURKEY
ERCIYES UNIVERSITY
GRADUATE SCHOOL OF NATURAL AND APPLIED SCIENCES
CHAIRMAN OF THE DEPARTMENT OF MECHANICAL
ENGINEERING
DEPARTMENT OF MECHANICAL ENGINEERING**

**NUMERICAL INVESTIGATION OF THERMAL AND
HYDRAULIC PERFORMANCE A TWISTED TUBE
MODIFIED BY USING “CUO/WATER” NANOFUID**

**Prepared by
Mohammed Ahmed Mousa AL-HAMEEDAWI**

**Supervisor
Prof. Dr. Veysel ÖZCEYHAN**

MSc Thesis

**March 2020
KAYSERİ**

**REPUBLIC OF TURKEY
ERCIYES UNIVERSITY
GRADUATE SCHOOL OF NATURAL AND APPLIED SCIENCES
CHAIRMAN OF THE DEPARTMENT OF MECHANICAL
ENGINEERING
DEPARTMENT OF MECHANICAL ENGINEERING**

**NUMERICAL INVESTIGATION OF THERMAL AND
HYDRAULIC PERFORMANCE A TWISTED TUBE
MODIFIED BY USING (CUO/WATER) NANOFUID**

(MSc Thesis)

**Prepared by
Mohammed Ahmed Al-HAMEEDAWI**

**Supervisor
Prof. Dr. Veysel ÖZCEYHAN**

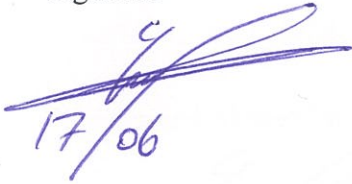
**March 2020
KAYSERİ**

SCIENTIFIC ETHICS SUITABILITY

I, hereby, declare that all information in this work was obtained in accordance with the academic and ethical rules. All results and materials that not been at the essence of this work are also transferred and expressed by giving reference as required by these rules and behavior.

Mohammed Ahmed Mousa AL-HAMEEDAWI

Signature



17/06

SUITABILITY FOR GUIDE

The MSc / thesis entitled “**Numerical Investigation On Thermal And Hydraulic Performance Of A Twisted Tube By Using Cuo-Water Nano-Fluids**” has been prepared in accordance with Erciyes University Graduate Education and Teaching Institute Thesis Preparation and Writing Guide.

Student

Mohammed Ahmed Mousa Al-Hameedawi

Supervisor

Prof. Dr. Veysel ÖZCEYHAN

Chairman of the Department of Mechanical Engineering

Prof.Dr. Necdet ALTUNTOP

ACCEPTANCE AND APPROVAL PAGE

This study entitled “**Numerical Investigation On Thermal And Hydraulic Performance Of A Twisted Tube By Using CUO-Water NANO-FLUIDS**” prepared by “**Mohammed Ahmed AL-Hameedawi**” under the supervision of **Prof. Dr. Veysel ÖZCEYHAN** was accepted by the jury as MSc. Thesis in Mechanical Engineering department.

..... / / 2020

JURY:

Supervisor : Prof. Dr. Veysel ÖZCEYHAN

Juror : Prof. Dr. Necdet ALTUNTOP

Juror : Prof. Dr. Hüseyin AKILLI

APPROVAL

That the acceptance of this thesis has been approved by the decision of the Institute’s Board of Directors with the date and numbered decision.

..... / /

Prof. Dr. Mehmet AKKURT

Director of the Institute

ACKNOWLEDGEMENTS

I am most grateful to my supervisor professor Veysel Ozceyhan for his excellent support and guidance throughout my master degree. I have been very fortunate to work under his supervision and I thank him sincerely for his advice, encouragement and patience.

I would like to thank Esenay Arslan and Mr. Ahmet Çabaş for their helpful comments regarding the numerical aspects of my study

I would like to thank Turkish people for their kindness and affection, which has made us doesn't feel homesick

A special thanks to my family. Who have always been proud of me and encouraged me to pursue my interests.

Mohammed Ahmed AL-Hameedawi

KAYSERI, 2020

NUMERICAL INVESTIGATION ON THERMAL AND HYDRAULIC PERFORMANCE OF A COILED TUBE BY USING “CuO-Water” NANO-FLUIDS

Mohammed Ahmed AL-Hameedawi

Erciyes University, Graduate School of Natural and Applied Sciences

Msc. Thesis, March 2020

Thesis Supervisor Prof. Dr. Veysel ÖZCEYHAN

ABSTRACT

In this study, several numerical simulations were constructed in order to enhance the heat transfer performance by exploiting smooth and twisted tubes with three different pitch lengths was (50mm, 100mm, 250mm). Water was selected as base fluid for analysis, and the (CuO-Water) nano-fluids effect was tested on the heat transfer through a circular tube in order to improve the thermal and hydraulic performances. The nano-fluid used was a single-phase of four different volume fractions: 1, 2, 3, and 4%. The analysis was experimented for Reynolds number values between 6000-40000. Constant uniform heat flux of $50,000 \text{ W/m}^2$ was applied to the outer surface of the test tube. Besides; k-epsilon standard turbulence model was adopted through the use of CFD (ANSYS) program. The inlet fluid temperature was taken as 293K and a constant hydraulic diameter of 26.9mm was considered. The optimum results ($\text{Nu} = 443.76$, $h=12129.98 \text{ W/m}^2$, $f = 0.1582$, $\Delta p = 2782.85 \text{ Pa}$, $\text{PEC}=2.39$) obtained were at pitch length of 50 mm, Reynolds number of 35613 and volume fraction of 4% (CuO-Water) in base fluid. Finally, The results in terms of thermal and hydraulic performances showed decreasing Nusselt number, heat transfer coefficient, friction factor and pressure as the number of pitches length in twisted tube increased. In addition, the thermal and hydraulic characteristics increased too when increasing the value of CuO-water nano-fluid fraction.

Keywords: Heat Transfer Enhancement, CuO/Water Nanofluid, Twisted tube modified, Pressure drop, Reynolds Number.

**“Bakır Oksit-Su” NANO AKIŞKANLIĞI KULLANARAK HELEZON
HORTUMUN TERMAL VE HİDROLİK PERFORMANSININ SAYISAL
İNCELEMESİ**

**Mohammed Ahmed AL-Hameedawi
Erciyes Üniversitesi, Fen Bilimleri Enstitüsü
Yüksek Lisans Tezi, Mart 2020
Tez Danışmanı Prof. Dr. Veysel Özceyhan**

ÖZET

Bu çalışmada, farklı hatve uzunluklarına sahip bükülmüş boru ve farklı hacimsel oranlara sahip CuO-Su nano akışkanının termal ve hidrolik performansına etkisinin sayısal araştırmasını sunmaktadır. Hatve uzunlukları 50 mm, 100 mm ve 250 mm olarak göz önünde bulundurulmuştur. Nano akışkanın hacimsel oranları ise %1, %2, %3 ve %4 ve su sıvısı olarak göz önünde bulundurulmuştur. Sınır şartı olarak sabit ısı akısı uygulanan boru içindeki akış Reynolds sayısının 6000 ile 40000 arasında olduğu türbülanslı akıştır. Akışkanın giriş sıcaklığı 293 K ve hidrolik boru çapı 26.9 mm dir. Türbülanslı akış için k-epsilon standart model CFD (ANSYS) programını kullanarak seçilmiştir.

Sonuç olarak, en yüksek değerler aşağıdaki gibi elde edilmiştir:

$$Nu=443.76, h=12129.98 \text{ W/m}^2, f=0.1582, \Delta p=2782.85 \text{ Pa}, PEC=2.39$$

50 mm hatve uzunluğu, Reynolds sayısı 35613 ve hacim fraksiyonu Pürüzsüz tüp ve su akışından% 4 (CuO-Su) nano akışkanlık olarak gösterilmiştir.

Son olarak, termal ve hidrolik performans açısından sonuçlar, oluklu borudaki hatve uzunluğunu arttırırken, Nusselt sayısının, ısı transfer katsayısının, sürtünme faktörünün ve basınç düşüşünün değerinin azalmasına yol açtığını göstermektedir.

Ancak CuO-su nano akışkanlığı değerini arttırırken termal ve hidrolik özellikleri de artacaktır.

Anahtar Kelimeler: Isı Transferi Arttırımı, CuO / Su Nano-akışkanlık, Oluklu boru modifiye, Basınç düşümü, Reynolds Sayısı.

TABLE OF CONTENTS

NUMERICAL INVESTIGATION ON THERMAL AND HYDRAULIC PERFORMANCE OF A COILED TUBE BY USING “CUO-Water” NANO-FLUIDS

SCIENTIFIC ETHICS SUITABILITY	i
SUITABILITY FOR GUIDE.....	ii
ACCEPTANCE AND APPROVAL PAGE	iii
ACKNOWLEDGEMENTS	iv
ABSTRACT.....	v
ÖZET	vi
TABLE OF CONTENTS.....	vii
LIST OF NOMENCLATURE.....	xii
LIST OF FIGURES	xiii
LIST OF TABLES	xvii
INTRODUCTION	1

CHAPTER 1

GENERAL INFORMATION

1.1 The mechanisms of enhancement heat transfer	2
1.1.1. The heat transfer enhancement techniques	3
1.1.1.1 Passive techniques.....	3
1.1.1.2. Active techniques	5
1.1.1.3. Compound technique	6
1.2. Contrastive additions	Hata! Yer işareti tanımlanmamış.
1.2.1 The features of twisted tube	6
1.2.3 The Technology of twisted tube	6
1.2.4 Thermal boundary layer of hydrodynamic	7
1.2.5 The advantages using of twisted tube over smooth tube:.....	7
1.3. The benefits of enhanced heat transfer	8
1.4 Introduction to Nanofluids	8
1.5.1. Nanofluids Preparation	9
1.5.1.1 The method of single-step.....	9
1.5.1.2. The method of two-step	10

1.5.2. Thermal conductivity of Nano fluids.....	10
1.5.2.1. Brownian motion	11
1.5.2.2. Interfacial layer	11
1.5.2.3. Volume fraction	12
1.5.3. The heat transfer improves by using nano fluid.....	12
1.5.4 The applications of nanofluid	13

CHAPTER 2

LITERATURE REVIEW

2.1. Nano fluid inserted through the smooth tube.....	14
2.2. Investigation with water fluid inserted	15
2.3. The twisted tube with contains nano-fluid inside it	16

CHAPTER 3

THE METHODOLOGY

3.1. Fluid flow by heat transfer	18
3.1.1. The boundary layer of Velocity	18
3.1.2. The boundary layer of thermal.....	19
3.1.3. Pure fluids correlations	20
3.1.3.1 The correlations of water fluids	20
3.1.3.2. The correlations (CUO-Water) nano-fluid:	21
3.2. helpful formulations.....	21
3.3. Numerical Analysis Process	23
3.4. The Geometry of Profiles	25
3.5. The CFD-models validation.....	26
3.6. The benefits of the CFD	26
3.7 Governing Equation	28
3.8 The test of grid Independence.....	28
3.8.1. Smooth tube is modified for the test of independence	29
3.9. Investigation of properties of the thermal and hydraulic into (CuO-water) nanofluid	31

CHAPTER 4

THE RESULTS AND DISCUSSION

4.1. The validation of Smooth Tube and different ratio of diameter(D1/D2) in water fluid	33
4.1.1.1 The convective of heat transfer	34
4.1.1.2 The friction factor.....	36
4.2. Smooth Tube and different ratio of diameter (D1/D2) in (CuO-Water) Nanofluid flow	37
4.2.1. Effect on Nu	37
4.2.1.1 At (D1/D2) =1 [circular smooth tube].....	37
4.2.1.2 Ellipse at the diameter ratio (D1/D2=1.5)--(33-22mm)	38
4.2.1.3 Ellipse at the diameter ratio (D1/D2=2) -(40-20mm)	39
4.2.2 Effect on (h).....	39
4.2.2.1 At (D1/D2) =1 [circular smooth tube].....	39
4.2.2.2 Ellipse at the diameter ratio (D1/D2=1.5) --(33-22mm)	40
4.2.2.3 Ellipse at the diameter ratio (D1/D2=2) -(40-20mm)	41
4.2.3. The friction factors	41
4.2.3.1 At the diameter ratio (D1/D2) =1 [circular smooth tube].....	41
4.2.3.3 At the diameter ratio (D1/D2=1.5) --(33-22mm).....	42
4.2.3.2 At the diameter ratio (D1/D2=2) --(40-20mm).....	43
4.3 Different ratio of twisted tube modified with a Smooth tube and different diameter ratios in water fluid	43
4.3.1 Effect on Nusselt number (Nu).....	43
4.3.1.1 At the diameter ratio (D1/D2=1.5) --(33-22mm).....	43
4.3.1.2 At the diameter ratio (D1/D2=2) --(40-20mm).....	44
4.3.2. Effect on heat transfer coefficient (h)	45
4.3.2.1 At the diameter ratio (D1/D2=1.5) --(33-22mm).....	45
4.3.2.2 At the diameter ratio (D1/D2=2) --(40-20mm).....	45
4.3.3 Effect on friction factor (f).....	46
4.3.3.1 At the diameter ratio (D1/D2=1.5) --(33-22mm).....	46
4.3.3.2 At the diameter ratio (D1/D2=2) --(40-20mm).....	47
4.3.4 Effect on pressure drop (Δp)	47
4.3.4.1 At the diameter ratio (D1/D2=1.5) --(33-22mm).....	47

4.3.4.2 At the diameter ratio ($D1/D2=2$) --(40-20mm).....	49
4.3.5.1 investigate PEC with elliptical different diameter ratio twisted and smooth tubes in water fluid	50
4.4. Investigation of twisted tube modified with Nanofluid CuO-Water	52
4.4.1. Effect on Nusselt number with twisted tubes modified and smooth tube ..	52
4.4.1.1 Effect of heat transfer coefficient (h)	53
4.4.1.2 Effect of Nu	53
4.4.1.3 Effect on heat transfer coefficient (h)	54
4.4.1.4 Effect on Nu	55
4.4.1.5 Effect on heat transfer coefficient (h)	55
4.4.1.6 Effect on Nu	56
4.4.1.7 Effect on heat transfer coefficient (h)	57
4.4.2. The friction factor	58
4.4.2.1 Effect on (Δp)	58
4.4.3 The friction factor	59
4.4.3.1 Effect on pressure drop (Δp)	60
4.4.3.2 Effect on friction factor.....	61
4.4.3.3 Effect on pressure drop (Δp) with volume fraction $\phi=3\%$	62
4.4.3.4 Effect on friction factor.....	63
4.4.3.5 Effect on pressure drop (Δp)	64
4.4.4 Thermo-Hydraulic Performance factor (THP) or performance evaluation criteri (PEC)	65
4.4.5 Investigation of (PEC) performance evaluation criteri with (CuO-Water) Nanofluid inserted.....	66
4.4.5.1 PEC with volume fraction $\phi=1\%$	66
4.4.5.2 PEC with volume fraction $\phi=2\%$	67
4.4.5.3 PEC with volume fraction $\phi=3\%$	68
4.4.5.4 PEC with volume fraction $\phi=4\%$	68
4.4.6 The analysis of performance evaluation (η)	69
4.4.6.1 η with volume fraction $\phi=1\%$	69
4.4.6.2 η with volume fraction $\phi=2\%$	70
4.4.6.3 η with volume fraction $\phi=3\%$	71
4.4.6.4 η with volume fraction $\phi=4\%$	72

CHAPTER 5

CONCLUSION AND RECOMMENDATIONS

5.1 The conclusion of this research.....	73
5.2 The Recommendations	74
REFERENCES	75
CURRICULUM VITAE	81



LIST OF NOMENCLATURE

C_p	: Specific heat (J/kg K).
C_{uo}	: Cupper Oxide.
D	: Diameter of a tube (m).
f	: friction factor.
h	: heat transfer coefficient (W/m ² .K).
h_E	: Heat transfer coefficient with inserts (Enhanced).
h_{NE}	: Heat transfer coefficient without inserts (Non-Enhanced).
K	: Thermal conductivity (W/m. K).
L	: Length (m).
L_1	: Entrance Section length (m).
L_2	: Test Section length (m).
L_3	: Exit Section length (m).
Nu	: Nusselt number.
Pr	: Prandtl number.
Re	: Reynolds number.
T_b	: Bulk temperature of a fluid (k).
T_{in}	: Inlet thermal temperature (K).
T_s	: Surface temperature (K).
T_w	: Temperature at the wall (K).
V	: Fluid velocity (m/s).
Δp	: Pressure drop (Pa).
q	: Heat flux of the tube (W/m ²).

Greek symbols

η	: Performance enhancement coefficient.
μ	: Dynamic viscosity (kg/m s).
ρ	: Density (kg/m ³).
Φ	: Nanofluids volume fractions.

Subscripts

bf	: Base fluid.
W	: Water.

LIST OF FIGURES

Figure 1.1.	The boundary layer for flowing over a flat plate from various flow system.....	3
Figure 1.2.	Flow chart techniques of enhanced heat transfer	3
Figure 1.3.	Apparatus of passive techniques a) Segmented fin sink, b) Helical insertsed,.....	5
Figure 1.4.	Geometric shape of smooth tube modified with twisted tube.....	5
Figure 1.5.	The inner foundation of twisted tube	6
Figure 1.6.	Schematic of thermal boundary layer of hydraulic	7
Figure 1.7.	T.E.M (Transmission electron microscopy) Photographs illustrating the CuO nanoparticles structure and size	9
Figure 1.8.	Graphic of single-step method.....	10
Figure 1.9.	Graphic of two-step method	10
Figure 1.10.	The motion of Brownian's nanomaterials	11
Figure 1.11.	The cross section nanofluid structure scheme with nanoparticles.....	12
Figure 3.1.	The boundary layer of Velocity.....	19
Figure 3.2.	Thermal boundary layer	20
Figure 3.3.	The diagram of CFD analyzing procedure	24
Figure 3.4.	The graphic body of numerical research	25
Figure 3.5.	Geometry with different pitch lengths of twisted tubes	25
Figure 3.6.	The diagram of turbulence models	26
Figure 3.7.	Turbulence model compression with the influence of the Reynold and Nusselt numbers.....	27
Figure 3.8.	Turbulence model with control of the numbers Reynold and Nusselt ...	27
Figure 3.9.	Smooth tube in Ansys program at 4.0mm	28
Figure 3.10.	The test of grid independence for smooth tube simulate.....	29
Figure 3.11.	The twisted tube in mesh longitude was generated	30
Figure 4.1.	The smooth tube with (4.0mm) was selected in this study, Nusselt number (with Dittus-Boelter correlation) vs Reynolds number for water fluid.....	35
Figure 4.2.	The relationship between the Nusselt number by using Dittus-Boelter correlation vs Reynolds number for water fluid in smooth tube for different ratio of diameter	36
Figure 4.3.	The Friction factor by using Blasius correlation vs Reynolds	36
Figure 4.4.	The relationship between the friction factor by using Blasius correlation versus Reynolds number for water fluid in smooth tube for different ratio of diameter	37
Figure 4.5.	The relationship between Nusselt and Reynolds numbers with different volume fractions of CuO/Water for smooth tube	38
Figure 4.6.	The relationship between Nusselt and Reynolds numbers with different volume fractions of CuO/Water for different diameters was ratio (1.5).	38

Figure 4.7.	The relationship between Nusselt and Reynolds numbers with different volume fractions of CuO/Water for different diameters was ratio (2)	39
Figure 4.8.	The relationship between heat transfer coefficient and Reynolds numbers with different volume fractions of CuO/Water for different diameters was ratio (1).	40
Figure 4.9.	The relationship between heat transfer coefficient and Reynolds numbers with different volume fractions of CuO/Water for different diameters was ratio (1.5).	40
Figure 4.10.	The relationship between heat transfer coefficient and Reynolds numbers with different volume fractions of CuO/Water for different diameters was ratio (2).	41
Figure 4.11.	Nusselt number relationship with Reynolds numbers variant volume fractions of CuO / Water for a smooth tube	42
Figure 4.12.	The relationship between Nusselt and Reynolds numbers with different volume fractions of CuO/Water for different diameters was ratio (1.5)	42
Figure 4.13.	The relationship between Nusselt and Reynolds numbers with different volume fractions of CuO/Water for different diameters was ratio (2)	43
Figure 4.14.	Effect of twisted tube modified with the Nusselt number of water in different pitch lengths	44
Figure 4.15.	Effect of twisted tube modified Nusselt number with Reynolds number of water in $D1/D2=2$	44
Figure 4.16.	Effect of twisted tube modified with heat transfer and Reynolds number of water in $D1/D2=1.5$	45
Figure 4.17.	Effect of twisted tube modified with heat transfer and Reynolds number of water in $D1/D2=2$	46
Figure 4.18.	Relation between friction factor and Re with different pitch length modified 1.5 ratio	46
Figure 4.19.	Effect of twisted tube modified with the friction factor of water in different diameter ratios (2).....	47
Figure 4.20	Relation between pressure drop and Re with different pitch length modified.....	48
Figure 4.21	Pressure counter for $D1/D2=1.5$ at $Re=18000$	48
Figure 4.22.	Effect of twisted tube modified with the pressure drop and Re of water in different diameter ratios (2).....	49
Figure 4.23.	Pressure counter for $D1/D2=2$ at $Re= 18000$ 4.3.5 Performance Evaluation Criteria	49
Figure 4.24.	The relationship between performance of enhancement coefficient and Reynolds number for water in elliptical of different diameter ($D1/D2=2$)	50

Figure 4.25. The relationship between performance of enhancement coefficient and Reynolds number for water in elliptical of different diameter ($D1/D2=1.5$) 51

Figure 4.26. The relationship between the Nusselt number and Reynolds number in volume fraction 1% (CuO-water) nano-fluid with different twisted tubes and smooth tube. 52

Figure 4.27. The relationship between the convective heat transfer coefficient and Reynolds number in volume fraction 1% (CuO-water) nano-fluid with different twisted tubes and smooth tube..... 53

Figure 4.28. The relationship between the Nusselt number and Reynolds number in volume fraction 2% (CuO-water) nano-fluid with different twisted tubes and smooth tube. 54

Figure 4.29. The relationship between the convective heat transfer coefficient and Reynolds number in volume fraction 1% (CuO-water) nano-fluid with different twisted tubes and smooth tube..... 54

Figure 4.30. The relationship between the Nusselt number and Reynolds number in volume fraction 1% (CuO-water) nano-fluid with different twisted tubes and smooth tube. 55

Figure 4.31. The relationship between the convective heat transfer coefficient and Reynolds number in volume fraction 3% (CuO-water) nano-fluid with different twisted tubes and smooth tube..... 56

Figure 4.32. The relationship between the Reynolds number and Nu with 4 % volume fraction of nano-fluid in a twisted tube and smooth tube with a different diameter pitch ratio were modified 56

Figure 4.33. The relationship between the Reynolds number and heat transfer coefficient with 4 % volume fraction of nano-fluid in a twisted tube and smooth tube 57

Figure 4.34. The relationship between the friction factor and Reynolds number with $\phi = 1\%$ of nano-fluid in a twisted tube and smooth tube..... 58

Figure 4.35. Relationship between pressure drop and Re and $\phi=1\%$ with a twisted tube and smooth tube 59

Figure 4.36. Comparison of total pressure counters between smooth tube and different pitch length (50,100,250mm) with volumetric concentration= $\phi=1\%$ CuO-water nanofluid at Re=18000..... 59

Figure 4.37. The relationship between friction factor and the Re with $\phi = 2\%$ with a twisted tube and smooth tube 60

Figure 4.38. The relationship between pressure drop the Re and with $\phi = 2\%$ with a twisted tube and smooth tube 60

Figure 4.39. Comparison of total pressure counters between smooth tube and different pitch length (50,100,250mm) with volumetric concentration= $\phi=2\%$ CuO-water nanofluid observed at Re=18000 61

Figure 4.40.	The relationship between the Reynolds number and friction factor with.....	62
Figure 4.41.	Relation between pressure drop and Re with $\phi=3\%$ with a twisted tube and smooth tube.....	62
Figure 4.42.	Total pressure counters between smooth tube and different pitch length (50,100,250mm) with volumetric concentration= $\phi=3\%$ CuO-water nanofluid observed at Re=18000.....	63
Figure 4.43.	The relationship between the Reynolds number and friction factor with a twisted tube and smooth tube.....	64
Figure 4.44.	Relationship between pressure drop and Re with a twisted tube and smooth tube modified.....	64
Figure 4.45.	Total pressure counters between smooth tube and different pitch length (50,100,250mm) with volumetric concentration= $\phi=4\%$ CuO-water nanofluid observed at Re=18000.....	65
Figure 4.46.	The coefficient of performance enhancement with water fluid in the twisted tube and smooth tube was modified.....	66
Figure 4.47.	The relation between performance enhancement and Reynolds number for Nano fluid with volume concentration of 1%.	67
Figure 4.48.	The relation between performance enhancement and Reynolds number $\phi=2\%$ nanofluid with inserted different pitch ratios	67
Figure 4.49.	The relation between performance enhancement and Reynolds number with nano fluid at volume concentration of 3% with inserted different pitch ratios.	68
Figure 4.50.	The relation between performance evaluation criteria and Reynolds number for Nano fluid with volume concentration of 4 % with inserted different pitch ratios.....	69
Figure 4.51.	The effect of performance evaluation analysis and Reynolds number for Nano fluid with volume concentration at $\phi=1\%$	70
Figure 4.52.	The effect of performance evaluation analysis and Reynolds number into the nano fluid with volume fraction at $\phi=2\%$ with modified different pitch ratios.	70
Figure 4.53.	The effect of performance evaluation analysis and Reynolds number for Nano fluid with volume concentration at $\phi=3\%$ with modified different pitch ratios	71
Figure 4.54.	The effect of performance evaluation analysis and Reynolds number for Nano fluid with volume concentration at $\phi=4\%$ with modified different pitch ratios	72

LIST OF TABLES

Table 3.1. The results of mesh sensitivity	29
Table 3.2. CuO nanoparticles and water physical and thermal properties at T=273k, from Cengel Y.].....	32
Table 3.3. The physical thermal properties of nanofluid CuO / water	32
Table 4.1. The different types of ellipse diameters	34



INTRODUCTION

The heat transfer field is considered to be one of the most important active fields in today's world. Many engineering studies try different techniques to increase the rate of heat transfer. The methods for improving the rate of heat transfer are mainly classified into three types: passive, active and compound methods. In addition, many manufacturing processes require heat transfer in various forms; it could be the cooling of a machine tool, the pasteurization of food or the change in temperature to cause a chemical process. Researchers have worked to develop thermal systems efficiency and increased the size and thereby increase the rate of energy consumption. Heat transfer is one of the physical phenomena most important researchers have investigated and developed. The heat transfer coefficient and pressure drop are among the most important factors affecting the performance of any heating system. Several types of research were conducted to get an understanding of heat transfer efficiency in their practical applications for heat transfer improvement. Due to its compact structure, greater heat transfer faces and higher heat transfer capacity are used in manufacturing facilities and power areas, this is achieved by decreasing the thermal resistance of the bordering layer and increasing the fluid flow interference. The results were solved in (h , Nu , f , T_s , and Δp) compared to the nine Reynolds numbers that ranging between 6,000 and 40,000.

One of the most important problems faced by academics is that the improved fluid interruption was using to improve heat transfer by increasing primary layer resistance results in a major drop in pressure which results in increased pressure costs.

Also often studies on finding solutions or reducing power, but many studies in the thermal engineering department are trying to find new ways and processes that include modifying equipment and machinery designs in various methods, Improve the heat transfer cycle and work towards substantial and the improved ascent between the surface and the surrounding liquid Bergles et al.[1]. Heat is widely used in engineering purposes by heat exchangers, in house atmospheric conditioning, in large industrial plant operation and in devices such it might be provide in many regions.

CHAPTER 1

GENERAL INFORMATION

1.1 The mechanisms of enhancement heat transfer

In several application systems heat transfer plays an important role. For example, into proper operation heat generated by the prime mover needs to be removed for vehicles. Similarly, electronic devices that heat wasted, which needs a cooling system. The other heat transfer processes include heating, ventilation and air conditioning systems. In thermal power stations, heat transfer is the main method. In addition, many production processes include heat transfer in various forms; it could be the cooling of a machine tool, the pasteurization of food or the adjustment of temperature to move a chemical process. It is useful to increase the heat transfer enhancement of these devices which is important for compact applications. because the space consumed by the device can be reduced by increasing efficiency,

Bergles et al.[1] was investigated when a fluid flows over a stationary surface, e.g. the flat plate, the bed of a river, or the wall of a pipe, the fluid touching the surface is brought to rest by the shear stress to at the wall. The concept of boundary layers is of importance in all of viscous fluid dynamics and also in the theory of heat transfer.

Boundary layers may be either laminar, or turbulent depending on the value of the Reynolds number. Basic characteristics of all laminar and turbulent boundary layers that developing flow over a flat plate are shown in figure 1.1

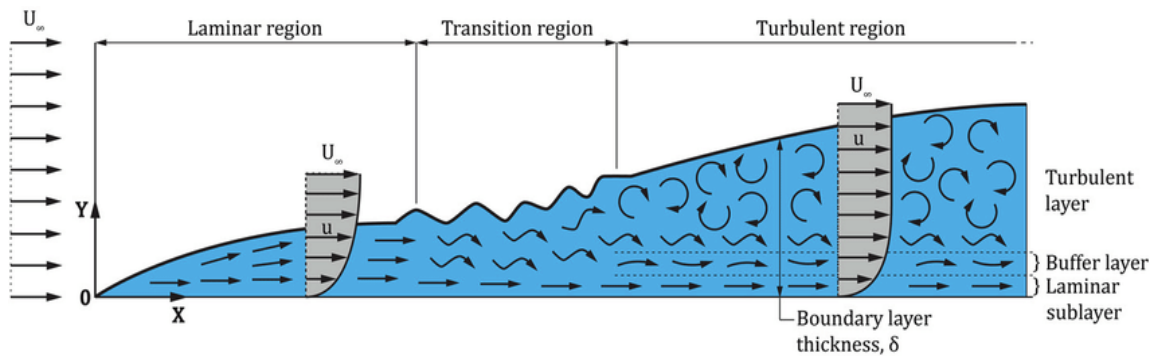


Figure 1.1. The boundary layer for flowing over a flat plate from various flow system [2]

1.1.1. The heat transfer enhancement techniques

The heat transfer enhancement have three types of mechanisms from Adrian Bejan et al.[3] (passive-active and compound) to improve heat transfer as below :

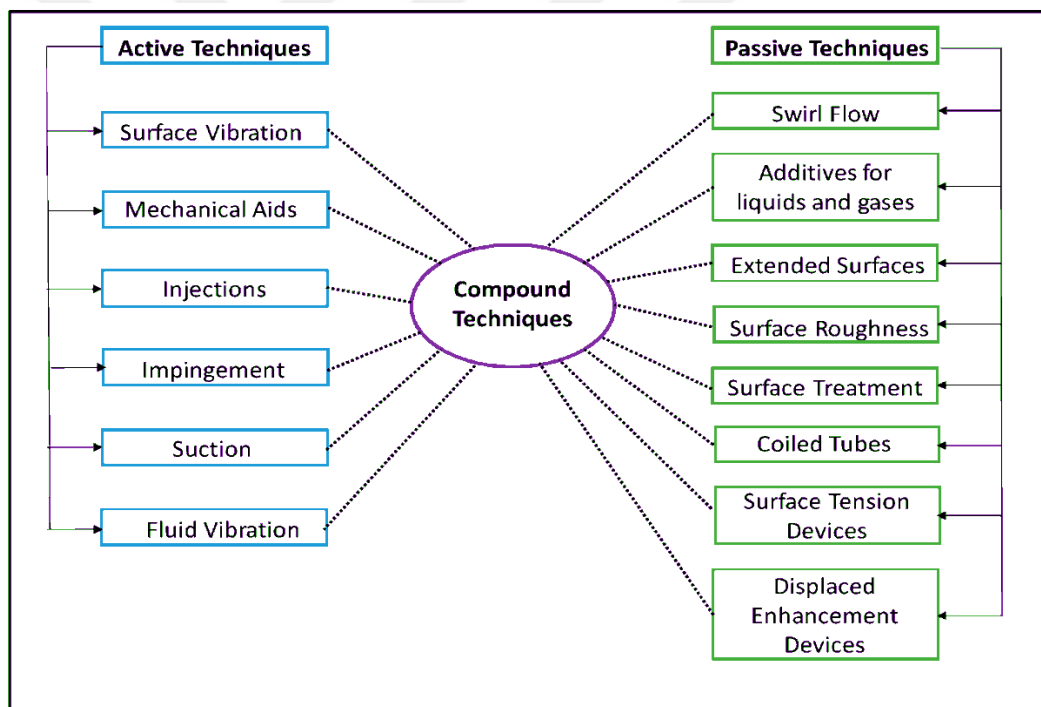


Figure 1.2. Flow chart techniques of enhanced heat transfer[2]

1.1.1.1. Passive techniques

Passive techniques are external power that don't required to improve heat transfer. The joints and rough surfaces will be used to support the vortex in the flow, which will lead to an increase in heat transfer. Due to its lower installation cost and compact size of heat exchangers, passive techniques are a good method because it's can be accomplished

with enhanced heat transfer, and it's utilizes to:

- **Coated or Treated facet** It is a surface for heat transfer with a shift in the final scale to spacing or washing. The changeover may be defined or undefined, that the flatness is rather lower than the one affects single-stage heat transfer and is used mainly for boiling activity
- **Rough facets** Two different methods provide it: the integrated system in which the roughness is introduced into the surfaces and extracted or reconstructed. The other is a non-integral approach made to maximize heat transfer by positioning the roughness close to the surface. Those same methods are facet adjustments which typically raise the instability stream but not to raise the heat transfer surface of the area and are used mainly in a single-phase flow.
- **Extended facets** The flat fin can just improve the field, but properly designed extended facets may increase the coefficient of heat transfer, Improve the area of heat transfer which increases the heat transfer format string.
- **Displaced enhancement device:** The purpose of this approach is to raise the combining of fluids, that leads to better energy delivery. Strips such as tapered ring modules, copper mesh, tapes, and cable wraps are classified as the devices for displaced enhancement.
- **The tube of Coiled:** Makes heat exchangers marginally quite lightweight. Winding tube deformation causes alternative currents, this promotes higher heat transfer parameters in single-stage phase currents and most boiling regions.
- **The apparatus of tension in surfaces:** Contains surfaces that guarantee and increase the flow of liquid from the condensation surfaces to the boiling surfaces.
- **Liquid and gas additives:** Include solid particulate matter, porous trace chemicals, gas bubbles and liquid droplets. Thus, that the fluid resistance in single-phase fluids, these particles are applied thus liquids or gases.

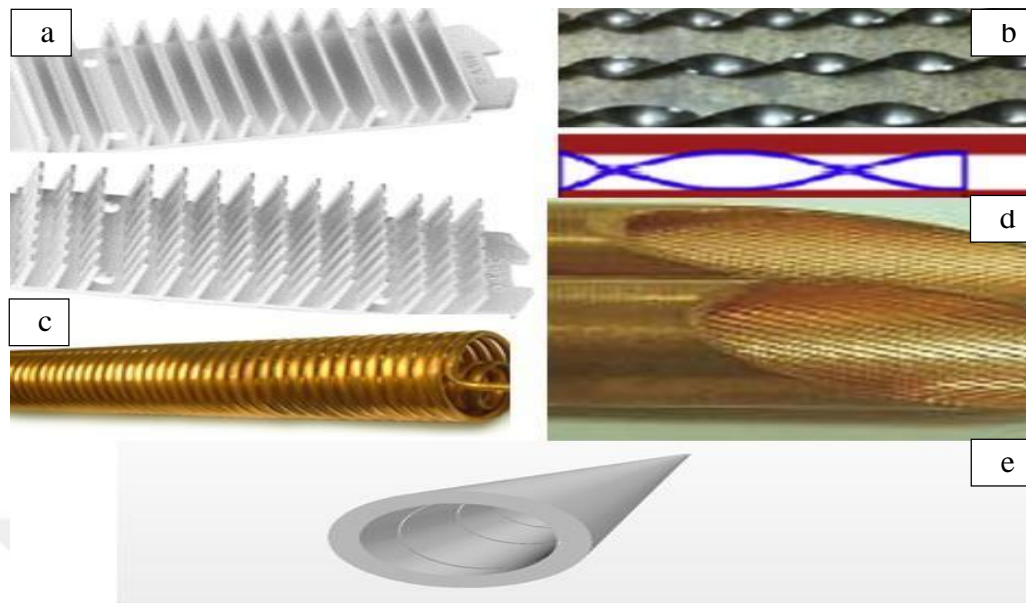


Figure 1.3. Apparatus of passive techniques a) Segmented fin sink, b) Helical inserted, c) Coiled tubes, d) Internally finned tube, and twisted tube e) Grooved Tube [4].

1.1.1.2. Active techniques

From Manglik [4], the power outlet needs to encourage the rate of heat transfer. Due to the design and higher device costs compared to passive methods, their application was limited. Some active methods are as follows:

- **Mechanical aids** Need devices which are rotated or rubbed mechanically. The heat exchanger rotator pipes for example are utilized commonly.
- **The vibration of surface** Is added to enhance low or high frequency heat transfer, such as piezoelectric appliances.
- **The vibration of fluid** Is also where the pulsation is produced in the fluid instead of in the surfaces themselves. Single phase flows are effective.
- **Jet Impingement** it utilized for both single-stage and two-stage heat transfer processes. In this process, the single-stage of fluid is pushed to the heat transfer surface in usual or vertical or diagonal direction.

1.1.1.3. Compound technique

The technique of compound enhancement is a mixture from more than one enhancement method (whether the passive or active techniques) to improve the thermal efficiency of heat exchanger apparatuses, transfer method and geometry classification, a single-phase flow with a forced convection approach is used in this analysis for the flow of internal grooved tubes.

1.2.1 The features of twisted tube:

1. Turbulence is created at low fluid speeds to improve the heat transfer in the pipe.
2. Smooth curved interior profile offers easy cleaning.
3. Fouling the surface of the tube is reduced.
4. Available in a wide range of diameters and styles. [5]

1.2.3 The Technology of twisted tube:

A twisted tube is created by indenting a spiral patterned, plain tube. This provides various flow regimes at the periphery-spiral in the heart and eddies.

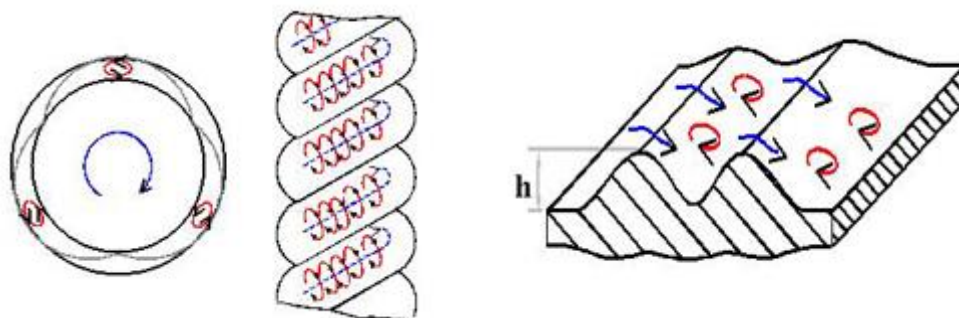


Figure 1.4. the inner foundation of twisted tube[5]

The helical flow leads to the situation where the fluid particles are respectively located near the tube wall and then in the main flow. Between the helical impressions, secondary flow occurs around the circumference of the channel, typically in the form of

eddies.

The flow regime ensures the rate of decrease in the resistance of boundary layers exceeds the rate of increase in the loss of pressure. In other words, high coefficients for heat transfer with minimal pressure drop increase.

1.2.4 Thermal boundary layer of hydrodynamic

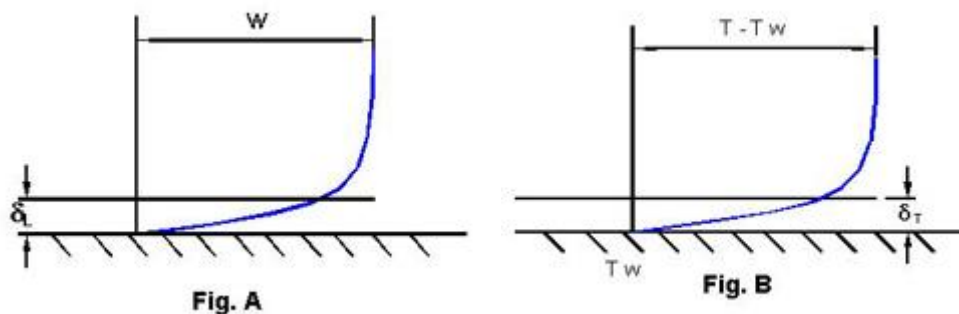


Figure 1.5. schematic of thermal boundary layer of hydraulic[5]

Increasing the coefficient of heat transfer brings the temperature of the tube wall equal to that of the bulk fluid on the tube. The roughness elements need a minimum height to control the flow (Figure A) and hence the heat transfer (Figure B). To ensure that the heat transfer is enhanced by the roughness components, the flow within the heat conduction layer must be affected

1.2.5 The advantages using of twisted tube over smooth tube:

Twisted tube shell and tube heat exchangers have many benefits and advantages over comparable smooth tube versions:

1. Long run times because of turbulent flow
2. Very low maintenance costs, minimal need for savings
3. Due to turbulence created by eddies on the periphery or tube wall, fouling is minimized
4. Uniform thermal transformation

5. More flexibility to size annular areas

1.3. The benefits of enhanced heat transfer

Naik, M., et al. [6]. The benefits of enhanced heat transfer as follows:

1. The device is makes compact.
2. It achieves rising in heat transfer rate by using optimize hydraulic pump capacity.
3. The cost of energy and material is reducing.
4. The efficiency of operation and system is rises.
5. The volume and weight is reduce.

1.4 Introduction to Nanofluids

Nanofluids are suspensions of nanoparticles, the term nanoparticle is derived from the 'nano' Latin prefix. It is used as prefix to indicate the 10^{-9} portion of a unit. In this context, nano-particles in the range of a few nanometers can be called the particles with a dimension. Nanoparticles have historically a size of between 100-2500 nm. Particulate content smaller than 100 nm is considered ultrafine. Because of their possible applications in the fields of medicine, optics and electronics such objects are extensively researched. A variety of processes such as gas condensation, mechanical wear, or chemical precipitation techniques may create nano particles. Gas condensation has benefits against other techniques. Nanoparticles used to make nanofluids include: aluminum oxide (Al_2O_3), copper (Cu), copper oxide (CuO), gold (Au), silver (Ag), silica nanoparticles and carbon nanotube. water, oil, acetone, decene and ethylene glycol were used as the base fluids. Nanoparticles can be formed from a variety of processes, including gas condensation, mechanical attrition or chemical precipitation. from Lee S [7]. Preparation of a nanofluid starts by combining the foundation fluid directly with nanoparticles. Sensitive nanofluid processing is necessary since nanofluids require discrete conditions, like even absorption, lasting suspension, Reliable probation, low carbon dioxide accumulation and no chemical fluid adjustments. from Xuan Y, [8].

The methods suggested for sustaining the suspensions as follows:

- a) changing the pH value of suspension
- b) using surface activators or dispersants
- c) using ultrasonic vibration.

Particles can fracture or agglomerate after mixing into liquid. Transmission electron microscopy (TEM) is widely used to observe the characteristics of particles before and after dispersion in liquid.

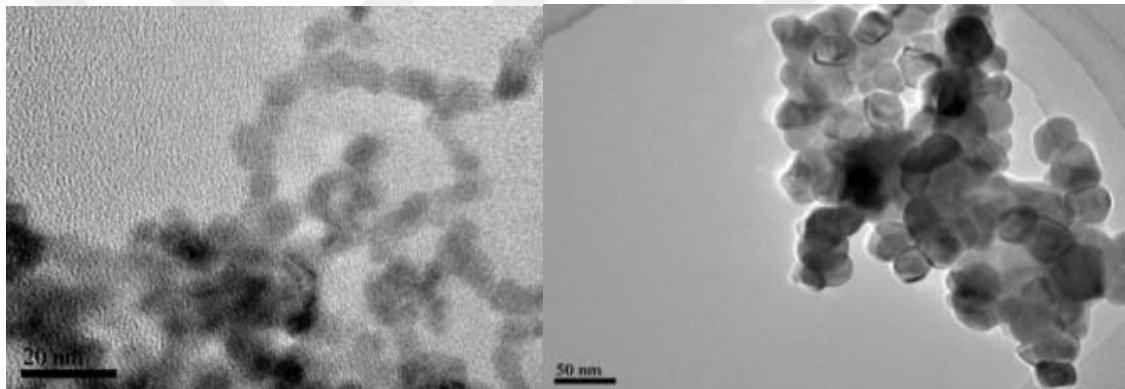


Figure 1.6. T.E.M (Transmission electron microscopy) Photographs illustrating the CuO nanoparticles structure and size [9].

1.5.1. Nanofluids Preparation

1.5.1.1 The method of single-step

- The one-step operation involves the combined production and dispersal of the molecules in the base fluid.
- The suction-SANSS (system for submerged arc nanoparticles) is indeed an efficient way for the preparation of nanofluids utilizing specific insulation liquids.
- Physical one-step process can't extract nanofluids on a large scale and the cost is also high, so that the one-step chemical method improves quickly.

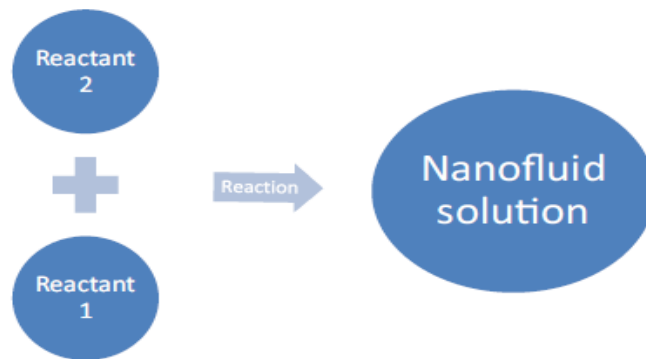


Figure 1.7. Graphic of single-step method [9]

1.5.1.2. The method of two-step

- Nanoparticles, nanofibers, nanotubes or other nanomaterials used in this process are first developed by chemical or physical methods as dry powders.
- In the second processing step, the nanosized powder will then be dispersed into a fluid with the aid of intensive magnetic force agitation, ultrasonic agitation, high-shear mixing, homogenization and ball friction.
- The method of two-step is the most economical approach for the wide-scale production of nanofluids.

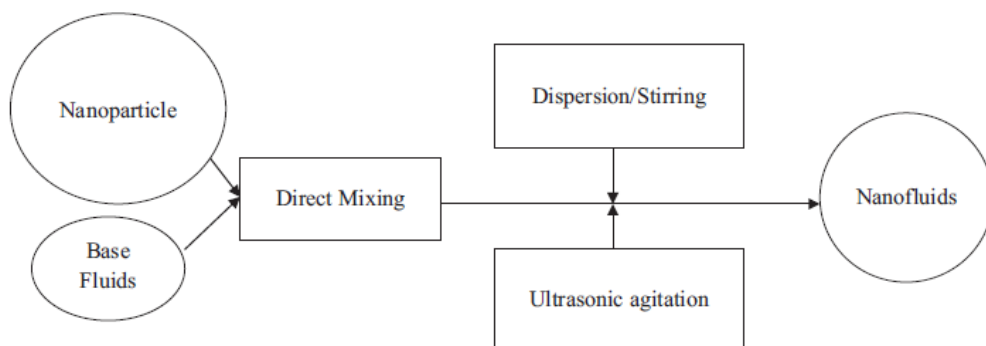


Figure 1.8. Graphic of two-step method [9]

1.5.2. Thermal conductivity of Nano fluids

- ❖ A quite poor thermal conduction of modern fluids was used in the heat transfer

applications.

- ❖ Considering the increasing demands of modern technology, this one has recently been suggested that the dispersion of small quantities of nanometer-sized solids into the fluid called nano fluids the increase the thermal conductivity of the fluids. [10].
- ❖ The nano fluids with the following thermal properties are:
 - Brownian motion
 - Interfacial layer
 - Volume fraction of particles.

1.5.2.1. Brownian motion

- Improvement of the efficient thermal conductivity of nano fluids is primarily due to localized convection caused by the nanoparticles ' Brownian movement.
- The motion of Brownian that causes micro-combining.
- It influence is an additive to the static dilute suspension's thermal conductivity.

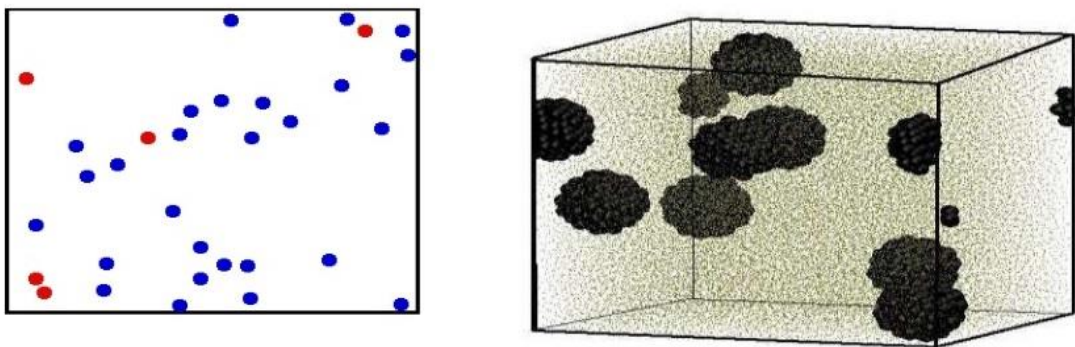


Figure 1.9. The motion of Brownian's nanomaterials [11]

1.5.2.2. Interfacial layer

- It's often supposed that the rigid-like nano surface acts as a thermal bridge between such a solid nanoparticle and a volume of liquid.

- A structural model of Nano fluids which consists of solid was suggested from this thermally bridging idea of the Nano sheet. Nanoparticles, liquid bulk, and Nano-like solids.
- This Nano layer does not have conventional photos of solid / liquid suspensions.

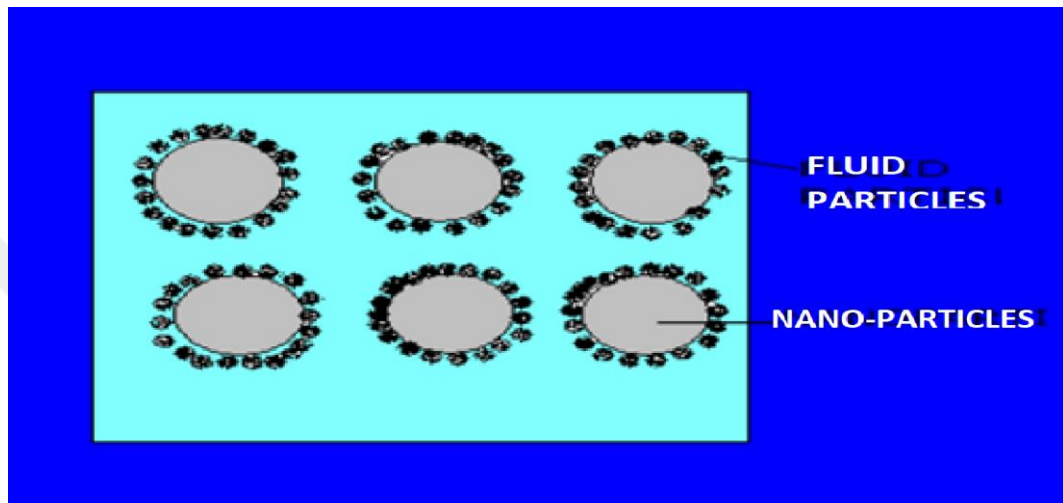


Figure 1.10. The cross section nanofluid structure scheme with nanoparticles [11]

1.5.2.3. Volume fraction

Highly conductive nanoparticles of very low volume fractions distributed in nanofluids may measurably increase the effective thermal conductivity of the suspension when compared to the pure liquid, Figure shows the thermal conductivity with volume fraction, R.Saidur (2011) [12]

1.5.3. The heat transfer improves by using nano fluid

- 1) Higher measurable surface area and thus greater surface heat transfer between particles and fluids
- 2) High flexibility of dispersion with prevalent Brownian particle motion.
- 3) Decreased pumping capacity to achieve equal heat transfer intensification compared to pure air.

- 4) Decreased cluttering of particles compared to conventional compost teas, thus facilitating miniaturization of the device.
- 5) Convertible properties including thermal conductivity and wet surface capacity by varying concentrations of particles to suit different applications. [13]

1.5.4 The applications of nanofluid

There are many applications of nanofluid [14] :

2. Engines cooling
3. Medical applications
4. Solar water heaters
5. Military applications
6. Automobile applications
7. Turning operations
8. Drilling operations
9. Refrigerants [14]

CHAPTER 2

LITERATURE REVIEW

2.1. Nano fluid inserted through the smooth tube

Vajjha et al. [15] were tested the behavior of a comprehensive heat transfer analysis and the decreasing of the pressure of two forms of (Al₂O₃ and CuO) nanoparticles; mixing ethylene glycol and water as flat tube operating fluid. At specific volume concentrations increasing to 5%. That results indicate that the coefficient of heat transfer and the friction factor increase at a fraction of volume of up to 4% and 3% combined with the greatest coefficient of heat transfer of CuO.

Fotukian S., Zeinali H. et al. [16] were investigated the convective heat transfer of Al₂O₃/water, CuO/water and Cu/water nanofluids through a square cross-section duct in laminar flow with constant temperature boundary conditions is numerically investigated. Because of the size and volume constraints, it may be required to use square flow-passage geometries. A square cross section duct has the advantage of lower pressure drop, but it has a lower heat exchange rate than that of a circular duct.

Pak B., Cho Y. et al. [17], in 1995 Studied the augmentation the term nanofluids was developed by the use of a functional phase of 1-100 nm small particles, Molecules, or pipes These particles improve the basic fluid properties such as thermal conduction until improve heat transfer coefficient.

Qiang, L., Yimin X. et al. [18] Researched on heat transfer and pressure decrease of three forms of nanoparticles (Al₂O₃, SiO₂ and CuO), Mixing methanol-glycol into water as the operation liquid at different volume fraction (0,1,2,3,4,5,6%). The results indicate that nano fluids have a greater efficiency in heat transfer chase by CuO and SiO₂. The pressure drop decreases as the volume fraction increases.

Namburu, P. Das, D., et al. [19] performed an experimental analysis on the transfer of heat and the decrease in pressure of three forms of nanoparticles (Al, CuO, and Al₂O₃) with particle diameter 25 nm, 30 nm, and 50 nm flowing through normal laminar water flow heated. The results indicate the increase in the coefficient of heat transfer for four forms of nanofluids (Al, Al₂O₃, Cu, and CuO) is 43%, 32%, and 25%, separately.

Gunes et al. [20] also examined the heat transfer and pressure drop with coiled wire inserted tube in turbulent current regime. The coiled wire was placed separately from the tube wall with two different distance ($s=1$ and 2). The experiments were practiced with three pitch ratios ($P/D = 1, 2$ and 3) at the range of Reynolds number from 4105 to 26,400. Regular heat flux was implemented to the exterior facet of the tube and air was the base fluid. The results revealed that utilizing coiled wire inserts lead to a considerable rise in the heat transfer and pressure drop, and the Nusselt number and friction factor rise with the decreasing pitch ratio and margin.

Sarkar J., et al. [21] has been inspected experimentally the heat transfer and friction factor of Cu-water nanofluid in tube. The results indicated which nano-fluid heat transfer with a volume concentration of 3 % vol. fraction increases by about 62 per cent. The friction factor was a low volume factor.

2.2. Investigation with water fluid inserted

Duangthongsuk, W., et al. [22] researched the coefficient of heat transfer and friction factor, twisted tubes and cold and hot water as a fluid that works in field heat pumps. Furthermore, it is positioned in two different cases in the test section: First, the traditional twisted full-length tape and the twisted strip with different blank spaces. The results showed heat transfer and friction factor were increased.

Kannadasan, N., et al. [23] inspect the validate for heat transfer and hypotension in a horizontal pair of stranded wires, where the finned tube's inner and outer diameters were 8.92 mm and 9.52 mm. Temperature varies from 15-20 ° C for cold and hot water. The results show a rise in a spiral wire spacer's heat transfer and an improvement in the friction factor.

Dawood, H., et al. [24], reviewed Enhancement of heat transfer and friction factor when

twisted tube and spiral tape are used along with air as the operating liquid in an axial pipe through a normal flux of heat. The axial and warped effect of the wire was measured, and wrapped tape results in a double increase in heat transfer according to the straight pipeline, and substantial pressure drop rise.

Vajjha, R., et al. [25] In the turbulent flow method, test the heat transfer and the pressure drop with a stranded wire. Coiled wire has a cross section which is equilateral. Trials were performed using three wall spacing numbers ($P / D = 0.5, 1.75, 2.5$ and 3.5) and pipe diameter equilateral triangle length ($L / D = 0,0624$ and $0,0957$) during 1 mm tube wall spacing ratios. Reynolds are numbered between 3,500 and 27,000. Regular heat flux was applied to the tube's exterior surface, and the primary liquid was air. The results showed that the use of spiral wire connections leads to a noticeable increase in heat transfer and a decrease in pitch diameter, a decrease in pressure and an increase in the Nu, with an increase in the Re and wire thicknesses.

2.3. The twisted tube with contains nano-fluid inside it

Abd, A., Al-Jabair, et al. [26] was inspected the analysis of heat transfer and friction factor in CuO and water with continuous heat flow and turbulent flow method with 0.1% friction rate, 0.2%, 0.3% in a hollow hollow tube. The heat transfer rate increases according to the test, And the drag factorize is roughly, likewise. The straight pipe and the surface temperature will be increase.

Vahidinia, F., et al. [27] inspected a parallel axial pipe nether reliable gas heating flux according to the surface liquid. Investigate heat transfer and a drop in pressure of Al₂O₃ nanoparticles with different fractions of weight (0.5 percent, 1 percent, and 2 percent). The research was conducted Re through 15 and 113 with. That outcomes Indicate the convection using a twisted tube are often extra efficient with nanofluid transmission. In addition, heat transfer raises further while both strategies are combined, In which heat transfer increases by Nearly 21.3 % of Al₂O₃ nano liquid stream on even a smooth pipe at the molecular fraction of 3%

Zarringhalam, M., et al. [28] have been investigated turbulent flow features in the tube by using CuO nanofluid experimentally. The friction factor and heat transfer coefficient are calculated respectively, and the effects of some factors as the volume fraction, flow

features and the Reynolds number have been discussed, from the experimental work a new correlation found from the data to calculate the heat transfer for nanofluids. The result shows the convective heat transfer remarkably increases when use nanoparticles with original flow than base fluid.

Abdolbaqi, M., Mamat et al. [29] have been examined the nanofluid (CuO/water) convective heat transfer in turbulent flow inside tube with nanoparticles volume fractions less than 0.3% was studied experimentally. The result shows that the value for heat transfer coefficient increasing about 25% compared with pure water, increasing the concentration does not Showcase significant effect on the improvement of heat transfer in turbulent conditions, the ratio of the convective heat transfer coefficient of nanofluid to that of pure water decreased as the number of Reynolds increased and through the work it is shown the wall temperature decreased noticeably when the nanofluid flowed in the tube.

CHAPTER 3

THE METHODOLOGY

In many cases, approximate solution is only found. Some of the mathematical techniques required for the thermo-hydrodynamic concern regarding the design of the structures of the heat exchanger are analytical while many are theoretical in nature. While the advancement of computers has rendered computational techniques more advantageous than traditional analytics in order to evaluate current and thermal fields in a heat flux stream, including or not including a particular twisted tube modified. A solution of equations (Navier-Stokes) with energy equation, continuity equation and momentum equations are needed.[30]

3.1. Fluid flow by heat transfer

The fluid flow and heat transfer remain a major area of interest for engineering and science researchers as well as designers, developers and manufacturers alike. The technology resources involve a wide range of energy device components and systems including general power systems, heat exchangers, high-performance gas turbines and other power conversion devices.[30] as shown in Figure (3.1)

3.1.1. The boundary layer of Velocity

The velocity boundary layer develops whenever there is flow over a surface. It is associated with shear stresses parallel to the surface and results in an increase in velocity through the boundary layer from nearly zero right at the surface to the free stream velocity far from the surface that outlined in Cengel [31]. The boundary layer thickness is by convention defined as the distance from the surface at which the velocity is 99% of the free stream velocity, as shown in figure 3.1:

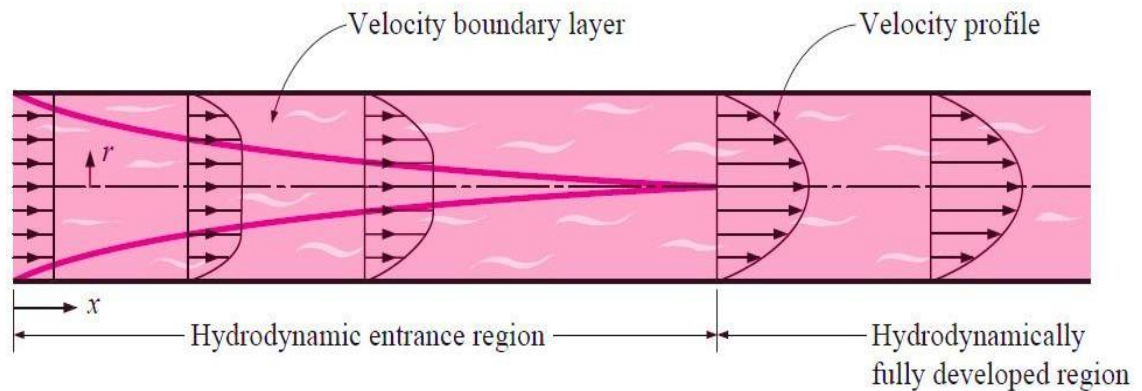


Figure 3.1. The boundary layer of Velocity[31].

It is useful to operate with an average velocity V_{avg} (is the average speed for a fully developed laminar pipe flow through a cross section, the average speed is half the maximum speed) in fluid flow, which remains constant in incompressible flow when the pipe's cross-sectional area is fixed. Due to changes in density and temperature, and due to friction, the increase in average velocity is usually small and is thus ignored in calculations.

3.1.2. The boundary layer of thermal

Similarly as a velocity boundary layer develops when fluid flows over a surface, if the bulk temperature and surface temperature differ, a thermal boundary layer shall develop. Think flowing over a flat isothermal plate at constant T_{wall} temperature. The temperature profile at the leading edge is uniform with T_{bulk} . Fluid particles which come into contact with the plate at the surface temperature of the plate achieve thermal equilibrium. Such particles share energy (by conduction and diffusion) with those in the adjacent fluid layer, as shown in figure 3.2 below as outlined in Cengel [31].

The thermal boundary layer is the area of the fluid in which those temperature gradients occur. Its thickness, x_t , is typically defined as the distance from the body at which the temperature is 99 percent of the temperature from an inviscid solution. The effects of heat transfer penetrate further into the stream with increasing distance from the leading edge, and the thermal boundary layer rises. The ratio of these two thicknesses (velocity and thermal boundary layers) is governed by the *Prandtl number*, which is defined as

the ratio of (diffusive momentum to thermal diffusivity).[32]

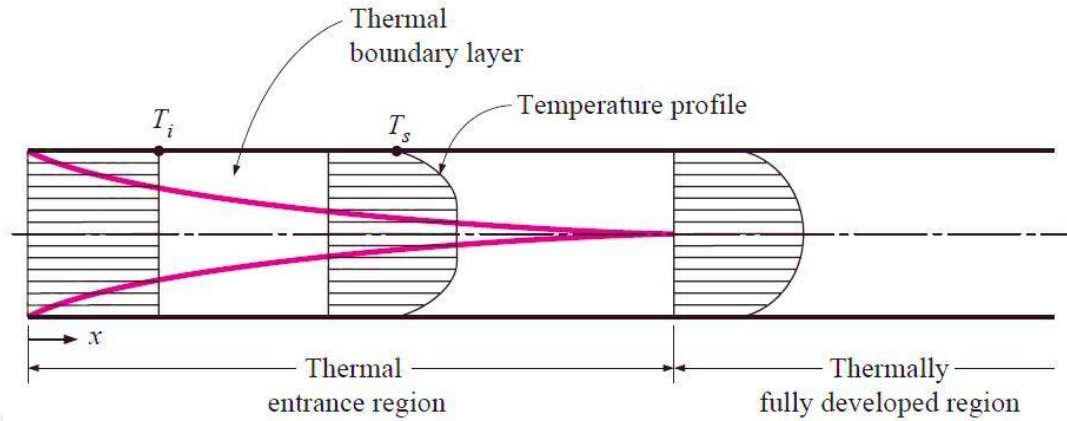


Figure 3.2. Thermal boundary layer[31].

3.1.3. Pure fluids correlations

3.1.3.1 The correlations of water fluids

a. The equation of Colburn [32]

$$(0.7 \leq Pr \leq 160)$$

$$(Re > 10,000)$$

b. The equation of Dittus-Boelter [33]

$$Nu = 0.023 Re^{0.8} Pr^n \quad (2)$$

Where $n=0.3$ flows into the tubes to cool, and 0.4 to heat for liquids.

c. The Equation of Petukhov [34]

$$f = (0.790 \ln Re - 1.64)^{-2} \quad (3)$$

$$(10^4 < Re < 10^6)$$

The Nusselt number, in the flow of turbulent, is applied to either the friction factor by measuring Chilton Colburn equation as follows:

$$Nu = 0.125 f Re Pr^{1/3} \quad (4)$$

This equation allows for proper assessment of the rough and smooth tubes in Nusselt number, if the friction factor was available.

d. The equation of Blasius [35]

Blasius [37] suggested the relation below to calculate the friction factor for pure fluids :

$$f = 0.316 Re^{-0.25} \quad (1)$$

(3000 < Re < 105)

3.1.3.2. The correlations (CUO-Water) nano-fluid:

A. Vajjha et al.'s empirical test [36]

This test is related with the equation of Gnilinsky as shown below:

$$Nu = 0.065 (Re^{0.65} - 60.22) (1 + 0.0169 Re^{1.5}) Pr^{0.542} \quad (6)$$

(0 < ϕ < 10.0 Vol %)
(3000 < Re < 1.6 x 10⁴)

B. The Experimental study of Pak & Cho. [37]

$$Nu = 0.021 Re^{0.8} Pr^{0.5} \quad (7)$$

(0 < ϕ < 3.0 Vol %)

$$(10^* < Re < 105) (6.5 < Pr < 12.3).$$

C. The numerical study of Maiga et al. [38]

$$Nu = 0.085 Re^{0.71} Pr^{0.35} \quad (8)$$

(0 < ϕ < 10.0 Vol %) (10⁴ < Re < 5 x 10⁵)
(6.6 < Pr < 13.9)

3.2. Helpful formulations

1. **The intensity of turbulence** is defined as the ratio of standard deviation of fluctuating wind speed to mean wind speed

$$I.T = 0.16 * Re^{-0.125} \quad (9)$$

2. **Bulk Temperature** The definition of bulk temperature is that adiabatic mixing of the fluid from a given cross section of the duct results in a certain temperature of equilibrium which accurately reflects the average temperature of the moving fluid (T_b).[39]

$$T_b = \frac{T_i + T_o}{2} \quad (10)$$

- 3. The coefficient of Heat transfer (hc):** The heat transfer rate between the surface of solid and one liquid per unit surface area over temperature difference. [40]

$$h = \frac{q}{T_s - T_b} \quad (11)$$

- 4. The Nusselt number (Nu):** Is the convective ratio to the conductive heat transfer at the fluid boundary. Convection includes advection (fluid movement) and diffusion (conduction) [40].

$$Nu = \frac{h * d}{k} \quad (12)$$

- 5. The Reynolds number** is the ratio of inertial forces to viscous forces within a fluid. The Reynolds number has wide-ranging applications ranging from liquid flow in a pipe to air passage over an airplane wing and it's used to predict the transition from laminar to turbulent flow [41].

$$Re = \frac{\rho \cdot v \cdot d}{\mu} \quad (13)$$

6. The Friction factor

Fluid friction is the force that prevents movement either within the fluid itself or through the fluid of another medium [42] as follows:

$$f = \frac{2D \Delta p}{\rho L v^2} \quad (14)$$

- 7. The Pressure Drop** The difference between the inlet and outlet pressures of the tube. It is a function of the tube's resistance to overflowing them [43]

$$\Delta P = \frac{f v^2 \rho l}{2d} \quad (15)$$

- 8. The Prandtl Number** It defined as the ratio of diffusive momentum to thermal diffusivity. It depends on fluid condition and fluid state [44].

$$\text{Pr} = \frac{\text{molecular diffusivity of momentum}}{\text{molecular diffusivity of heat}} = \frac{\nu}{\alpha} = \frac{\mu C_p}{K} \quad (16)$$

9. The Performance of Thermo-Hydraulic factor or Performance Evaluation Criteria

is a ratio of the change in the heat transfer rate to change in friction factor. Several types of inserts are used in many heat transfer enhancement devices is specified and used with the same fluid. [45]

$$\text{PEC} = \frac{NU_c/NU_o}{((f_c/f_o)^{1/3})} \quad (17)$$

C : is represent the all case of the twisted tube

O : is represent the all case of the smooth (circular) tube

11. Performance evaluation analysis (η) The applied factor is measured at the same hydraulic force as the enhanced heat transfer coefficient (h_E) to the non-enhanced heat transfer coefficient (h_{NE}) and is used with the nanofluid. [46]

$$\eta = \left(\frac{h_E}{h_{NE}} \right) \quad (18)$$

3.3. Numerical Analysis Process

1. The geometry was drawn (smooth tube) by using CAD program 2018.
- 2.. The mesh was generated by ANSYS 18.0.
3. The turbulent flow k- ϵ - Standard model was selected.
4. Test independence for the smooth tube was meshed of the first case and study the flow of water and nanofluid with multiple volume fractions (0%, 1%, 2%, 3% and 4%).
5. For the second situation, run the test with twisted tube insert with adjusted pitch ratios (50 mm, 100 mm, 250 mm) to generate mesh and examine the water flow and nanofluid and compare with the value of volume fractions, and all the results had been investigated.[47]

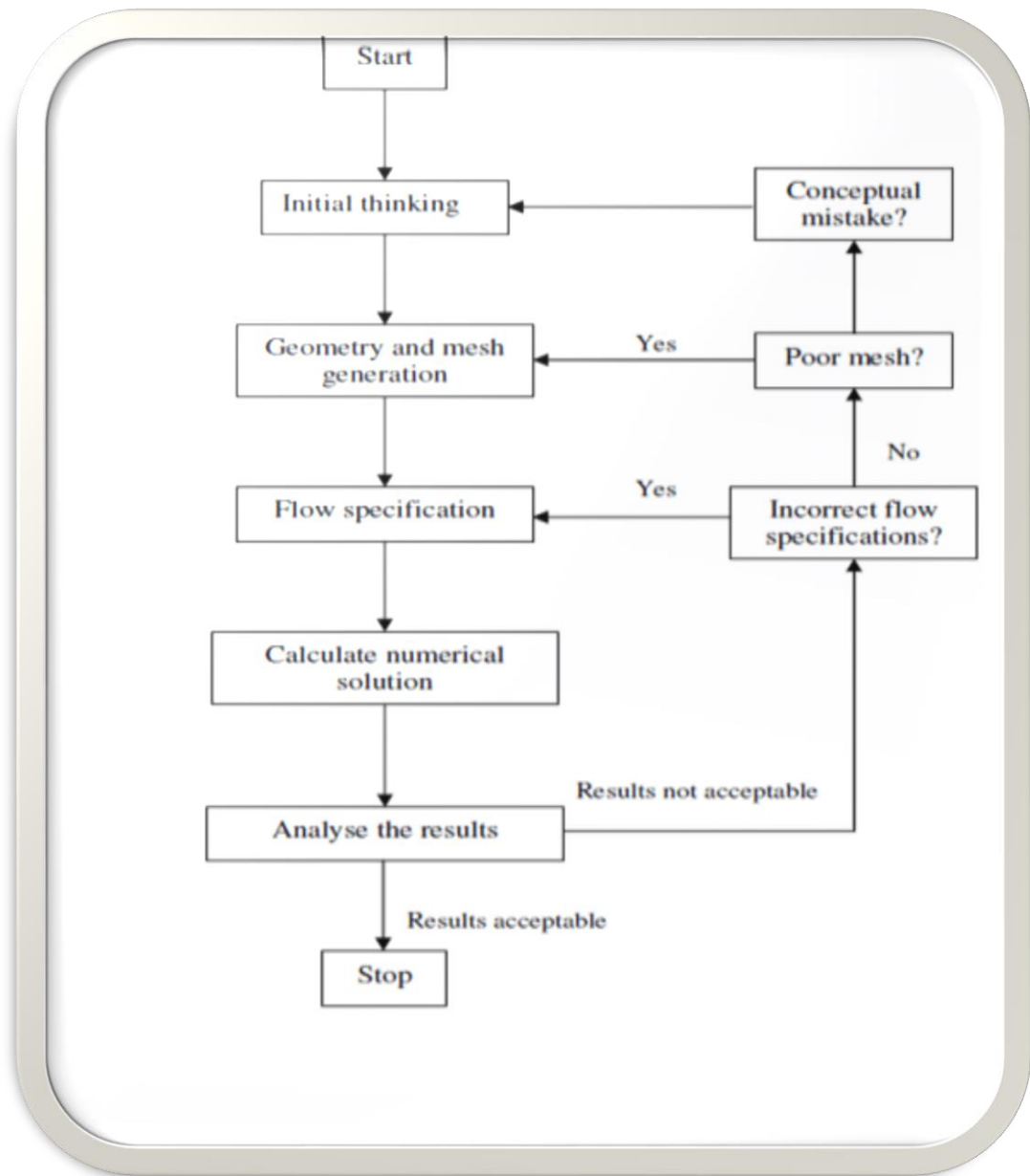


Figure 3.3. the diagram of CFD analyzing procedure [48]

3.4. The Geometry of Profiles

The shape included a straight pipe with a diameter of 26.9 mm and a length of 1000 mm with three sections: 300 mm entrance region, 1000 mm test section wall and 200 mm exit region as shown by the figure (3.4):

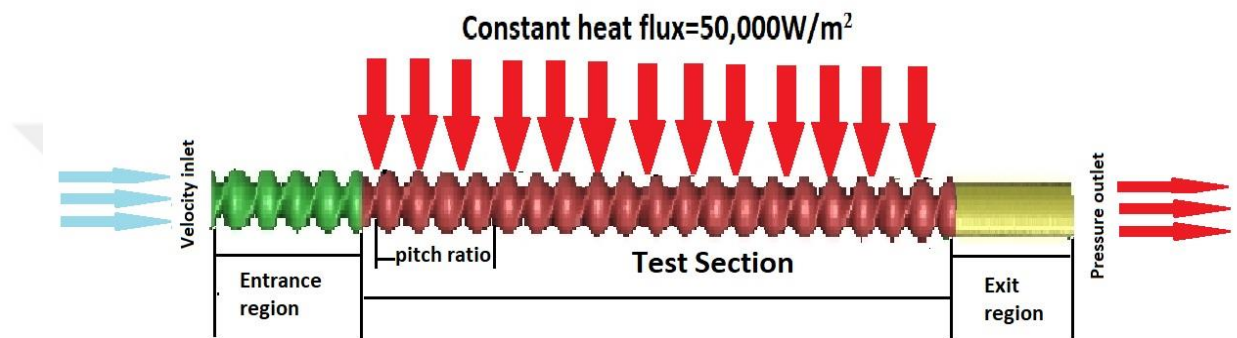


Figure 3.4. The graphic body of numerical research

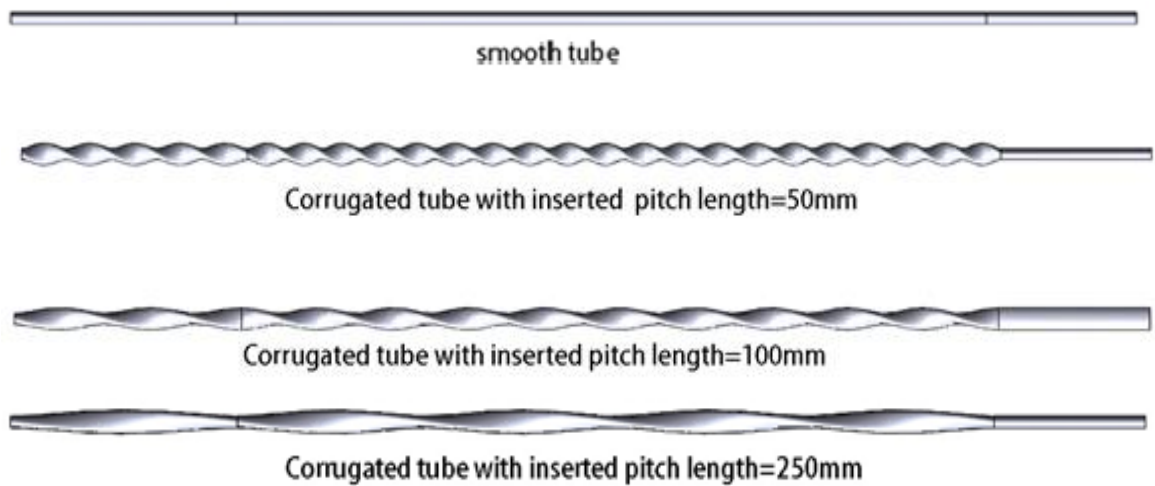


Figure 3.5. Geometry with different pitch lengths of twisted tubes

3.5. The CFD-models validation

According to Eesa [49] inspected, the validation of CFD models is often important to determine computational model accuracy. This calculation can make CFD models easier to develop. Associating the CFD results with existing experimental, theoretical or analytical data validates that as well.

3.6. The benefits of the CFD

The benefits of CFD According to Eesa [49] as follows:

1. In many industrial practices CFD will deliver comprehensive flow visualization
2. Ability to run systems that are not applicable to controlled experiments.
3. CFD can provide a variety of extensive data, since there are generally no similar limitations.
4. The intricate physically dealings with occur in the stream situation was been styled simultaneously, as there is usually no need to limit assumptions.

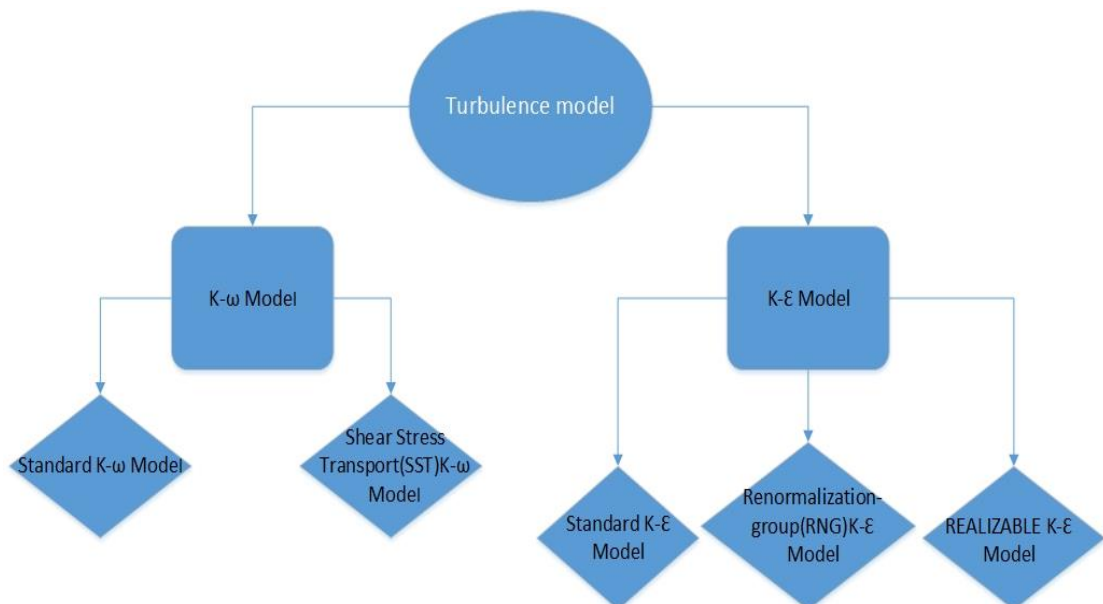


Figure 3.6. The diagram of turbulence models [50]

In the present study, the K- ϵ -standard model was chosen as the closest value for the Blasius correlation of friction factor and Dittus-Boelter correlation of Nusselt number was shown in Figure (3.7 and 3.8)

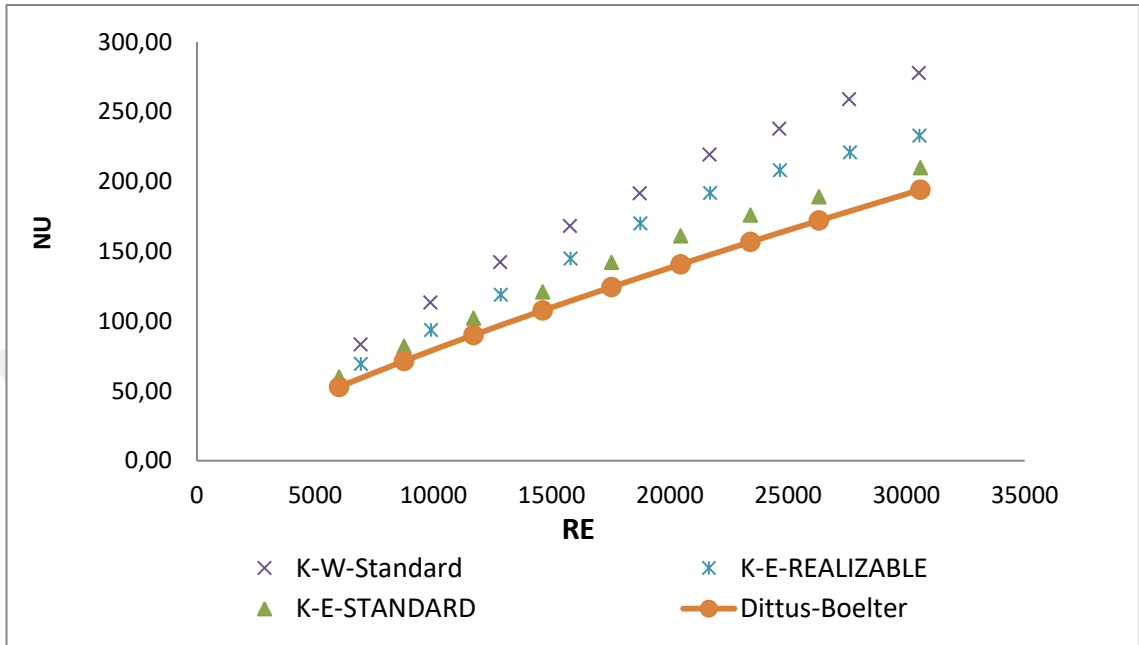


Figure 3.7. Turbulence model compression with the influence of the Reynold and Nusselt numbers

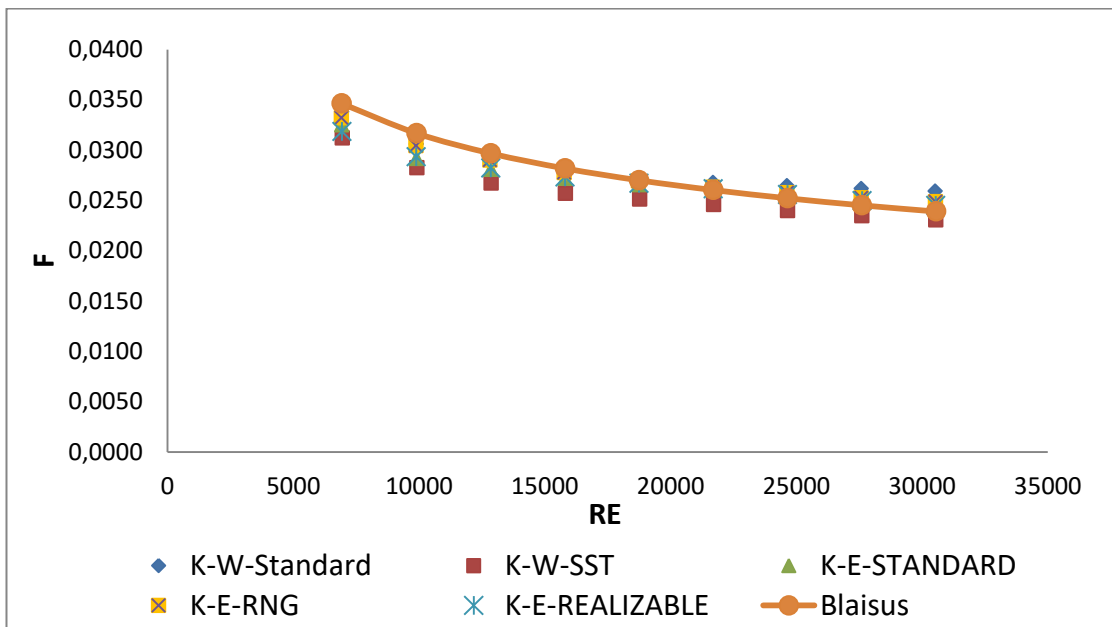


Figure 3.8. Turbulence model with control of the numbers Reynold and Nusselt

3.7 Governing Equation

The heat transfer analyzes are carried out through continuity, momentum and energy in this study [51].

The equation of Continuity:

$$\nabla \cdot (\rho_m \vec{v}_m) = 0 \quad (26)$$

Momentum equation

$$\nabla \cdot (\rho_m \vec{v}_m \vec{v}_m) = -\nabla P + \nabla \cdot [\mu_m (\nabla \vec{v}_m + \nabla \vec{v}_m^T)] + \nabla \cdot (\sum_{k=1}^n \phi_k \rho_k \vec{v}_{dr,k} \vec{v}_{dr,k}) \quad (27)$$

Energy equation

$$\nabla \cdot \sum_{k=1}^n (\phi_k \vec{v}_k (\rho_k h_k + p)) = \nabla \cdot (k_{eff} \nabla T) \quad (28)$$

3.8 The test of grid Independence

Grid-independent testing seems to mean the same thing, but the name is non-sensitive as no, or at least very few, The separate test is carried out using multiple mesh types and the quantities of the identical items are detected by Rashidi et al. [52] as illustrated in Figure (3.9), Figure (3.11) and Figure (3.12)

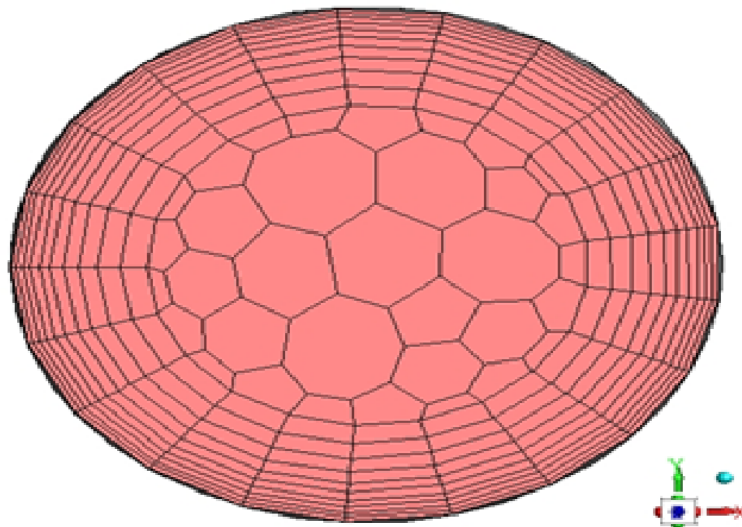


Figure 3.9 Smooth tube in Ansys program at 4.0mm [48]

3.8.1. Smooth tube is modified for the test of independence

For the first situation using a smooth tube this independence test shown in Figure 3.10 shows the Nusselt number value for elements is almost equal (3mm, 4mm and 5mm) after testing the 4.0 mm mesh was chosen.

Table 3.1. The results of mesh sensitivity

Element size	Cell number	Nu	f
1.0 mm	2,350,966	111.427	0.03194
2.0 mm	1,991,512	109.914	0.03144
3.0 mm	1,624,989	87.8185	0.02973
4.0 mm	491,990	74.3072	0.02797
5.0 mm	138,724	59.0122	0.02759

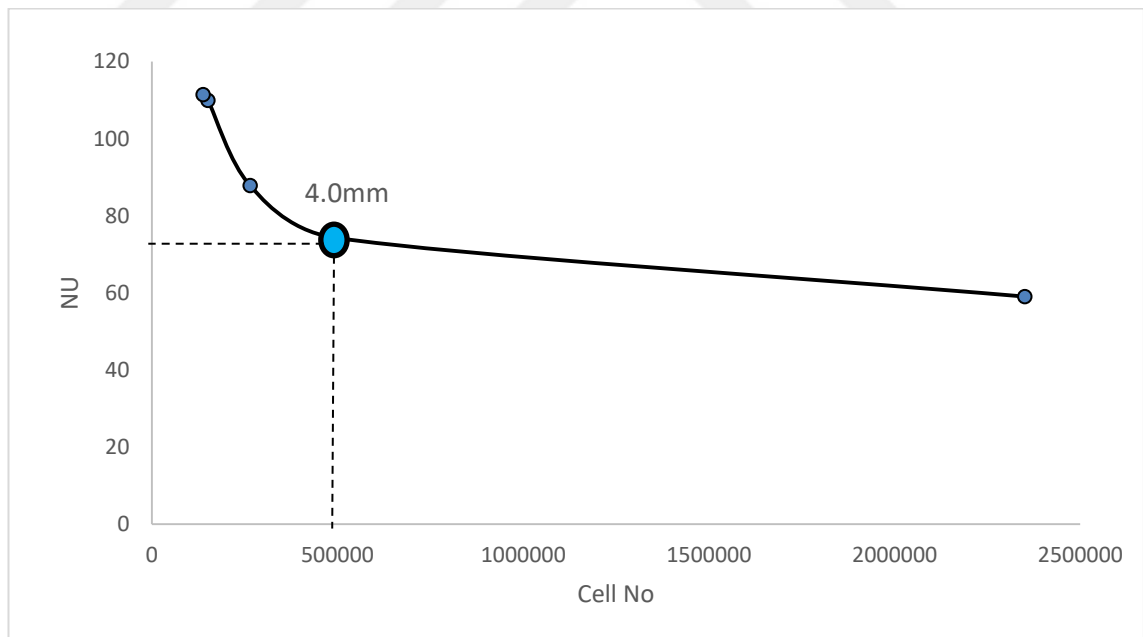


Figure 3.10. The test of grid independence for smooth tube simulate

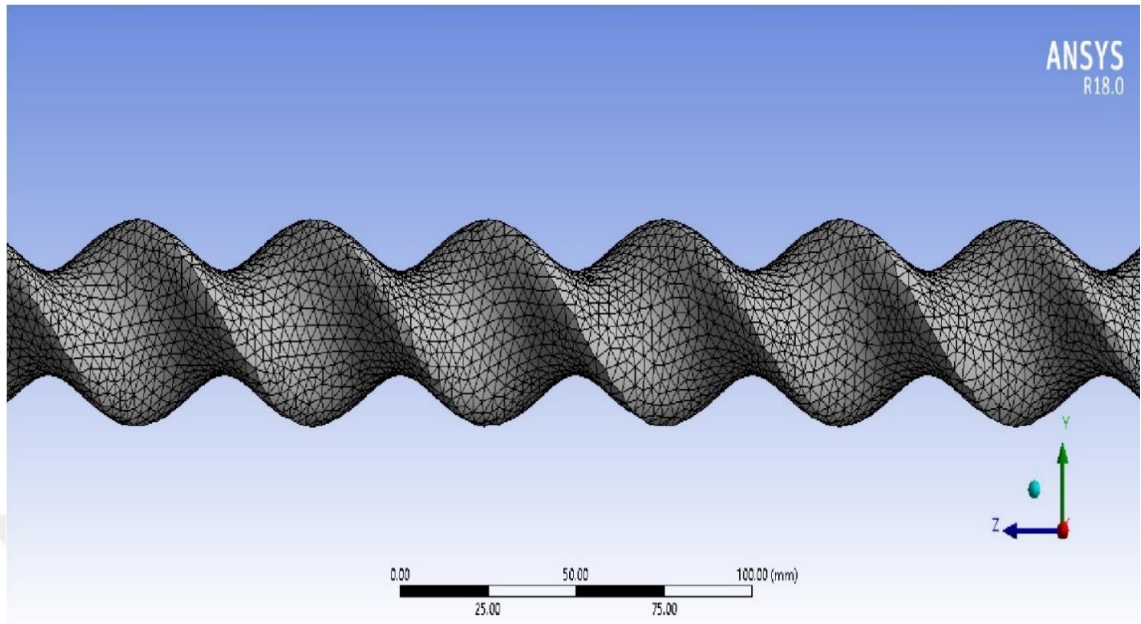


Figure 3.11. The twisted tube in mesh longitude was generated

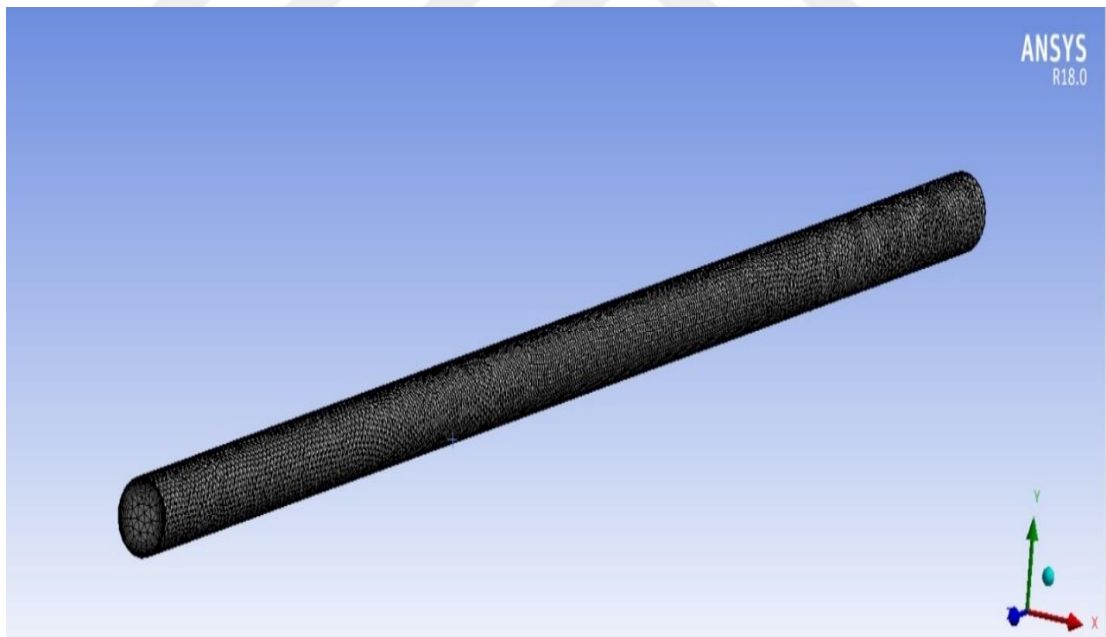


Figure 3.1 A view of mesh twisted tube section

3.9. Investigation of properties of the thermal and hydraulic into (CuO-water) nanofluid

Nano fluids includes particle accumulation in a stable system of metals, metal carbides, nitrides, carbon nanotubes, etc. like water, ethylene glycol, coolants and engine oil of less than 110 nm. According to Sharma et al. [53], Nanofluid thermo-physical characteristics are discovered to just be greater than stable liquid characteristics. The mixture is homogeneous when combining nanoparticles with a water base fluid , According to Demir et al.[54] Not a mixture proposed and that could be considered as a racemic mixture, from the Table 3.6 that relation to the particle size and shape and both characteristics depend on the volume fraction of nanoparticles with various physical characteristics. The formulations for obtaining nanofluid's physical are given below:

1. *The nanofluid specific heat capacity (C_p):* Is the heat energy measurement required to raise the temperature of the unit quantity of a substance by a specific temperature interval. It is inferior to liquid for fuel. Hence Nanofluid's specific heat is less than pure gas. Pak and Cho equation had been applied in this research.

$$C_{pnf} = \frac{\phi * (\rho_s * c_{ps}) + (1 - \phi) * (\rho_w * c_{pw})}{\rho_{nf}} \quad (29)$$

2. *The nanofluid density (ρ):* The equation for the density of two-phase mixtures for micrometer-sized particles is available in the slurry flow literature (Cheremisinoff, 1986). Pak and Cho (1998) adopted the same equation for nanometer size parts as formulated in the formula.

$$\rho_{nf} = \phi * \rho_s + (1 - \phi) * \rho_w \quad (30)$$

3. *The nanofluid viscosity (μ):* Einstein's fundamental research on infinite dilute suspensions of unloaded hard spheres based on the vorticity of the particle shear field was the first theoretical work available on the viscosity of suspension that provided the concept in Equation:

$$\mu_{nf} = \mu_w * (1 + 2.5 * \phi) \quad (31)$$

4. The nanofluid *thermal conductivity (k)*: This is a critical feature in heat transfer, since it can conduct heat. Therefore, metal's thermal conductivity is quite higher than air. Equation of Hamilton and Crosser [55],

$$K_{nf} = k_{np} \left[\frac{k_{np} + (n-1)k_{bf} - (n-1)\phi(k_{bf} - k_{np})}{k_{np} + (n-1)k_{bf} + \phi(k_{bf} - k_{np})} \right] \quad (32)$$

Table 3.2. CuO nanoparticles and water physical and thermal properties at T=273k, from Cengel Y. [31]

Physical properties	Base fluid (water)	CuO
Cp (J/kg.k)	4179	540
ρ (kg/m ³)	997.1	6500
K (w/m.k)	0.613	72

Table 3.3. The physical thermal properties of nanofluid CuO / water [55,56]

ϕ	ρ kg/m ³	Cp J/kg. k	k w/m.k	μ kg/m.s
1 %	1053.02	4145.536	0.6673466	0.00102705
2 %	1108.04	4109.072	0.686874	0.0010521
3 %	1163.06	4072.608	0.7067937	0.00107715
4 %	1218.08	4036.144	0.7271175	0.0011022

CHAPTER 4

THE RESULTS AND DISCUSSION

The calculation results obtained from Ansys.18.0 Fluent Software are available and investigated through this section. It contains test results of water, and water with volumetric concentrations of nanofluid (0%, 1%, 2%, 3% and 4%) for CuO – water nanofluid and nanofluid mixture percent in a plain tube, the twisted four pitch ratios modified (p=0” smooth tube”, 50mm,100mm, 250 mm). The analyzes were carried out with Reynolds number between (6000 < Re < 40,000) under the turbulent full development and a constant heat flux (50,000 W / m²).

4.1. The validation of Smooth Tube and different ratio of diameter(D1/D2) in water fluid

The convective heat transfer and friction factor tests of the current flat tube (before twisted modified) for water are checked. The friction factor and the convective heat transfer were used to validate this work because of the similarities in the thermal and hydraulic efficiency through this chapter, individually and for the schematic of ellipse tube then we used three types of elliptical cylinder ratios with a constant hydraulic diameter (D_h=26.9mm) The calculation methods to find the different diameters were :

$$\text{At } D_h=26.9 \text{ mm , } (D_1=2*D_2) , (r_1=2*r_2) \text{ -----(19)}$$

$$A= \pi r_1*r_2\text{-----(20)}$$

$$D_h = \frac{4*A}{p} \text{-----(21)}$$

$$P= 2*\pi \sqrt{(r_1^2 + r_2^2)} * 0.5 \text{-----(22)}$$

Since : A= the area of ellipse / P=perimeter of ellipse/ r= radius of ellipse.

$$\text{From eq.(3)} \rightarrow 26.9=4* \left[\frac{\pi*2*(r_2*r_2)}{2*\pi*\sqrt{(r_2^2+r_2^2)*0.5}} \right]$$

$$26.9 = 4* \left[\frac{r_2^2}{\sqrt{(2r_2^2+r_2^2)*0.5}} \right]$$

$$26.9= 4* \left[\frac{r_2^2}{\sqrt{1.5*r_2^2}} \right] = 4 * \frac{r_2^2}{1.5*r_2}$$

$$r_2=10.087\text{mm}-----\text{(23) in (19) } r_1=2*10.087=20.175\text{mm}$$

$$\text{therefor: } D_1=2* r_1=40.35\text{mm}$$

$$D_2=2* r_2=20.175\text{mm}$$

And the another of dimensions also the same steps above, and the results we placed it in the table below :

Table 4.1. The different types of ellipse diameters

D ₁ (mm)	D ₂ (mm)	D ₁ /D ₂
26.9	26.9	1
33.625	22.416	1.5
40.35	20.175	2

4.1.1.1 The convective of heat transfer

The results of the Nusselt number uses of a smooth tube and different diameter ratio were obtained. Agreement with the current of water defined in the Dittus-Boelter equation and the range deviation ratio was confined to the values between ($\pm 1,13\%$ to $8,88\%$), as shown in Figure (1);

$$Nu = 0.023Re^{0.8}Pr^{0.4} \quad (24)$$

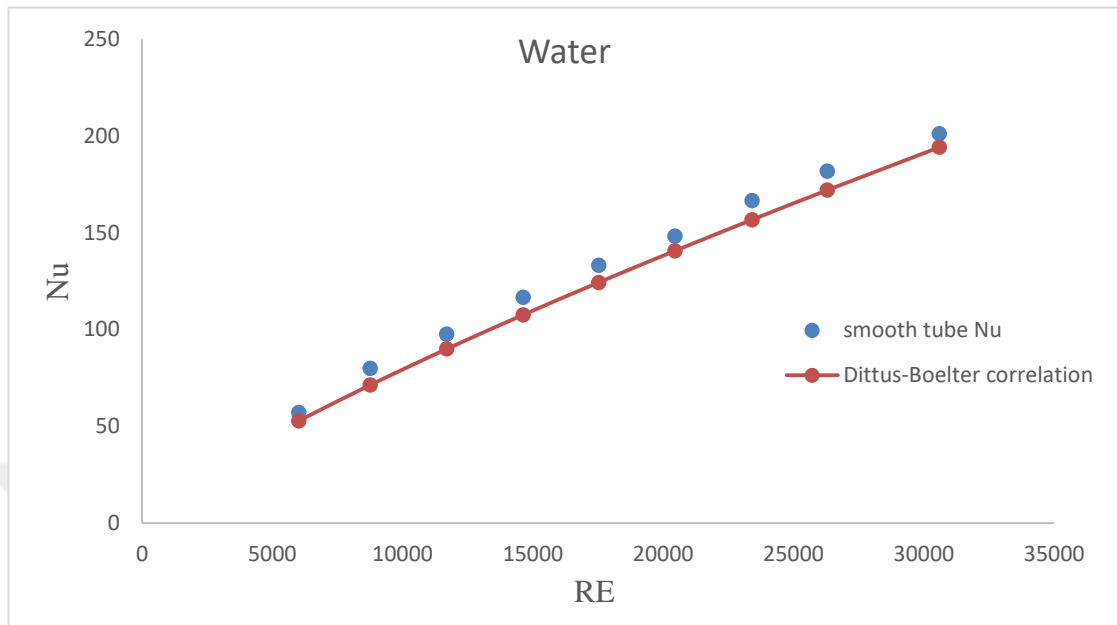


Figure 4.1. The smooth tube with (4.0mm) was selected in this study, Nusselt number (with Dittus-Boelter correlation) vs Reynolds number for water fluid

The Reynolds number versus Nusselt number through a smooth tube and the Dittus-Boelter correlation is given in fig. 4.1. The correlation to match the results attained with a deviation ratio below ± 10 percent was found; indicating a good match. The recorded correlation's maximum deviation ratio was (4.69 %), and the minimum deviation of the recorded correlation was (4.942%), in the elliptical cylinder ratios were ($D1/D2=1.5$) and ($D1/D2=2$) respectively. The fig.4.2. below shows Nu number variation with Reynolds number for different diameters.

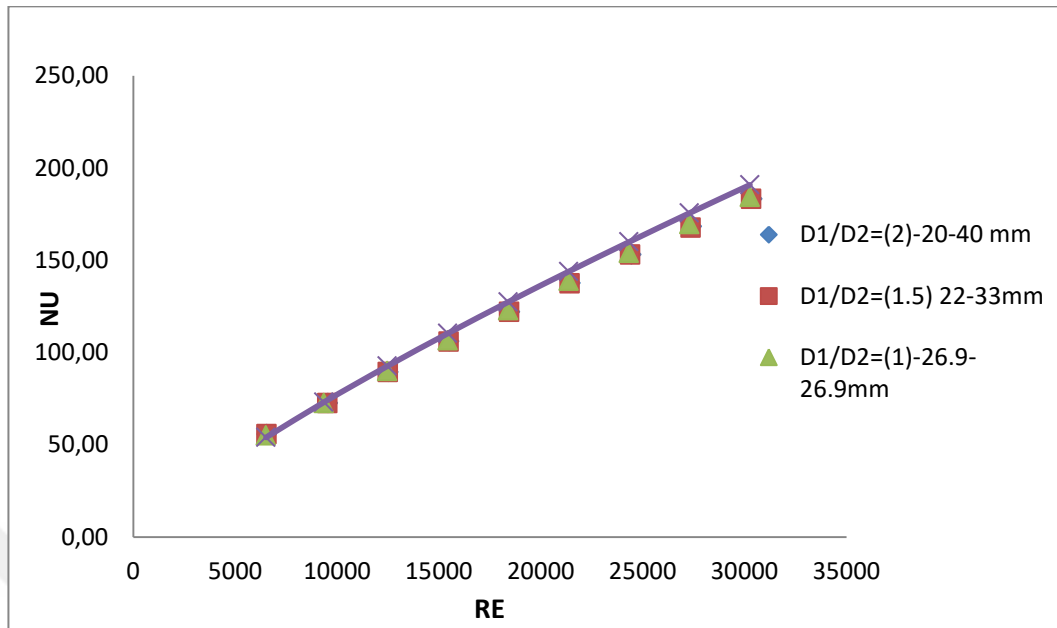


Figure 4.2. The relationship between the Nusselt number by using Dittus-Boelter correlation vs Reynolds number for water fluid in smooth tube for different ratio of diameter

4.1.1.2 The friction factor

The numerical results for the use of smooth tube with water as fluid were given in fig. 4.3. The specified friction factor for Blasius eq. correlation (25) [53] in which the range deviation ratio was between ($\pm 2.2\%$ to 8.07%) as shown in Figure 4.3.

$$f = 0.316 * Re^{-0.25} \tag{25}$$

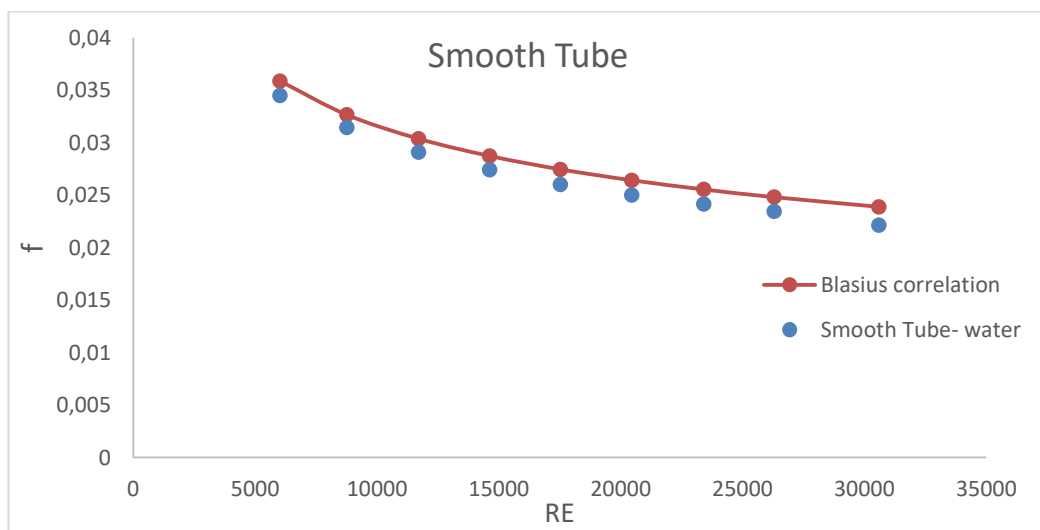


Figure 4.3. The Friction factor by using Blasius correlation vs Reynolds number for water fluid.

The correlation is found to match the results with a deviation ratio under the $\pm 10\%$ was obtained; indicating a good match. Figure 4.4 indicates friction factor changes by Reynolds number for different diameters.

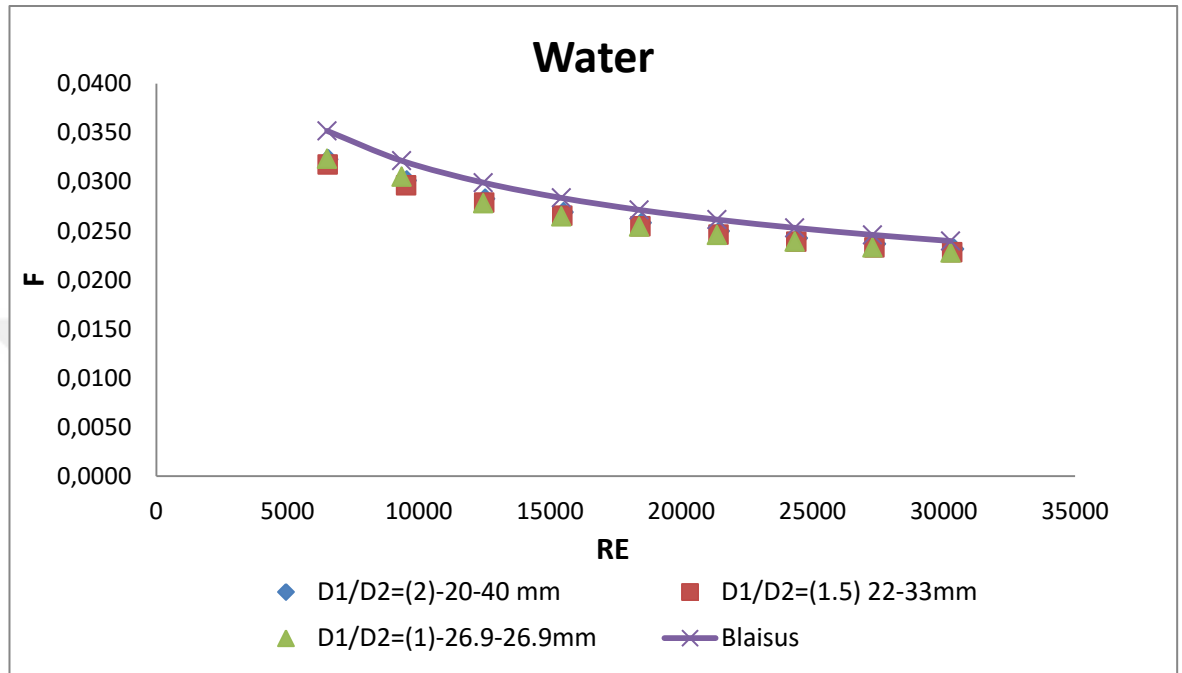


Figure 4.4. The relationship between the friction factor by using Blasius correlation versus Reynolds number for water fluid in smooth tube for different ratio of diameter

4.2. Smooth Tube and different ratio of diameter (D1/D2) in (CuO-Water) Nanofluid flow

4.2.1. Effect on Nu

4.2.1.1 At (D1/D2) =1 [circular smooth tube]

The Nusselt number increased with the increase of nanofluid (CuO-Water) fraction and also of increase of the Reynolds number, where the maximum value of Nu is (249.65) at (Re=30,449) in the volume fraction ($\phi=4\%$) CuO-Water nanofluid, and the minimum value of Nu is (53.08) at (Re=6,195) in the water fluid was obtained as shown below fig (4.5)

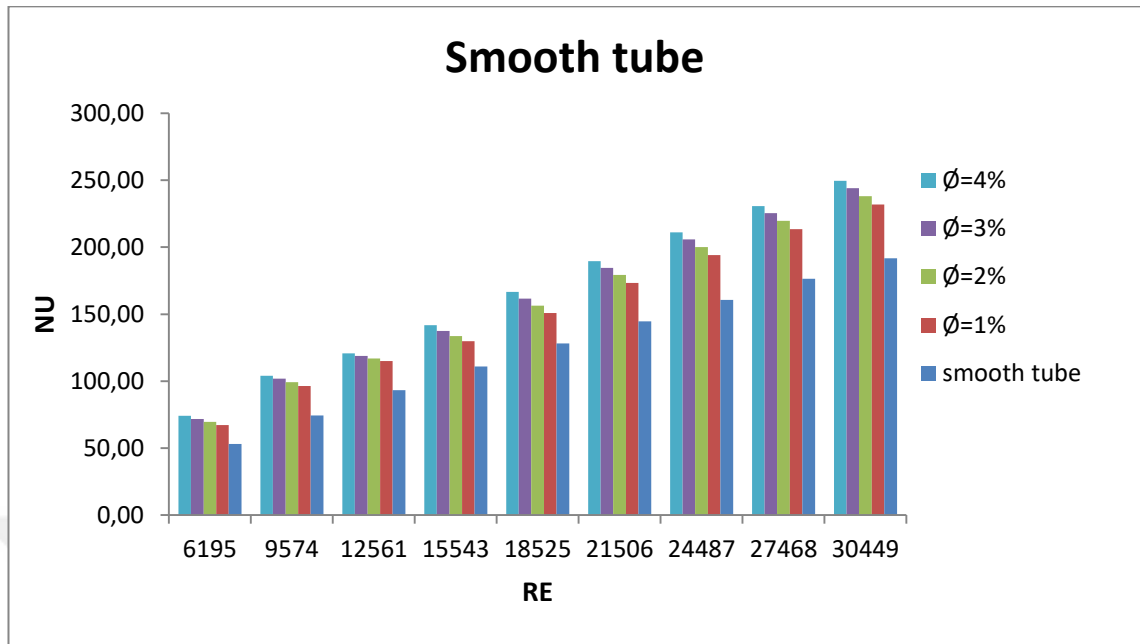


Figure 4.5. The relationship between Nusselt and Reynolds numbers with different volume fractions of CuO/Water for smooth tube

4.2.1.2 Ellipse at the diameter ratio (D1/D2=1.5)--(33-22mm)

The maximum value of Nu is (249.65 at (Re=30,449) in the volume fraction ($\phi=4\%$) CuO-Water nanofluid, and the minimum value of Nu is (62.13) at(Re=6,195) in the water fluid as shown in fig.4.6.

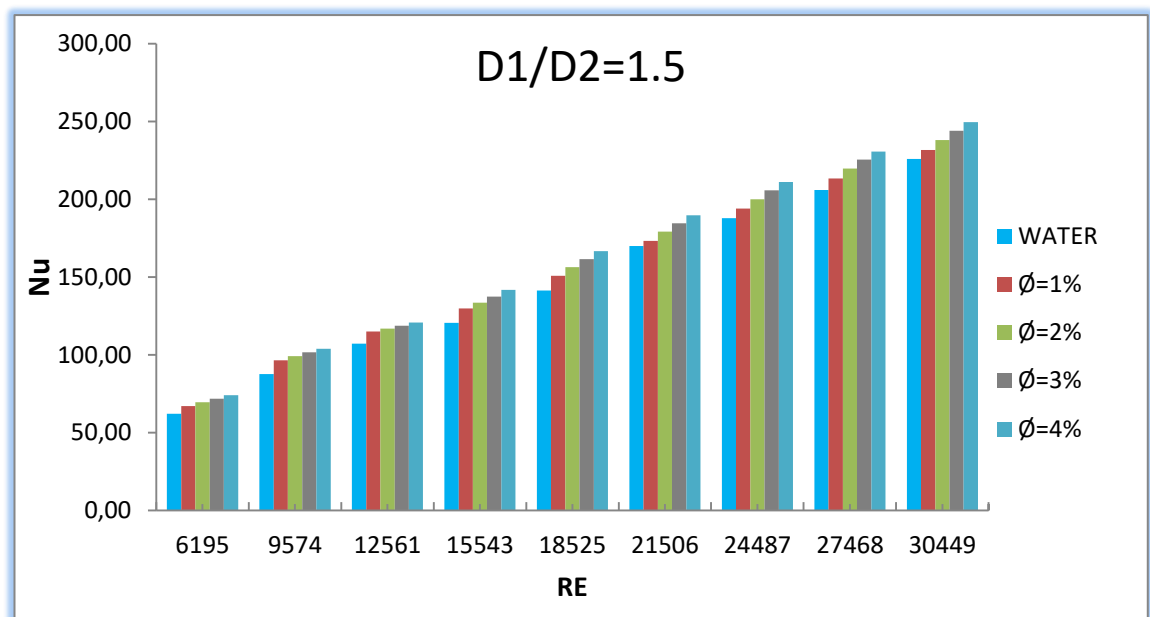


Figure 4.6. The relationship between Nusselt and Reynolds numbers with different volume fractions of CuO/Water for different diameters was ratio (1.5).

4.2.1.3 Ellipse at the diameter ratio ($D1/D2=2$) -(40-20mm)

The maximum value of Nu is 265.24 at $Re=30,399$ in the volume fraction (ϕ)=4% of CuO-Water nanofluid, and the minimum value of Nu is 55.75 at $Re=6,555$ in the water fluid as shown in fig. 4.7.

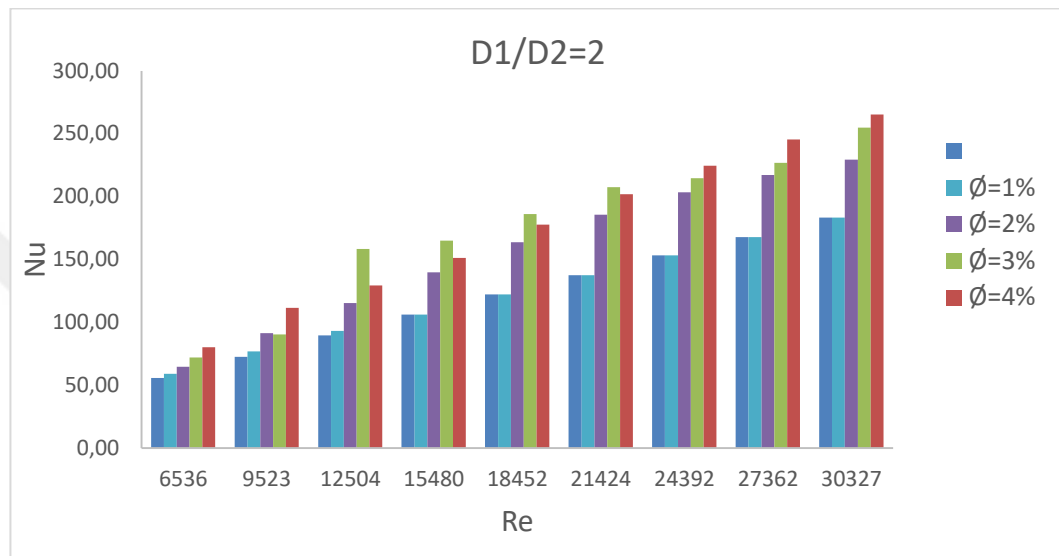


Figure 4.7. The relationship between Nusselt and Reynolds numbers with different volume fractions of CuO/Water for different diameters was ratio (2)

4.2.2 Effect on (h)

4.2.2.1 At ($D1/D2$) =1 [circular smooth tube]

Since the heat transfer coefficient is directly proportional with Nu, in the same condition, the (h) will be increased with the increase of (CuO-Water) nanofluid concentrations by also increases the Reynolds numbers, where the maximum value of h is 6821.33 at $Re=30,262$ in the volume fraction (ϕ)=4% of CuO-Water nanofluid, and the minimum value of h is 1239.86 at $Re=6,510$ in the water fluid was obtained as shown below fig. 4.8.

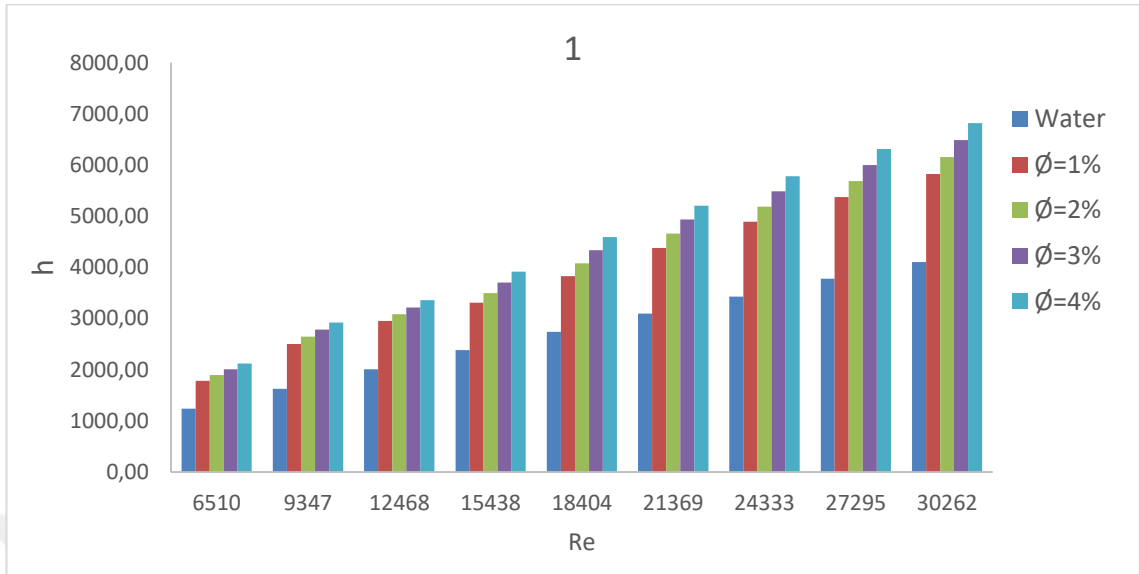


Figure 4.8. The relationship between heat transfer coefficient and Reynolds numbers with different volume fractions of CuO/Water for different diameters was ratio (1).

4.2.2.2 Ellipse at the diameter ratio (D1/D2=1.5) --(33-22mm)

The maximum value of h is 6821.33 at Re=33,649 in the volume fraction (ϕ)=4% of CuO-Water nanofluid, and the minimum value of h is 1255.01 at Re=6,519 in the water fluid as shown in fig.4.9.

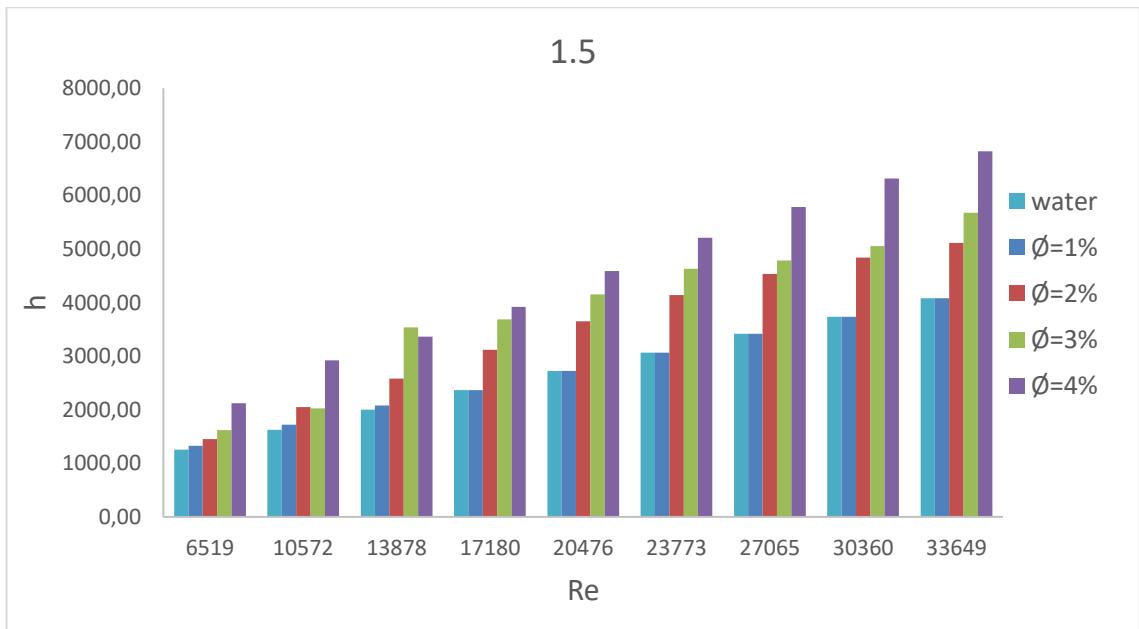


Figure 4.9. The relationship between heat transfer coefficient and Reynolds numbers with different volume fractions of CuO/Water for different diameters was ratio (1.5).

4.2.2.3 Ellipse at the diameter ratio (D1/D2=2) -(40-20mm)

The maximum value of h is achieved as 7289.11 at $Re=31,326$ in the volume fraction (ϕ)=4% of CuO-Water nanofluid, and the minimum value of h is obtained as 1255.2 at $Re=6,736$ in the water fluid as shown in fig. 4.10.

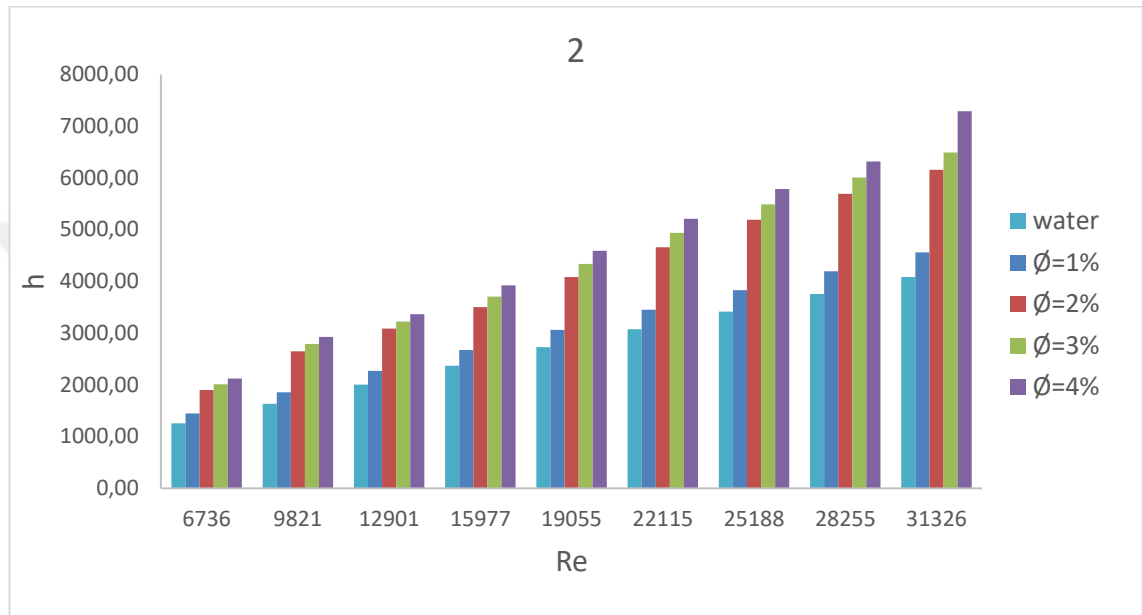


Figure 4.10. The relationship between heat transfer coefficient and Reynolds numbers with different volume fractions of CuO/Water for different diameters was ratio (2).

4.2.3. The friction factors

4.2.3.1 At the diameter ratio (D1/D2) =1 [circular smooth tube]

The maximum value of f is 0.0323 at $Re=31,059$ in the volume fraction (ϕ)=4% of CuO-water nanofluid, and the minimum value of f is 0.0228 at $Re=6,206$ in the water fluid as shown in fig. 4.11.

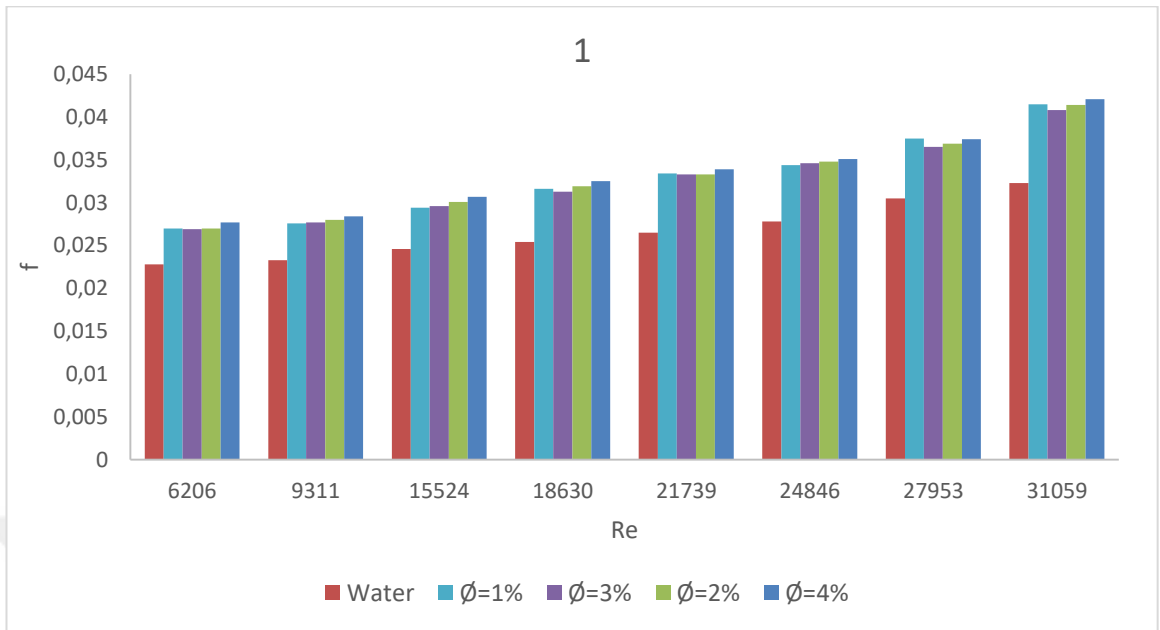


Figure 4.11. Nusselt number relationship with Reynolds numbers variant volume fractions of CuO / Water for a smooth tube

4.2.3.3 At the diameter ratio (D1/D2=1.5) --(33-22mm)

The maximum value of f is obtained as 0.0329 at $Re=30,399$ in the volume fraction (ϕ)=4% of CuO-Water nanofluid, and the minimum value of f is 0.02 at $Re=30,399$ in water fluid, as shown in fig. 4.12.

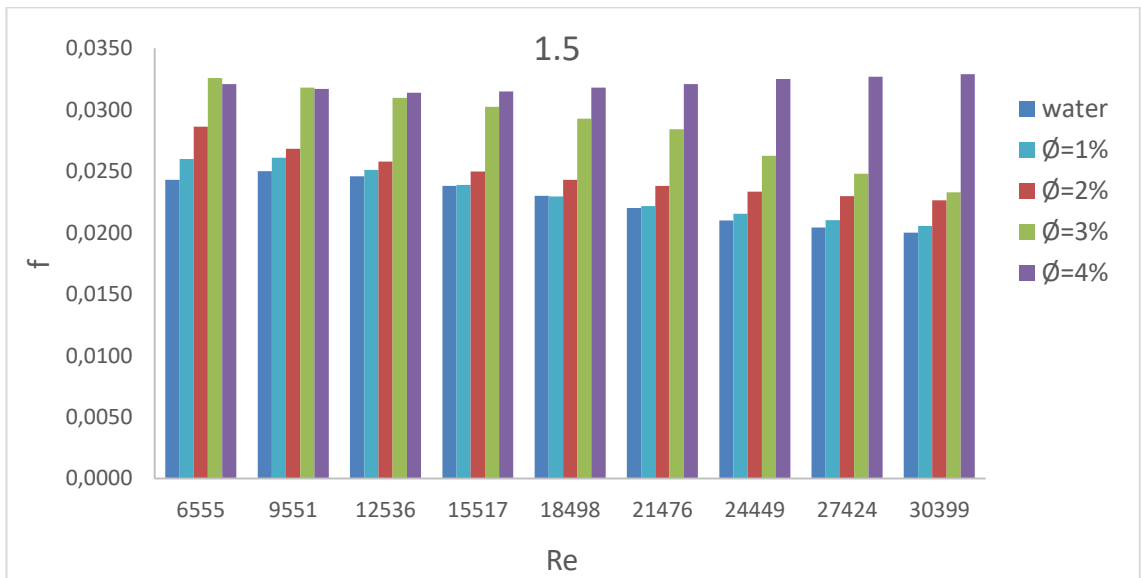


Figure 4.12. The relationship between Nusselt and Reynolds numbers with different volume fractions of CuO/Water for different diameters was ratio (1.5)

4.2.3.2 At the diameter ratio ($D1/D2=2$) --(40-20mm)

The maximum value of f is calculated as 0.0421 at $Re=31,059$ in the volume fraction (ϕ)=4% of CuO-Water nanofluid, and the minimum value of f is found as 0.0228 at $Re=6,206$ in the water fluid as shown in fig. 4.13.

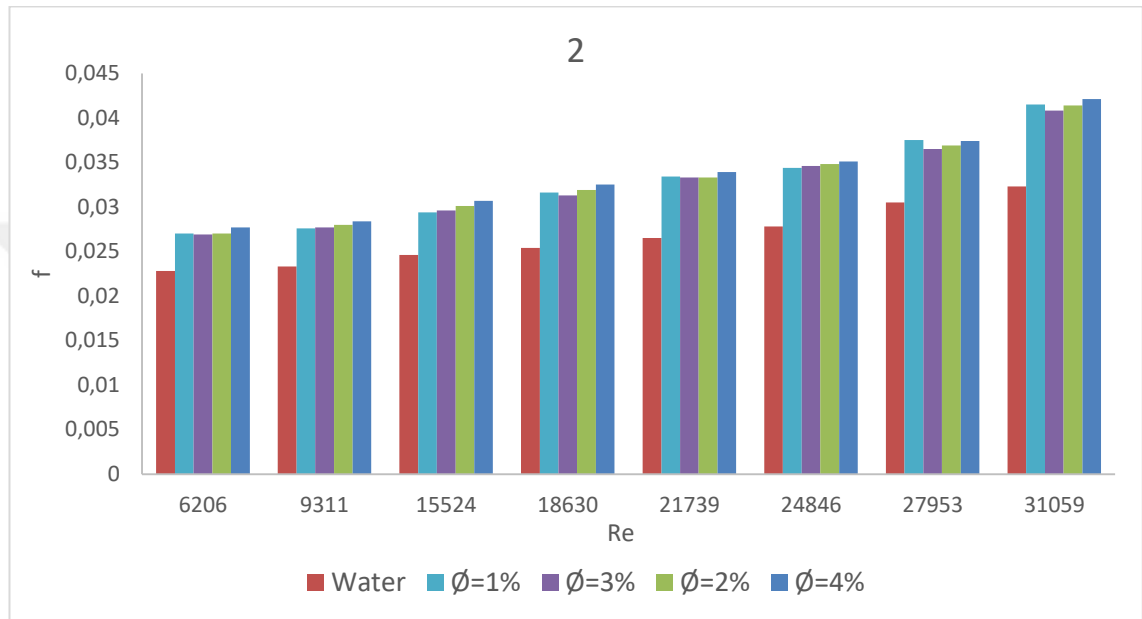


Figure 4.13. The relationship between Nusselt and Reynolds numbers with different volume fractions of CuO/Water for different diameters was ratio (2)

4.3 Different ratio of twisted tube modified with a Smooth tube and different diameter ratios in water fluid

4.3.1 Effect on Nusselt number (Nu)

4.3.1.1 At the diameter ratio ($D1/D2=1.5$) --(33-22mm)

The max.value of Nusselt number is found as 451.61 at the Reynolds number of 34,024 for *pitch length of 50mm*, and the min.value of Nusselt number is obtained as 67.5 at the Reynolds number of 7,217 for *smooth tube*. From fig. 4.14 also shows an increase in the Nusselt number, with a decrease in the pitch ratio of the twisted tube by increasing the value of the Reynolds number.

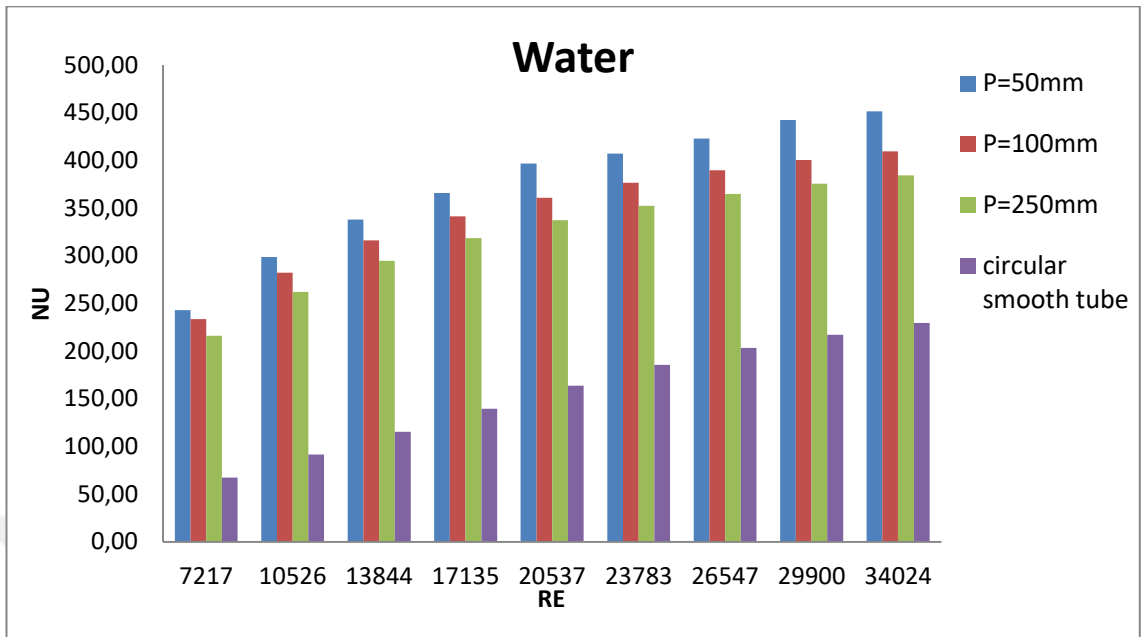


Figure 4.14. Effect of twisted tube modified with the Nusselt number of water in different pitch lengths

4.3.1.2 At the diameter ratio (D1/D2=2) --(40-20mm)

The maximum value of Nu is achieved as 314.59 at Re=32,090 in the pitch length of p=250mm in water fluid, and the minimum value of Nu is found as 55.75 at Re=7,025 in the smooth tube as shown in fig. 4.15.

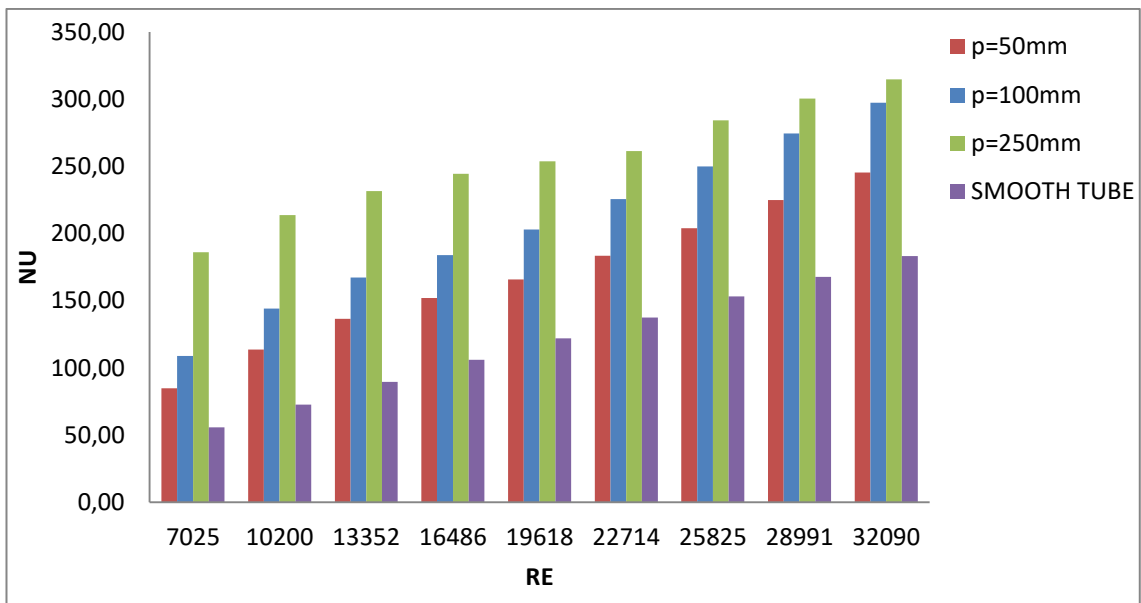


Figure 4.15. Effect of twisted tube modified Nusselt number with Reynolds number of water in D1/D2=2

4.3.2. Effect on heat transfer coefficient (h)

4.3.2.1 At the diameter ratio (D1/D2=1.5) --(33-22mm) The maximum value of *heat transfer coefficient* is found as 7405.4 w/m².K at Re=33,954 in the pitch length p=50mm water fluid, and the minimum value of *h* is calculated as 1255.2 w/m².K at Re=7,179 in the smooth tube as shown in fig. 4.16.

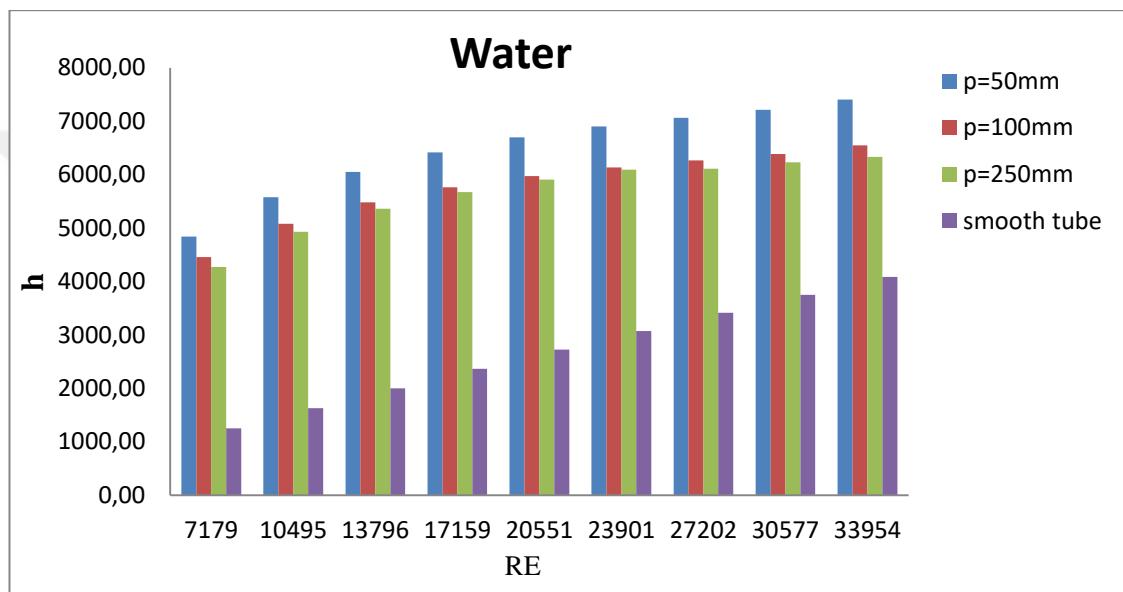


Figure 4.16. Effect of twisted tube modified with heat transfer and Reynolds number of water in D1/D2=1.5

4.3.2.2 At the diameter ratio (D1/D2=2) --(40-20mm)

The maximum value of *heat transfer coefficient* is achieved as 7008.8 w/m².K at Re=32,090 where the pitch length p is 250mm water fluid, and the minimum value of *h* is found as 1255.03 at Re=7,025 in the smooth tube as shown in fig. 4.17.

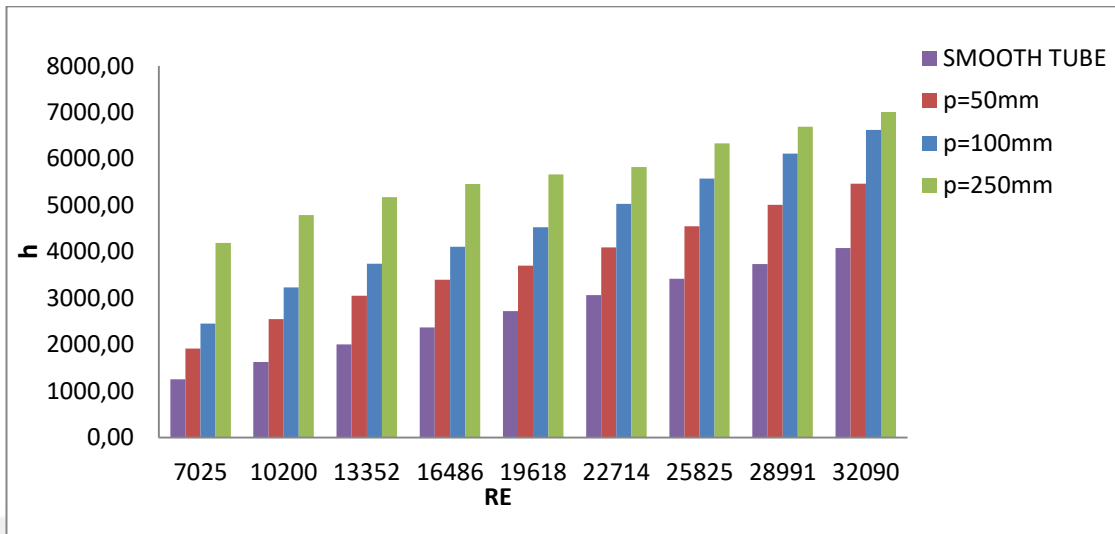


Figure 4.17. Effect of twisted tube modified with heat transfer and Reynolds number of water in $D1/D2=2$

From the upper figures noticed that; the value of heat transfer coefficient will increase with the increasing the number of pitch ratio and thus increasing Reynolds number.

4.3.3 Effect on friction factor (f)

4.3.3.1 At the diameter ratio ($D1/D2=1.5$) --(33-22mm)

The maximum value of f is found as the value of 0.0742 at $Re=7,025$ at pitch diameter is 50mm in the water fluid, and the minimum value of f is calculated as 0.0228 at $Re=32,090$ at the smooth tube as shown in fig. 4.18.

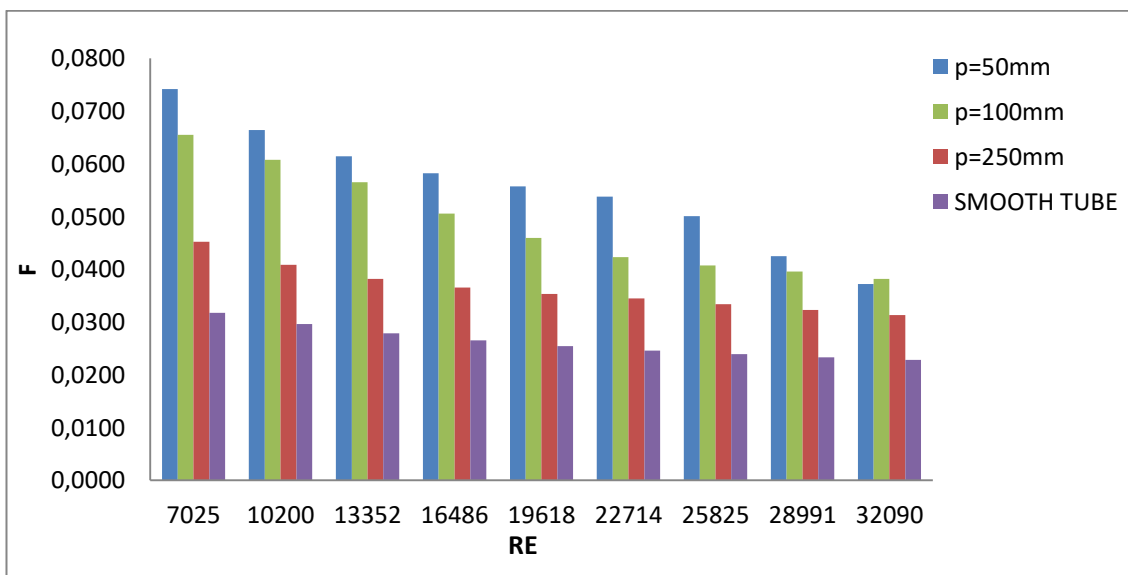


Figure 4.18. Relation between friction factor and Re with different pitch length modified 1.5 ratio

4.3.3.2 At the diameter ratio ($D1/D2=2$) --(40-20mm)

The maximum value of f is found as 0.01339 at $Re=7,179$ at pitch diameter of $p=50mm$ in the water fluid, and the minimum value of f is 0.0232 at $Re=33,954$ at the smooth tube as shown in fig. 4.19.

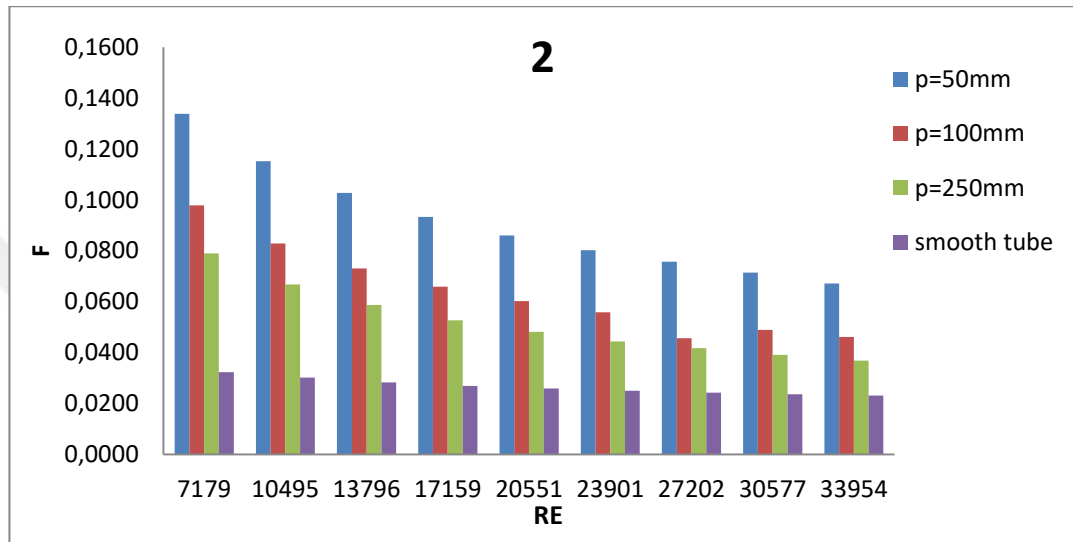


Figure 4.19. Effect of twisted tube modified with the friction factor of water in different diameter ratios (2)

From the figures noticed that; the value of friction factor will decrease with the increasing the number of pitch ratio and thus increasing Reynolds number.

4.3.4 Effect on pressure drop (Δp)

4.3.4.1 At the diameter ratio ($D1/D2=1.5$) --(33-22mm)

Figure 4.22 shows that the maximum value of pressure drop occurs when water as a base fluid at $Re=32,090$ as a value of 952.5 Pa and with pitch length of 50mm modified, while the maximum value was 29.13 Pa when circular smooth tube was used at $Re=7,025$.

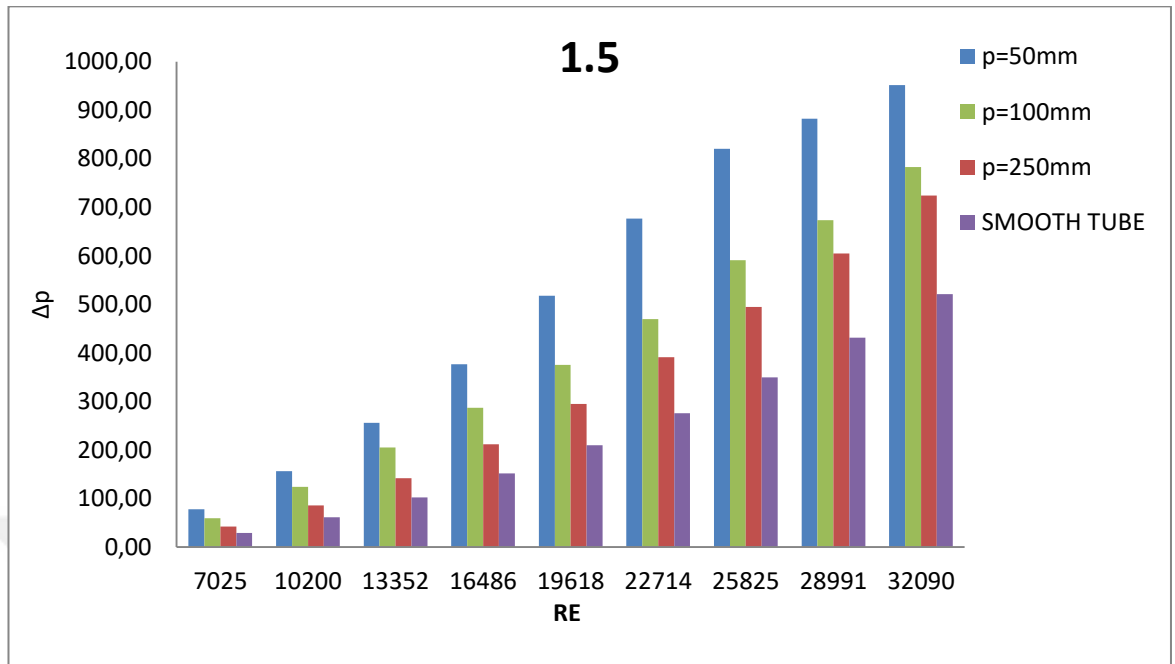


Figure 4.20 Relation between pressure drop and Re with different pitch length modified

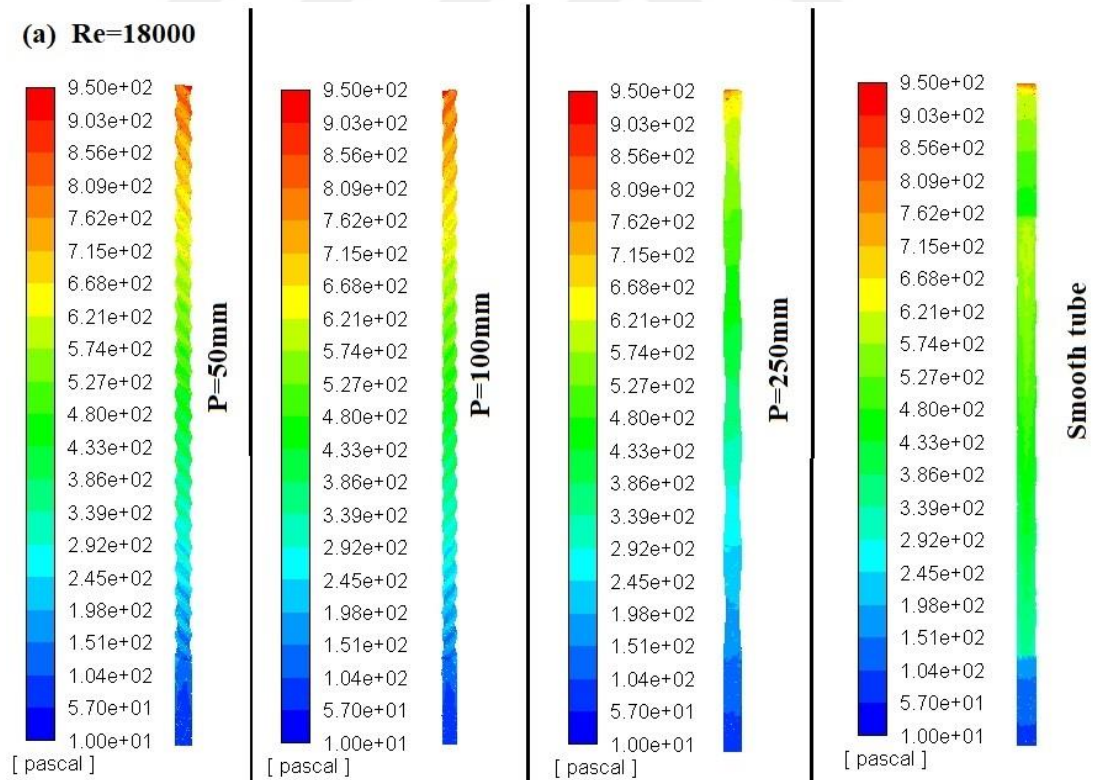


Figure 4.21 Pressure counter for D1/D2=1.5 at Re=18000

4.3.4.2 At the diameter ratio (D1/D2=2) --(40-20mm)

The maximum value of *pressure drop* is obtained as 1917.7 Pa at Re=33,954 at pitch diameter (p) =50mm in the water fluid, and the minimum value of pressure drop value is obtained as 29.71 Pa at Re=7,179 for smooth tube as shown in fig. 4.22.

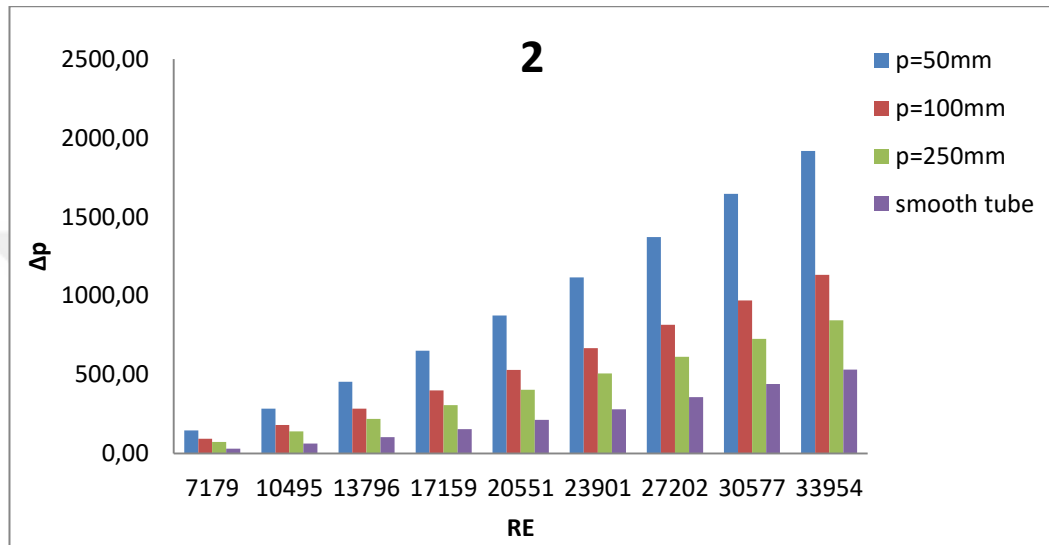


Figure 4.22. Effect of twisted tube modified with the pressure drop and Re of water in different diameter ratios (2)

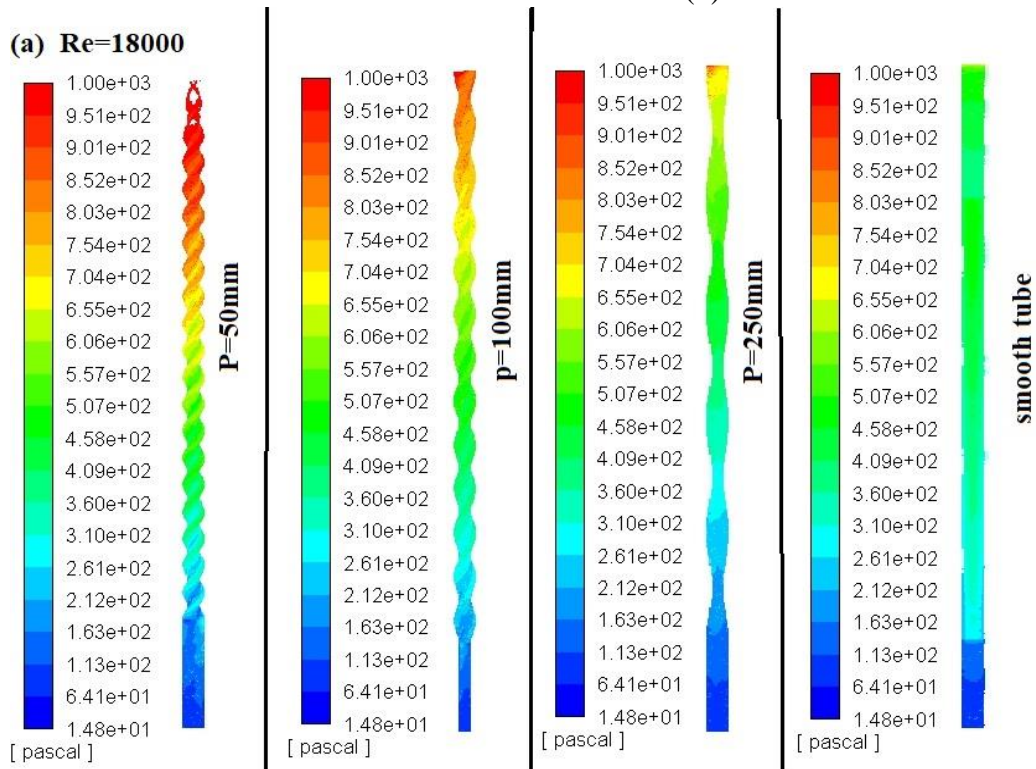


Figure 4.23. Pressure counter for D1/D2=2 at Re= 18000

4.3.5 Performance Evaluation Criteria

4.3.5.1 investigate PEC with elliptical different diameter ratio twisted and smooth tubes in water fluid

4.3.5.1.1 At the diameter ratio ($D1/D2=2$) --(40-20mm)

The maximum value of PEC is found as 1.392 at $Re=7,179$ in the pitch length (p) is 50mm, and the minimum value of PEC is calculated as 1 at all the values of Reynolds number because its water fluid in the smooth tube; The performance of enhancement coefficient (PEC) vs Reynolds number is clearly outlined. That points out that the coefficient of performance enhancement decreased while the pitch ratio increase and thus increasing Reynolds number as shown in fig. 4.24.

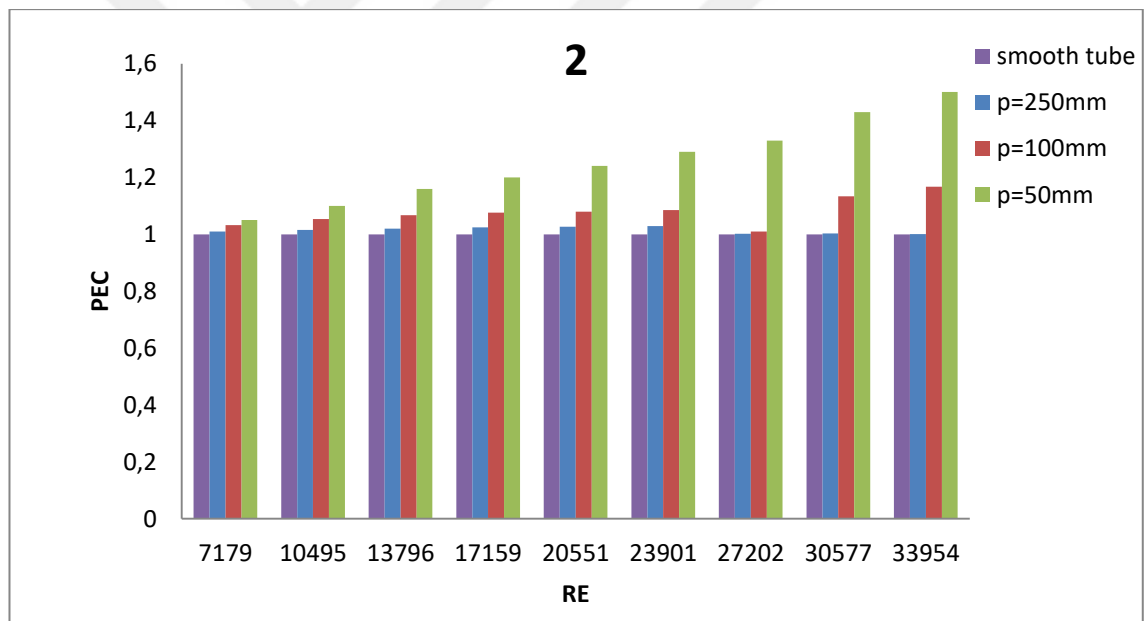


Figure 4.24. The relationship between performance of enhancement coefficient and Reynolds number for water in elliptical of different diameter ($D1/D2=2$)

4.3.5.1.2 At the diameter ratio ($D1/D2=1.5$) --(33-22mm)

The maximum value of PEC is found as 1.52 at $Re=33,954$ in the pitch length (p) is 50mm water fluid, and the minimum value of PEC is 1 for all range of Reynolds number because it base water fluid , as shown in fig. 4.25.

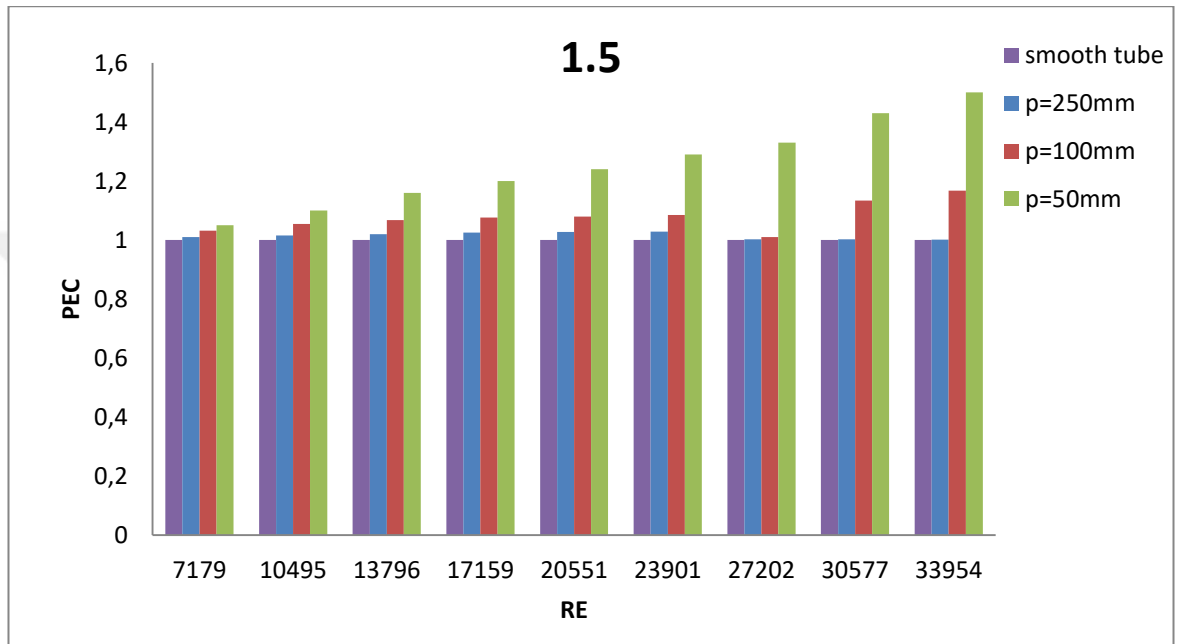


Figure 4.25. The relationship between performance of enhancement coefficient and Reynolds number for water in elliptical of different diameter ($D1/D2=1.5$)

4.4. Investigation of twisted tube modified with Nanofluid CuO-Water

4.4.1. Effect on Nusselt number with twisted tubes modified and smooth tube

Figure 4.26 shows relationship between the Nusselt number and Reynolds number in volume fraction 1% (CuO-water) nano-fluid with different twisted tubes and smooth tube. The maximum value of Nusselt number found as 330.95 at volume fraction at 1% (CuO-Water) nanofluid was used at $Re=34,705$ and with pitch length of 50mm, while the minimum value of Nu number as 55.89 calculated when circular smooth tube was used at $Re=7,349$.

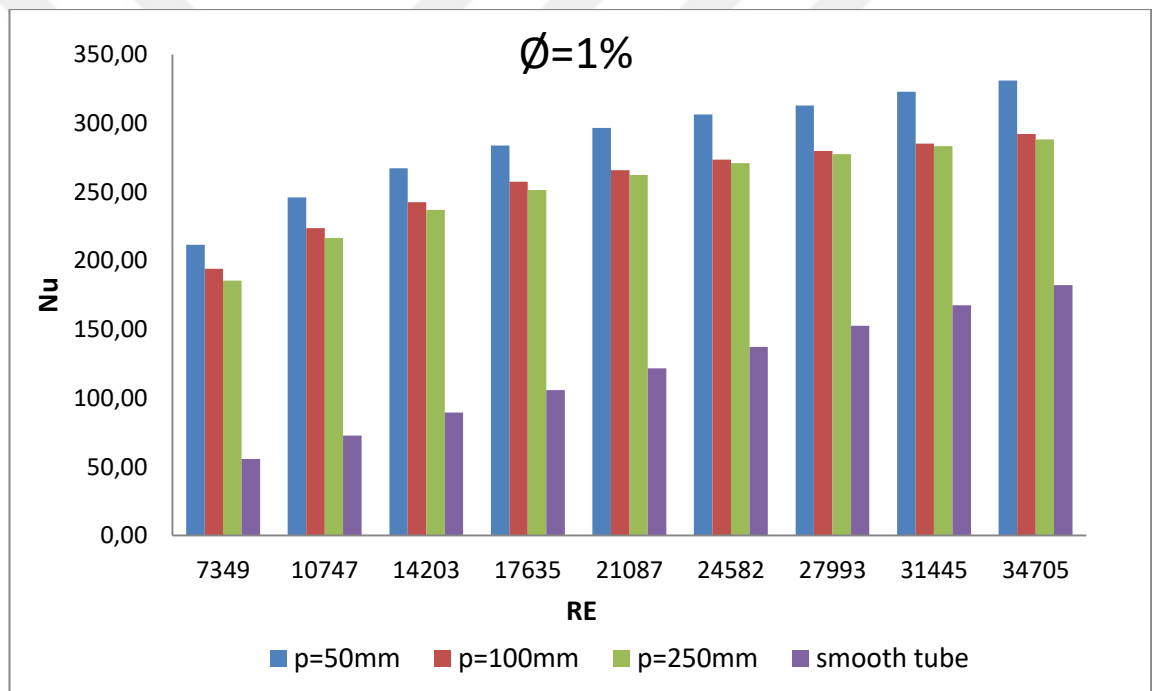


Figure 4.26. The relationship between the Nusselt number and Reynolds number in volume fraction 1% (CuO-water) nano-fluid with different twisted tubes and smooth tube.

Nusselt number result shows increment by using nanoparticles in base fluid and so, the twisted tube with a different diameter pitch ratio (50,100,250mm) and smooth tube was modified, and also supply increase in the value of Nusselt number. Additionally, this change is due to the decrease in the pitch ratio, thus increasing the Reynolds number to the same volume fractions 1%.

4.4.1.1 Effect of heat transfer coefficient (h)

The maximum value of heat transfer coefficient ($8283.71 \text{ w/m}^2 \cdot \text{K}$) is found when volume fraction at 1% (CuO-Water) nanofluid was used at $\text{Re}=34,705$ and with pitch length (50mm) modified and also the minimum value was $1444.75 \text{ w/m}^2 \cdot \text{K}$ when circular smooth tube was used at $\text{Re}=7,349$.

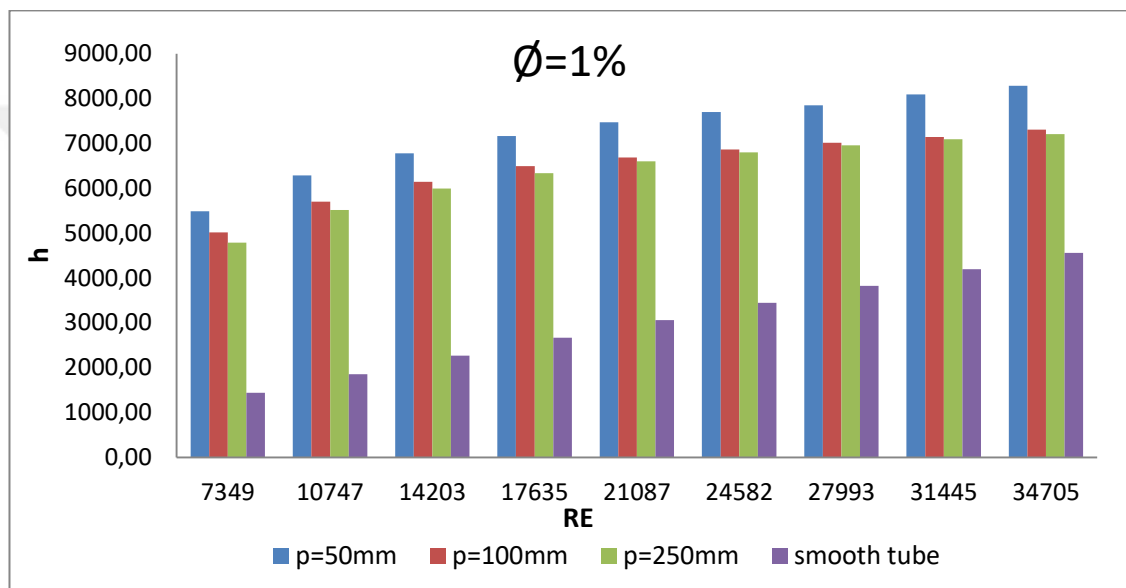


Figure 4.27. The relationship between the convective heat transfer coefficient and Reynolds number in volume fraction 1% (CuO-water) nano-fluid with different twisted tubes and smooth tube.

4.4.1.2 Effect of Nu

From the figure 4.28, the maximum value of Nu is found as 334.42 when (CuO-Water) nanofluid was used for $\text{Re}=36,563$ and with pitch length of 50mm, the minimum value was of Nu number is also calculated as 69.56 when circular smooth tube was used at $\text{Re}=7,133$.

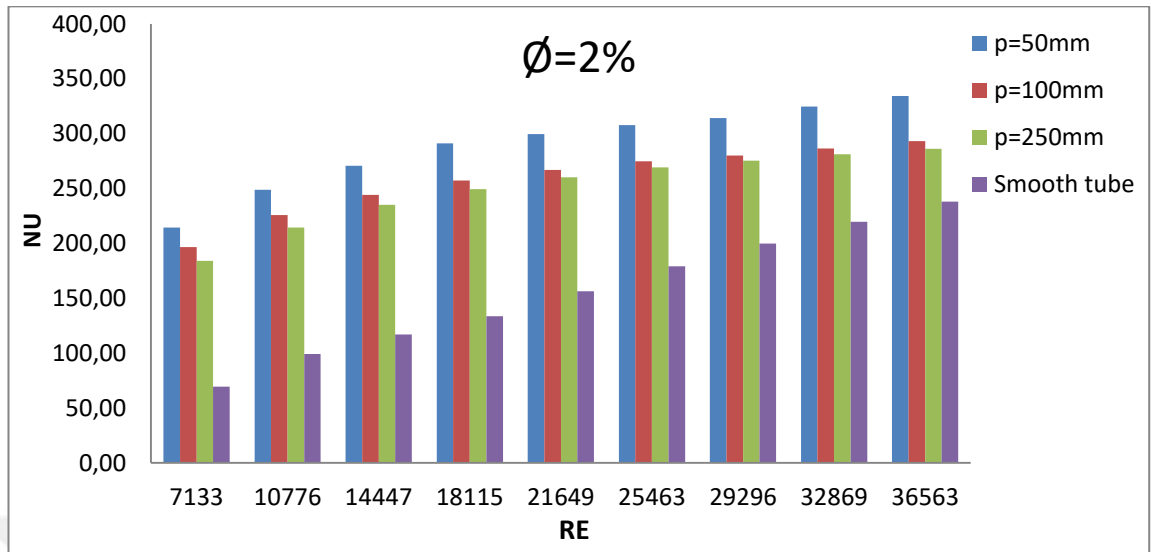


Figure 4.28. The relationship between the Nusselt number and Reynolds number in volume fraction 2% (CuO-water) nano-fluid with different twisted tubes and smooth tube.

4.4.1.3 Effect on heat transfer coefficient (h)

Figure 4.29 shows The relationship between the convective heat transfer coefficient and Reynolds number in volume fraction 1% (CuO-water) nano-fluid with different twisted tubes and also smooth tube. The highest value of heat transfer coefficient is found as 7405.4 $w/m^2 \cdot K$ when volume fraction at 2 % (CuO-Water) nanofluid was used at $Re=33,954$ and with pitch length of 50mm. The minimum value is calculated as 1255.2 $w/m^2 \cdot K$ where circular smooth tube is used at $Re=7,179$.

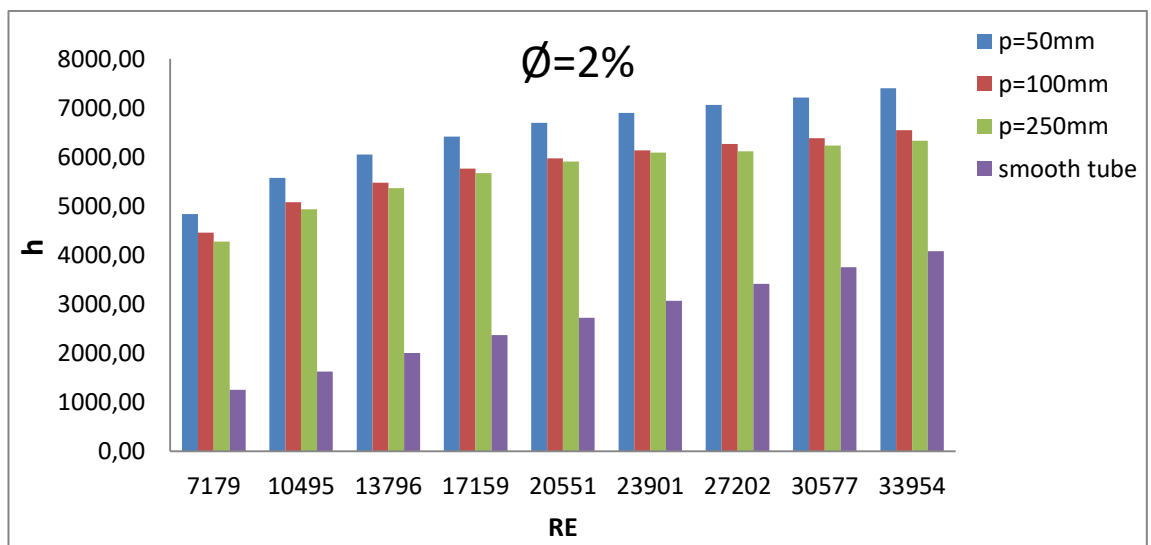


Figure 4.29. The relationship between the convective heat transfer coefficient and Reynolds number in volume fraction 1% (CuO-water) nano-fluid with different twisted tubes and smooth tube.

4.4.1.4 Effect on Nu

The maximum value of Nusselt number is found as 420.21 when volume fraction at 3% (CuO-Water) nanofluid was used at $Re=36,494$ while pitch length is chosen as 50mm as given in fig. 4.30. The lowest value is found as 71.85 when circular smooth tube was used at $Re=7,270$.

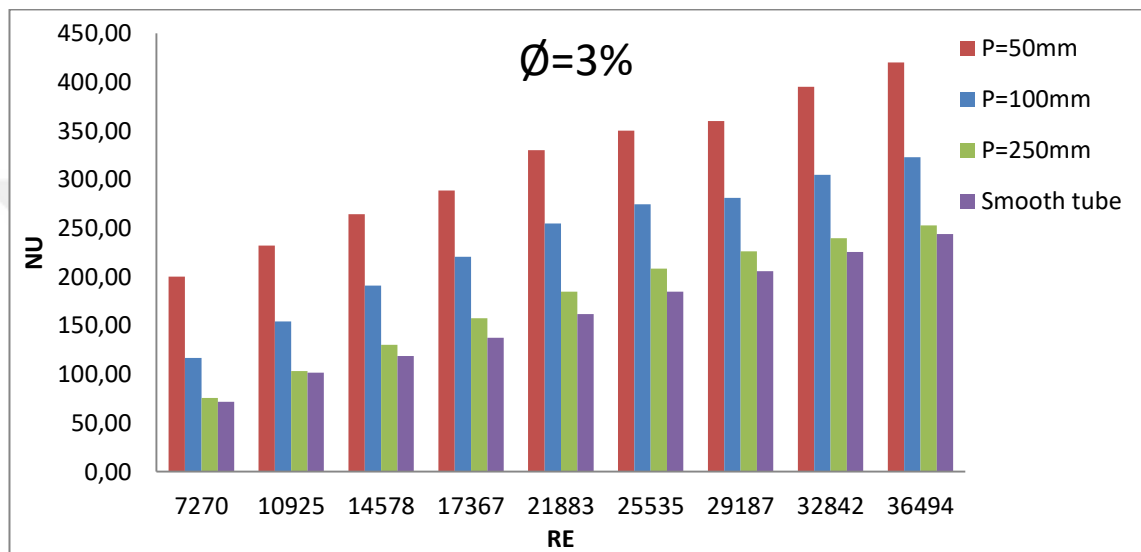


Figure 4.30. The relationship between the Nusselt number and Reynolds number in volume fraction 1% (CuO-water) nano-fluid with different twisted tubes and smooth tube.

4.4.1.5 Effect on heat transfer coefficient (h)

Figure 4.31 shows relationship between the convective heat transfer coefficient and Reynolds number in volume fraction 3% (CuO-water) nano-fluid with different twisted tubes and smooth tube. The maximum value of heat transfer coefficient is obtained as $6487 \text{ w/m}^2 \cdot \text{K}$ when volume fraction at 3 % (CuO-Water) nanofluid was used at $Re=36,494$ and $p=50\text{mm}$ case. The minimum value was $2007.51 \text{ w/m}^2 \cdot \text{K}$ when circular smooth tube was used at $Re=7,270$.

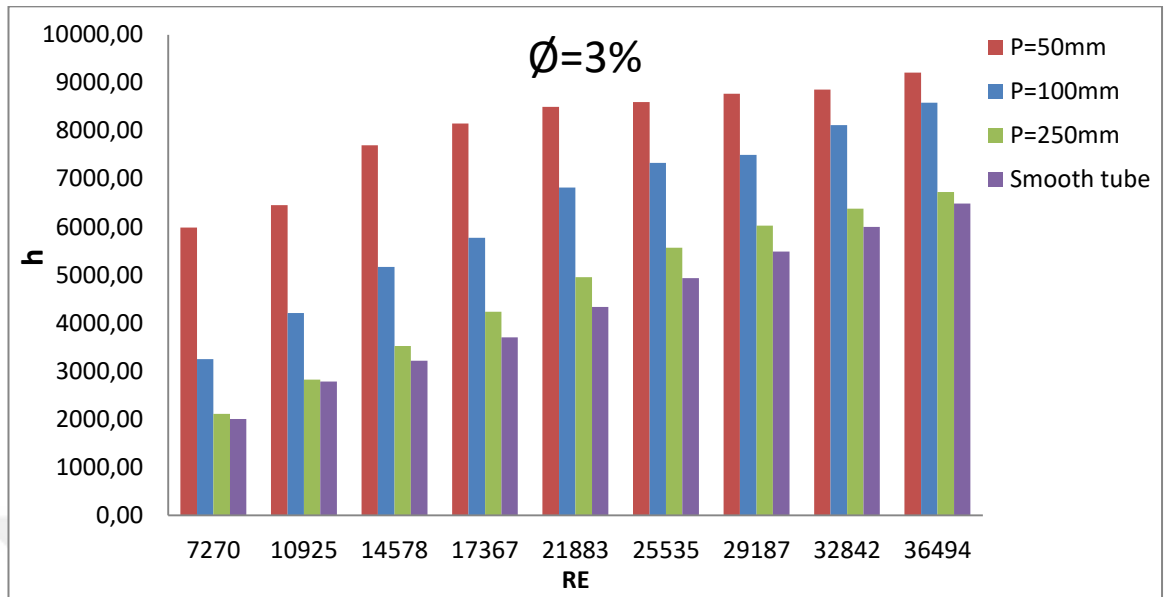


Figure 4.31. The relationship between the convective heat transfer coefficient and Reynolds number in volume fraction 3% (CuO-water) nano-fluid with different twisted tubes and smooth tube.

4.4.1.6 Effect on Nu

The relationship between the Reynolds number and Nu with 4 % volume fraction of nano-fluid in a twisted tube and smooth tube with a different diameter pitch ratio is given in fig. 4.32. The maximum value of Nusselt number is found as 443.76 when volume fraction at 4 % (CuO-Water) nanofluid was used at Re=35,613 and p=50mm. The lowest Nu number is calculated as 74.07 when circular smooth tube was used at Re=7,738.

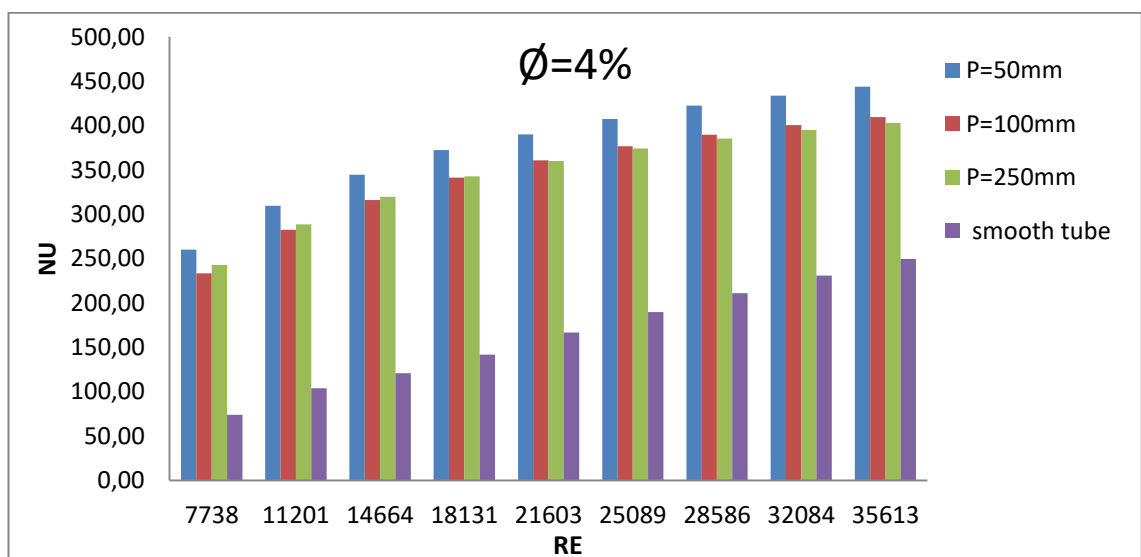


Figure 4.32. The relationship between the Reynolds number and Nu with 4 % volume fraction of nano-fluid in a twisted tube and smooth tube with a different diameter pitch ratio were modified

4.4.1.7 Effect on heat transfer coefficient (h)

Figure 4.33 represent the relationship between the Reynolds number and heat transfer coefficient with 4 % volume fraction of nano-fluid in a twisted tube and smooth tube. The maximum heat transfer coefficient value is found as 12122.9 w/m². K when volume fraction at 4 % (CuO-Water) nanofluid was used at Re=35,613 and p=50 mm case. The lowest h value is found as 2122.31 w/m². K when circular smooth tube was used at Re=7,738.

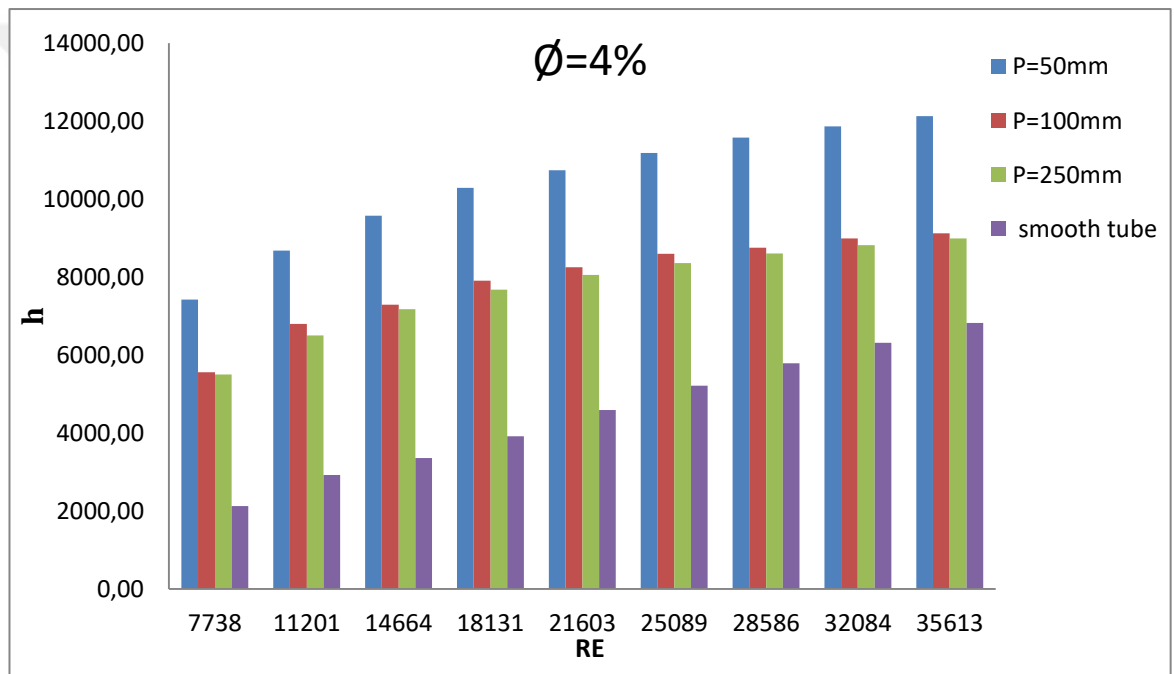


Figure 4.33. The relationship between the Reynolds number and heat transfer coefficient with 4 % volume fraction of nano-fluid in a twisted tube and smooth tube .

4.4.2. The friction factor

Figure 4.34 shows the relationship between the friction factor and Reynolds number with $\varphi = 1\%$ of nano-fluid in a twisted tube and smooth tube. The maximum value of friction factor (0.1352) is obtained when volume fraction at 1 % (CuO-Water) nanofluid was used at $Re=34,705$ and $p=50mm$. The minimum value (0.026) was found when circular smooth tube was used at $Re=7,349$.

From figure, it is pointed out that, the nano fluid had no effect on the friction factor but when modified the twisted tube the friction factor will increase significantly. When the pitch ratio in twisted tube decrease, the friction factor value will be increase.

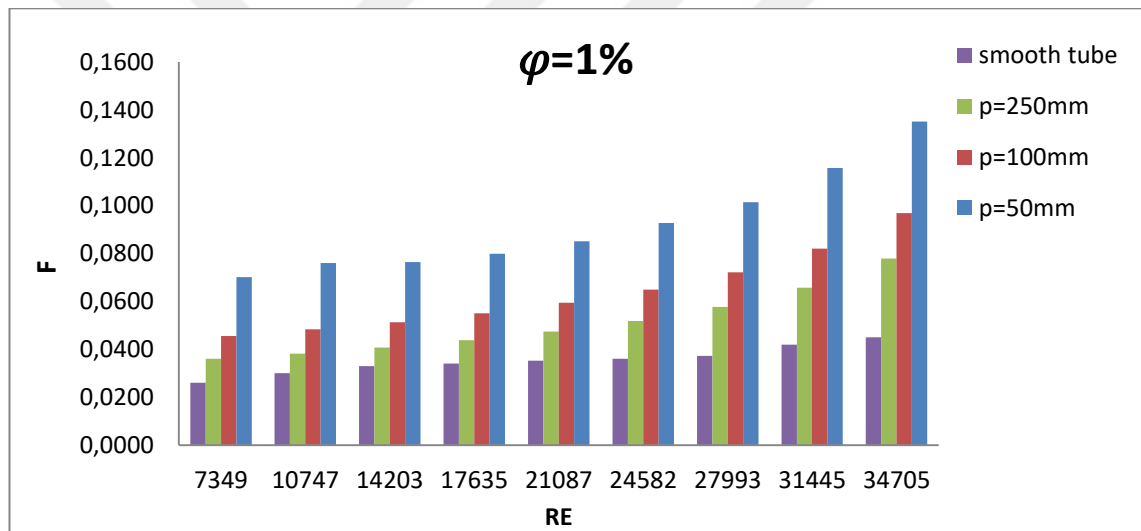


Figure 4.34. The relationship between the friction factor and Reynolds number with $\varphi = 1\%$ of nano-fluid in a twisted tube and smooth tube

4.4.2.1 Effect on (Δp)

From the fig. 4.35, it is shown that the maximum value of *pressure drop* (2126.5 Pa) is calculated at 1% (CuO-Water) nanofluid concentration is used in base fluid case at $Re=34,705$ and $p=50mm$. The lowest value of is found as 31.18 Pa while circular smooth tube was used at $Re=7,349$.

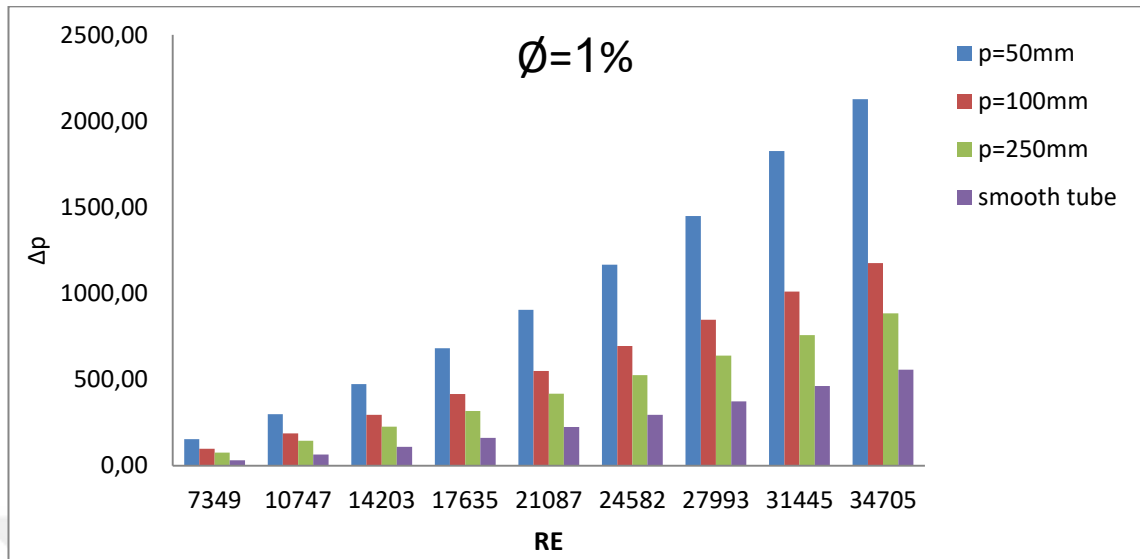


Figure 4.35. Relationship between pressure drop and Re and $\phi=1\%$ with a twisted tube and smooth tube

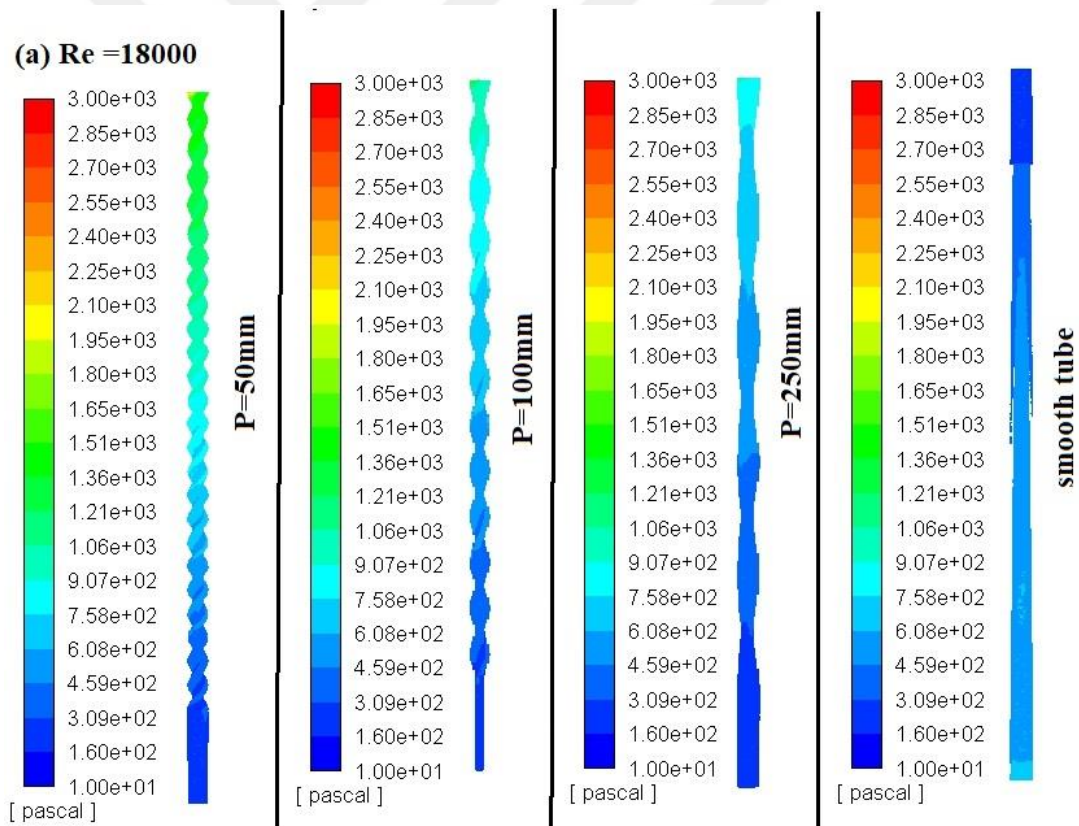


Figure 4.36. Comparison of *total pressure* counters between smooth tube and different pitch length (50,100,250mm) with volumetric concentration= $\phi=1\%$ CuO-water nanofluent at Re=18000

4.4.3 The friction factor

The relationship between friction factor and the Re with $\phi = 2\%$ with a twisted tube and smooth tube is given in fig. 4.37. The highest value of *friction factor* (0.1445) is obtained while (CuO-Water) nanofluent fraction ratio is used at Re=36,563 and pitch length is 50

mm. The lowest friction factor occurs as 0.0273 while circular smooth tube was used case at $Re=7,133$.

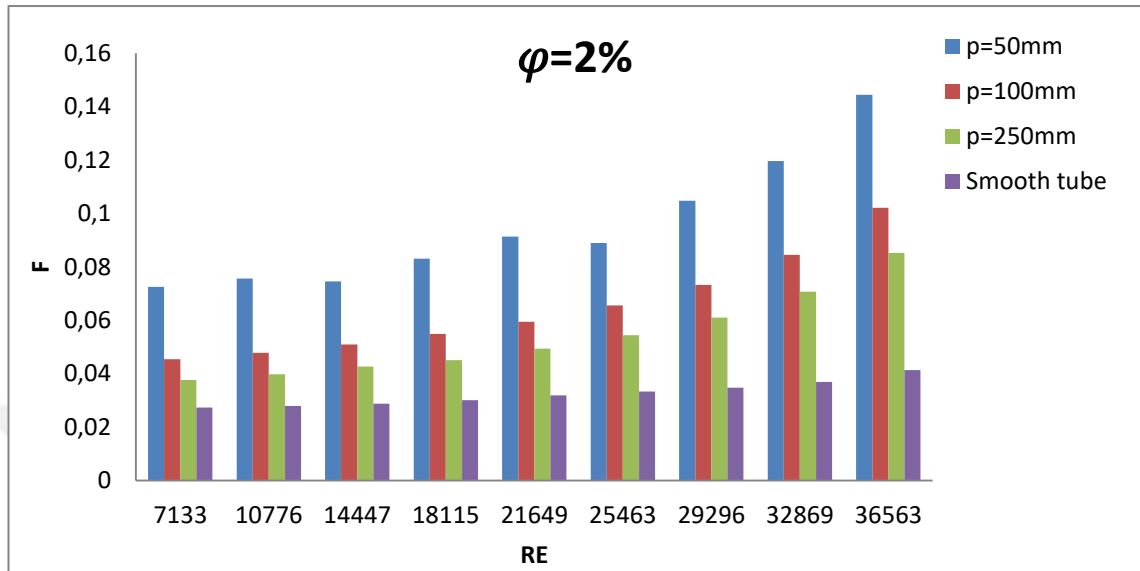


Figure 4.37. The relationship between friction factor and the Re with $\phi = 2\%$ with a twisted tube and smooth tube

4.4.3.1 Effect on pressure drop (Δp)

The relationship between pressure drop the Re number is given in fig. 4.38. The maximum value of *pressure drop* (2260.5 Pa) is calculated at 2% of nanofluid fraction ratio case at $Re=36,563$ and $p=50mm$. The minimum value (40.67 Pa) occurs when circular smooth tube was used at $Re=7,133$.

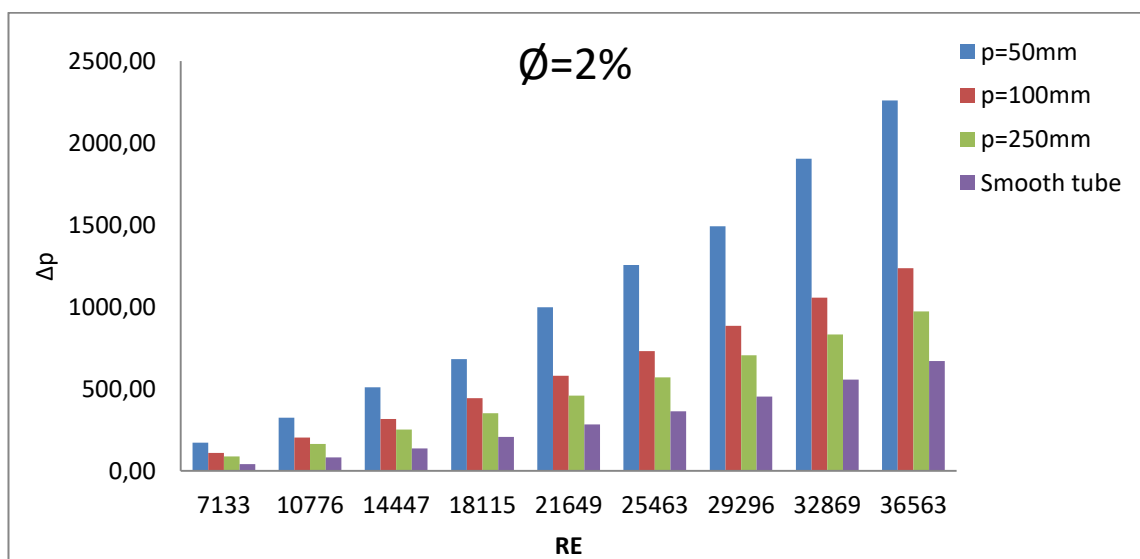


Figure 4.38. The relationship between pressure drop the Re and with $\phi = 2\%$ with a twisted tube and smooth tube

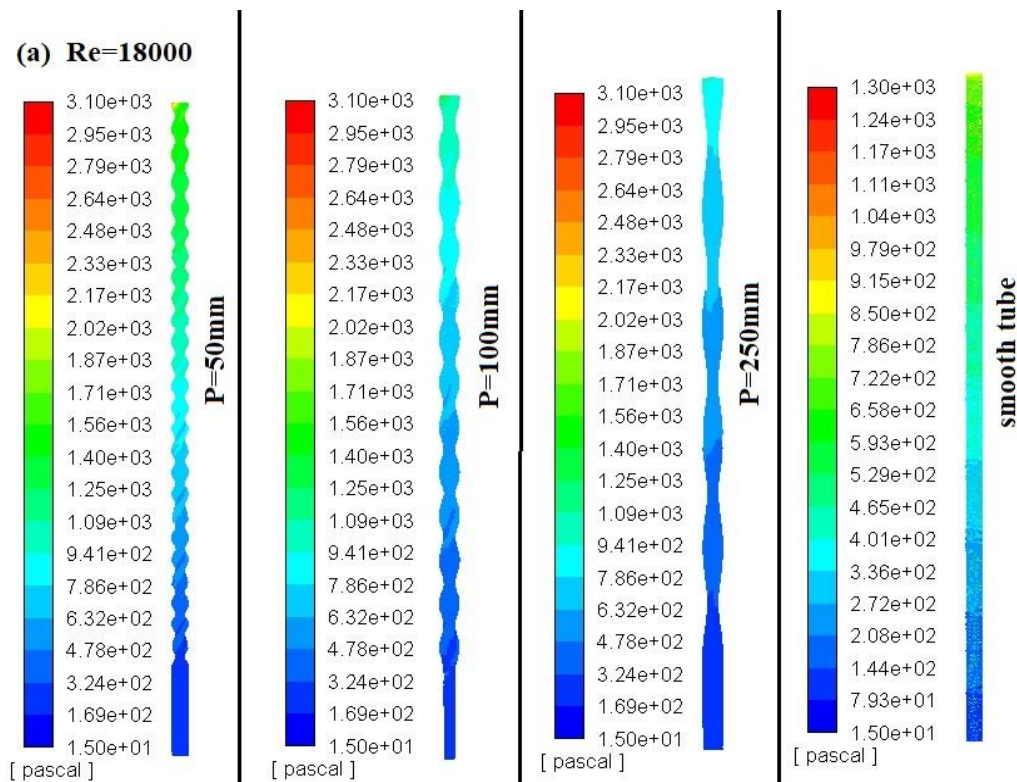


Figure 4.39. Comparison of total pressure counters between smooth tube and different pitch length (50,100,250mm) with volumetric concentration= $\phi=2\%$ CuO-water nanofluent observed at $Re=18000$.

4.4.3.2 Effect on friction factor

Fig. 4.40 shows relationship between the Reynolds number and friction factor with $\phi = 3\%$ of fraction . The highest value of *friction factor* at 3% (CuO-Water) nanofluent is found as 0.1285 at Reynolds number of=36,494 and $p=50\text{mm}$. The lowest value (0.0269) is found when circular smooth tube was used at $Re=7,270$.

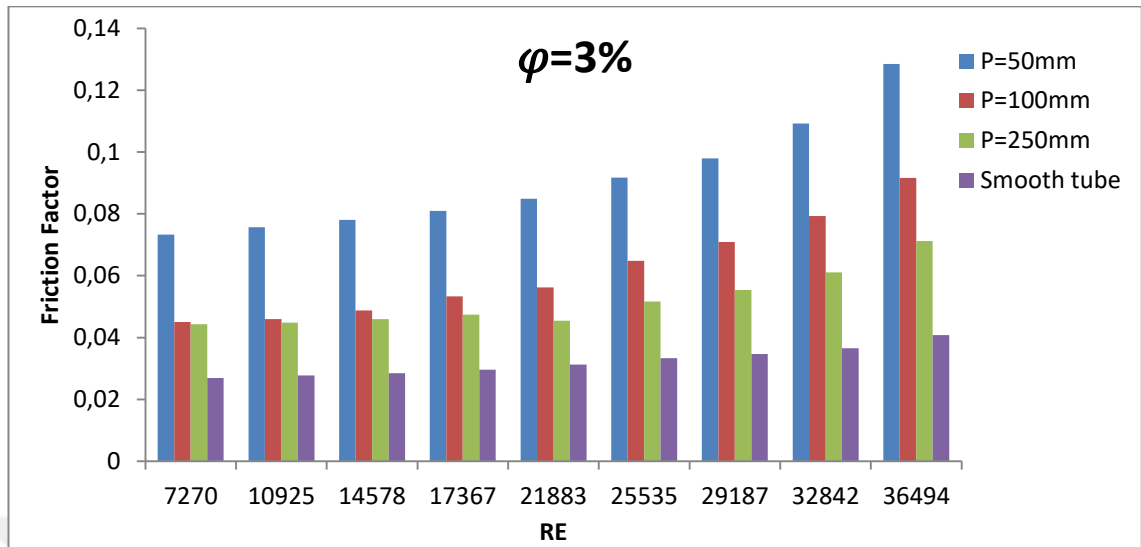


Figure 4.40. The relationship between the Reynolds number and friction factor with $\phi = 3\%$ with a twisted tube and smooth tube

4.4.3.3 Effect on pressure drop (Δp) with volume fraction $\phi=3\%$

Relation between pressure drop and Re with $\phi=3\%$ is presented in fig. 4.41. The maximum value of *pressure drop* at 3% (CuO-Water) nanofluid is calculated as 2121.2 Pa at Re=34,168 and p=50mm. The minimum value was (29.34 Pa) is obtained when circular smooth tube was used at Re=7,218.

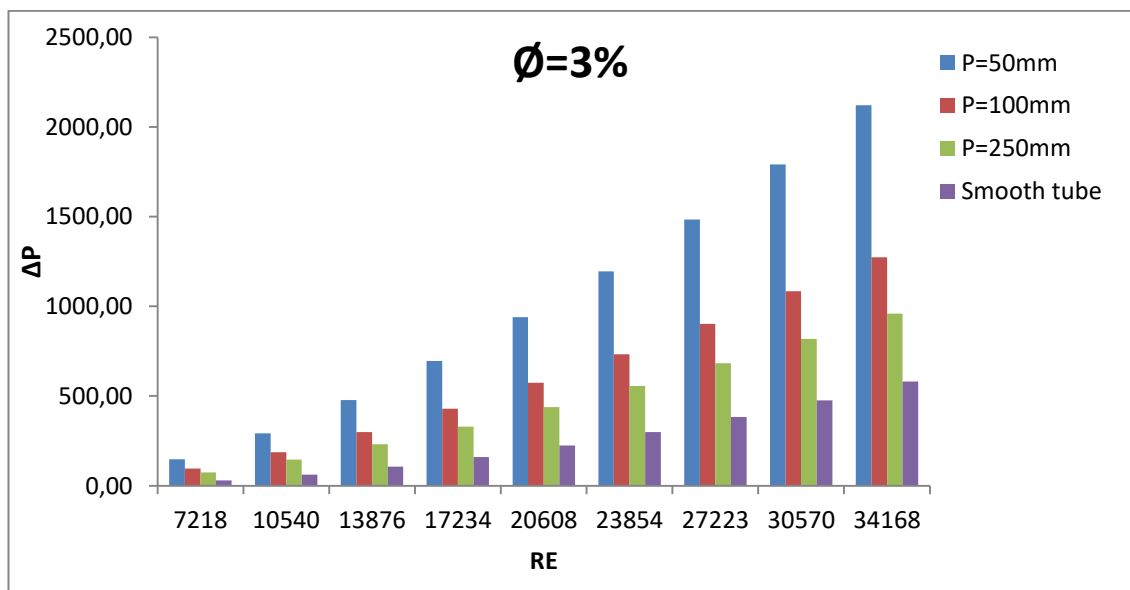


Figure 4.41. Relation between pressure drop and Re with $\phi=3\%$ with a twisted tube and smooth tube

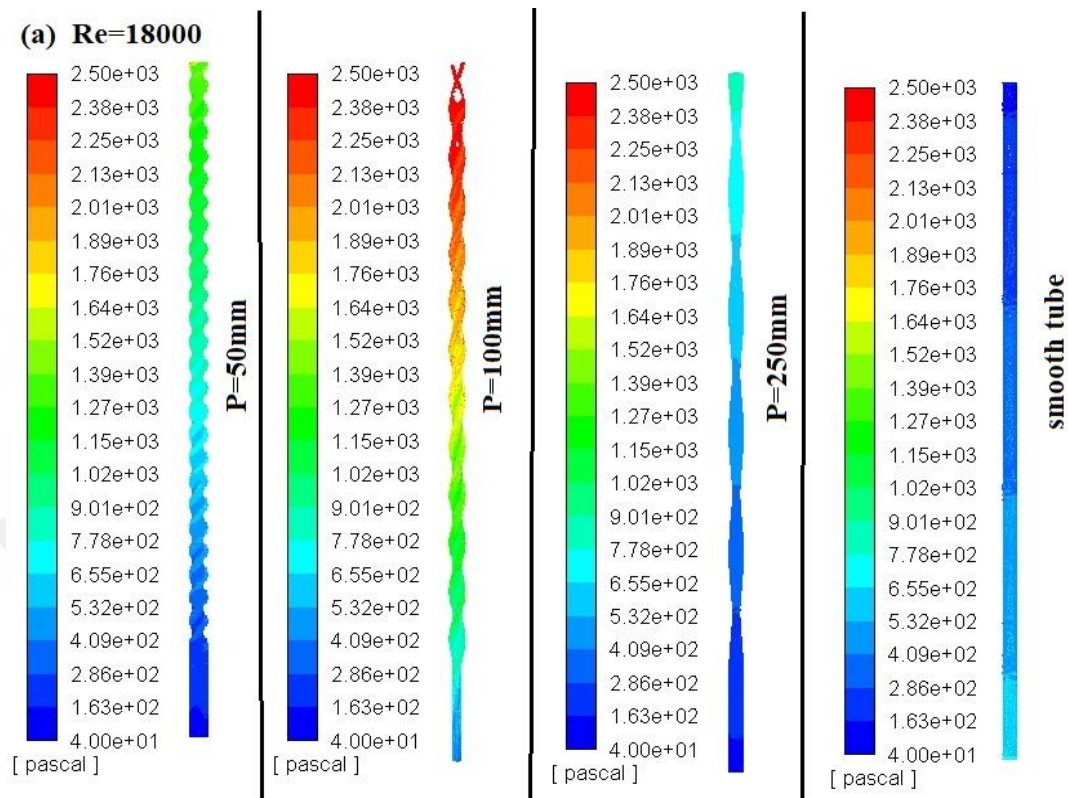


Figure 4.42. Total pressure counters between smooth tube and different pitch length (50,100,250mm) with volumetric concentration= $\phi=3\%$ CuO-water nanofluid observed at $Re=18000$.

4.4.3.4 Effect on friction factor

Figure 4.43 present the relationship between the Reynolds number and friction factor with a twisted tube and smooth tube. Highest *friction factor* value is found as 0.1778 at 4 % (CuO-Water) nanofluid used case at $Re=35,613$ and pitch length of 50mm. Lowest *friction factor* value is found as 0.0266 when circular smooth tube was used at $Re=7,738$.

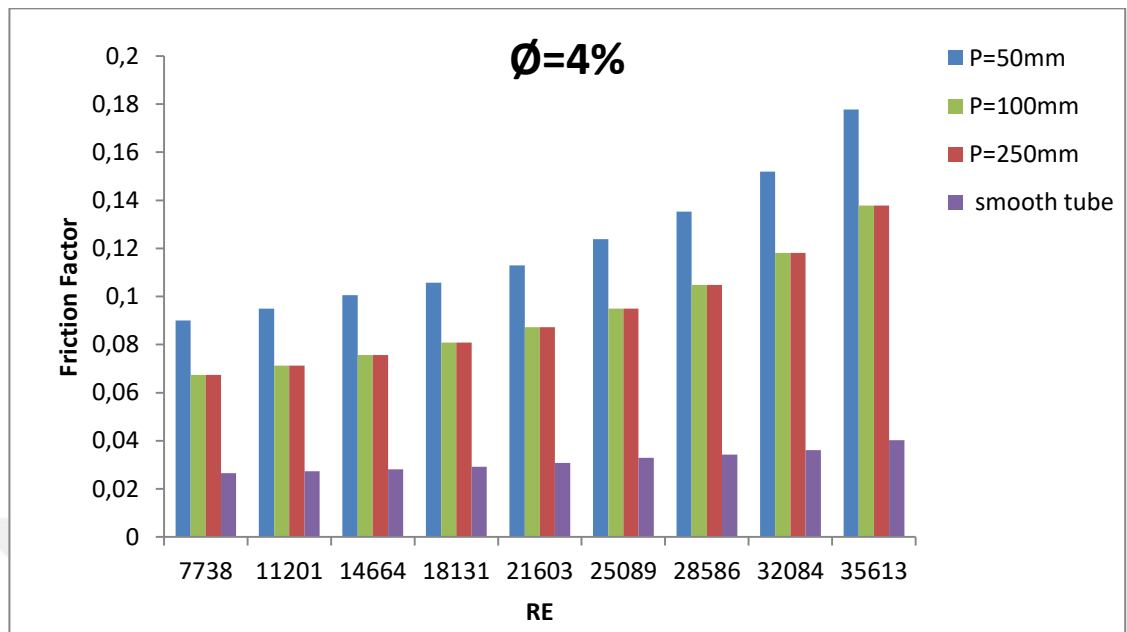


Figure 4.43. The relationship between the Reynolds number and friction factor with a twisted tube and smooth tube

4.4.3.5 Effect on pressure drop (Δp)

Pressure drop versus Reynolds number is presented in fig. 4.44. The maximum amount of pressure drop (2782.8 Pa) occurs at 4% (CuO-Water) nanofluid fraction at $Re=35,613$ and pitch length of 50 mm. The lowest pressure drop obtained as 43.37 Pa at circular smooth tube used case at $Re=7,738$.

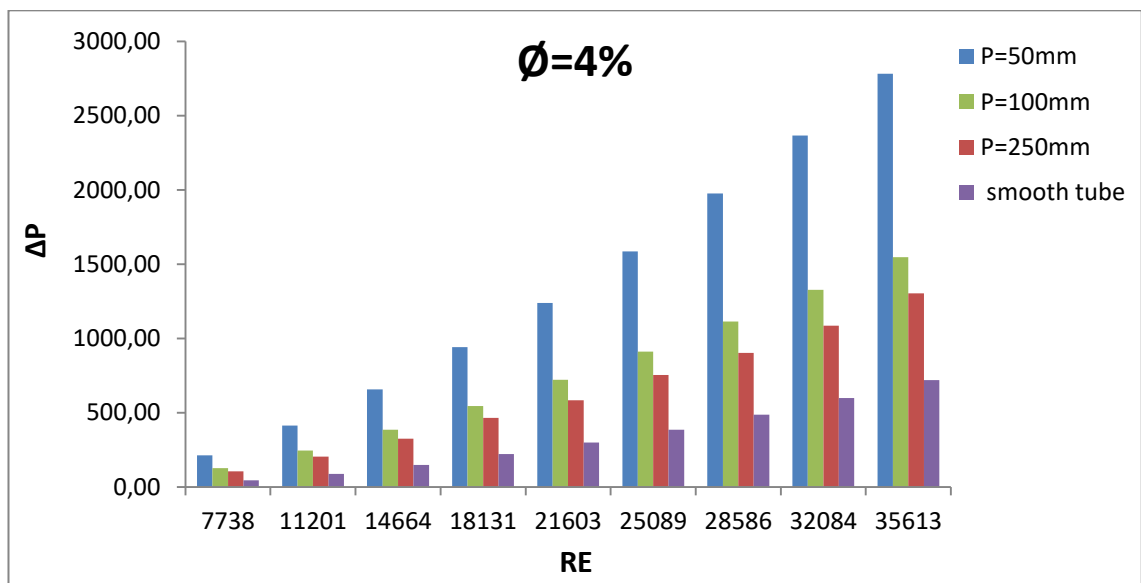


Figure 4.44. Relationship between pressure drop and Re with a twisted tube and smooth tube modified.

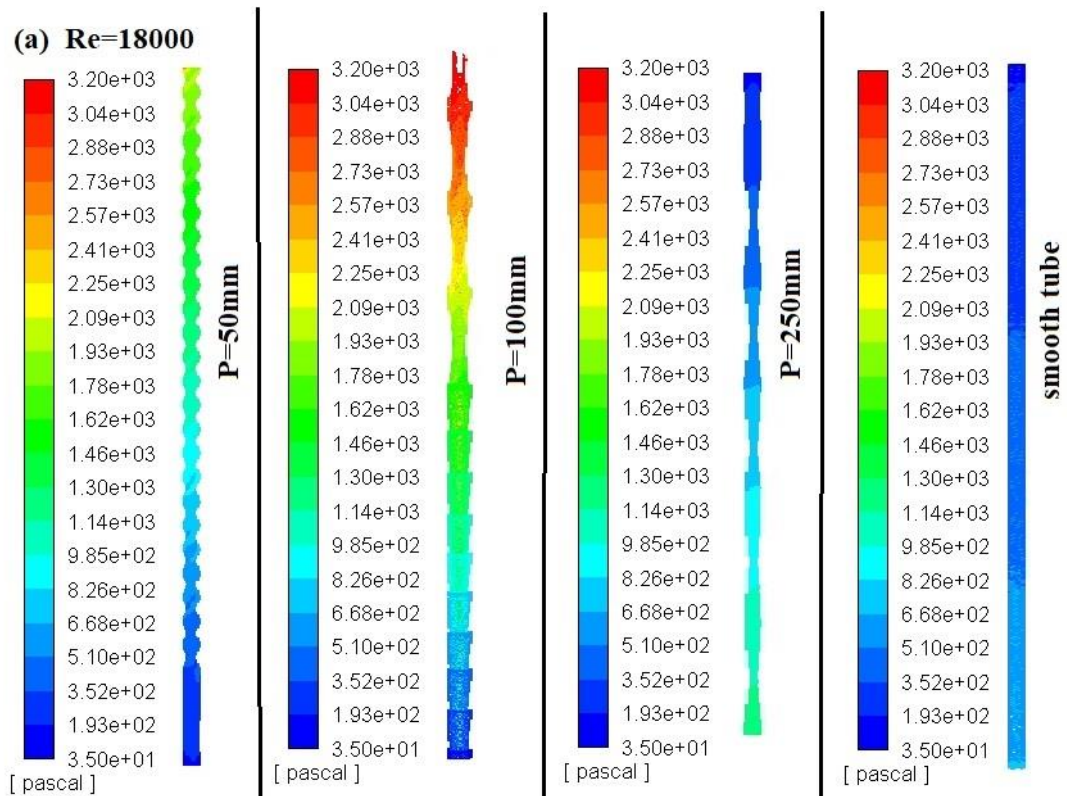


Figure 4.45. Total pressure counters between smooth tube and different pitch length (50,100,250mm) with volumetric concentration= $\phi=4\%$ CuO-water nanofluid observed at $Re=18000$

4.4.4 Thermo-Hydraulic Performance factor (THP) or performance evaluation criteria (PEC)

The coefficient of PEC and the effect of CuO and water contains on thermo-hydraulic performance factor respecting to the nanofluid to the ratio of four volume fractions (1 %, 2%, 3 %, and 4%) and water fluid.

PEC versus Reynolds number for different twisted tube is given in fig.4.46. The maximum value of PEC is achieved as 2.457 at $Re=34,024$ and $p=50$ mm, while the minimum value (1.0) at circular smooth tube is calculated at $Re=7,217$.

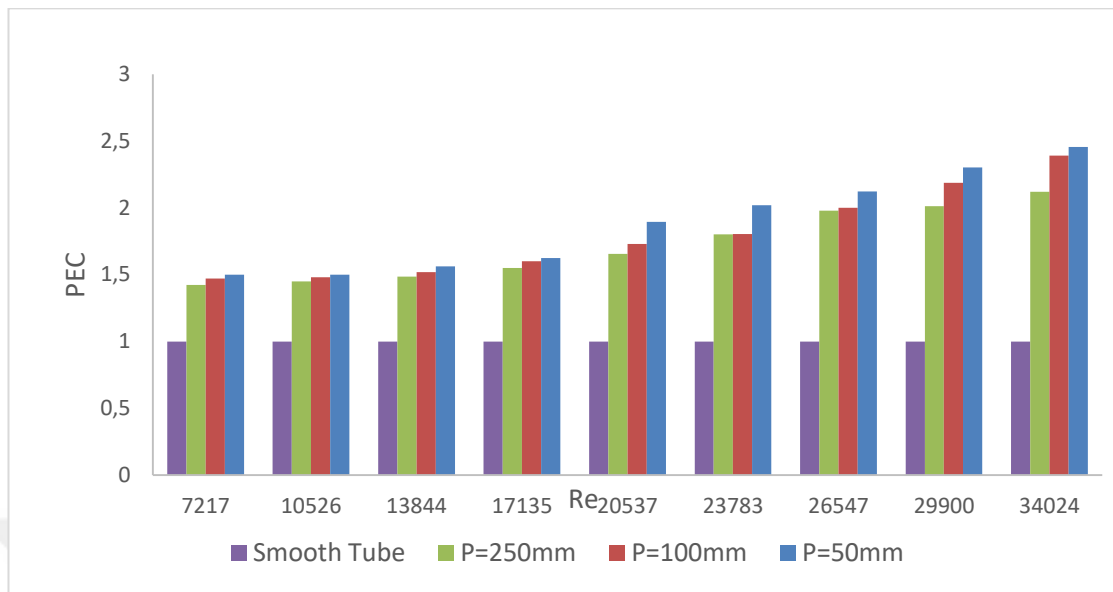


Figure 4.46. The coefficient of performance enhancement with water fluid in the twisted tube and smooth tube was modified

4.4.5 Investigation of (PEC) performance evaluation criteria with (CuO-Water) Nanofluid inserted

4.4.5.1 PEC with volume fraction $\phi=1\%$

From the fig. 4.47, highest amount of PEC value (2.21) obtained while the $p=50$ mm twisted tube used case at $Re=33,039$ and pitch length (50 mm) and the lowest one is also obtained at circular smooth tube.

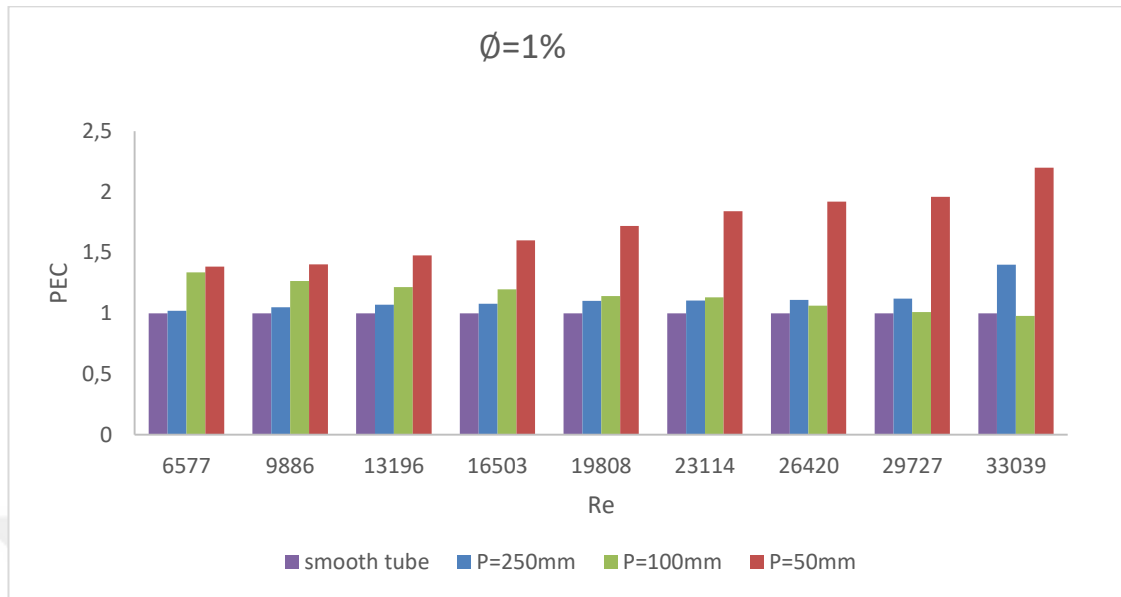


Figure 4.47. The relation between performance enhancement and Reynolds number for Nano fluid with volume concentration of 1%.

4.4.5.2 PEC with volume fraction $\phi=2\%$

Fig. 4.48 shows relation between performance enhancement coefficient and Reynolds number for $\phi=2\%$ nanofluid used cases for different pitch ratios. The highest PEC value is found as 2.2706 at $Re=34,700$ and pitch length of 50 mm. The minimum value occurs at circular smooth tube as expected.

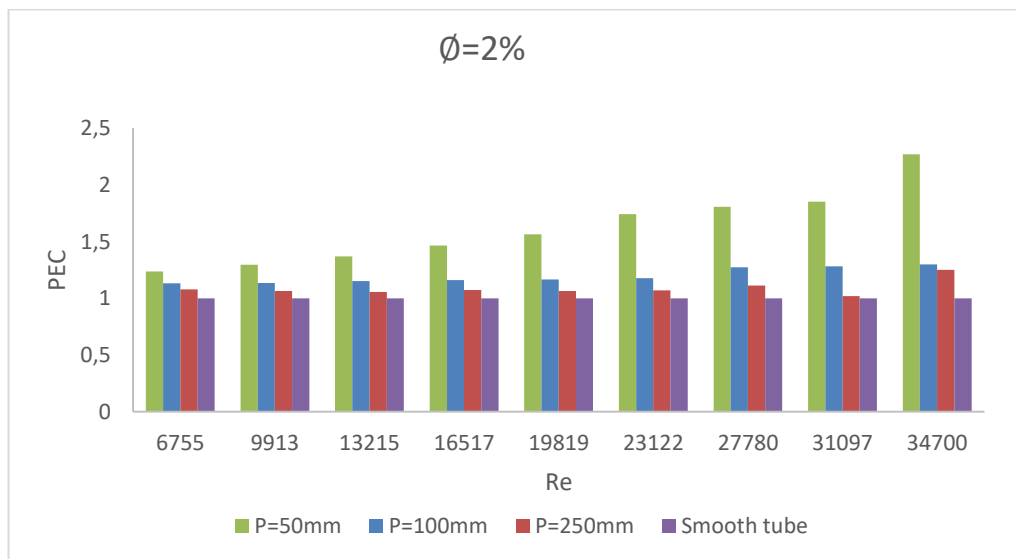


Figure 4.48. The relation between performance enhancement and Reynolds number $\phi=2\%$ nanofluid with inserted different pitch ratios

4.4.5.3 PEC with volume fraction $\phi=3\%$

From the fig. 4.49, the maximum value of *PEC* (2.28514) is found at Reynolds number of 36,494 and pitch length of 50 mm. The minimum value of *PEC* number is calculated while circular smooth tube was used for all range of Reynolds number.

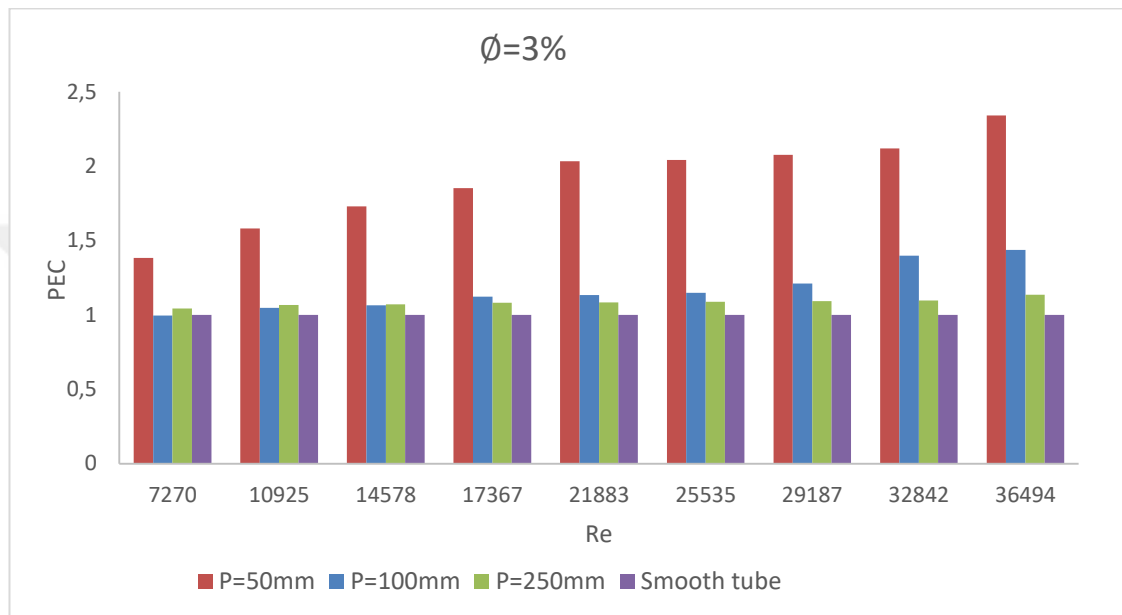


Figure 4.49. The relation between performance enhancement and Reynolds number with nano fluid at volume concentration of 3% with inserted different pitch ratios.

4.4.5.4 PEC with volume fraction $\phi=4\%$

Figure 4.50 indicates the relation between performance evaluation criteria and Reynolds number for Nano fluid with volume concentration of 4 % with inserted different pitch ratios. The highest *PEC* value (2.4045) is achieved at $Re=35,613$ and $p=50$ mm, while the minimum *PEC* value occurs at circular smooth tube used cases for all range of Reynolds numbers.

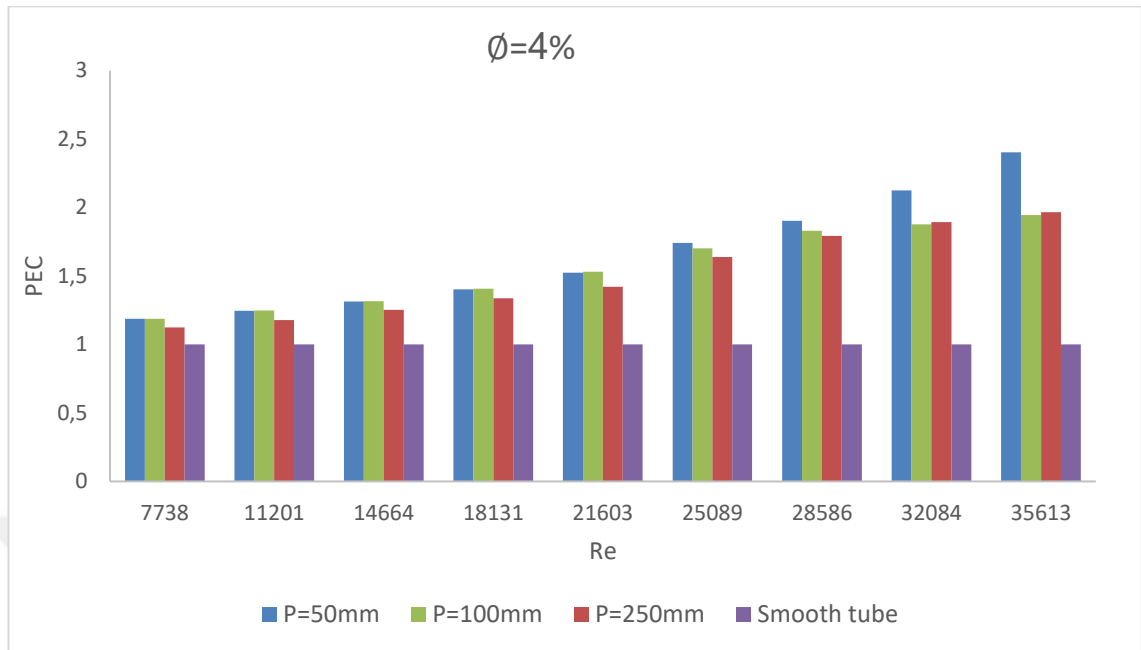


Figure 4.50. The relation between performance evaluation criteria and Reynolds number for Nano fluid with volume concentration of 4 % with inserted different pitch ratios

4.4.6 The Performance enhancement coefficient (η)

The analysis of performance evaluation is already listed through in the chapter 3 at section (3.2.11) eq.(2-4-B). The values of the analysis of performance evaluation increased when the (50mm, 100mm, 250mm) water or nanofluids were injected from the twisted tubes and taken from the reported values.

4.4.6.1 η with volume fraction $\phi=1\%$

The relation between performance enhancement coefficient and Reynolds number for Nano fluid with volume concentration $\phi=1\%$ case presented in fig. 4.51. The highest (2.2) and lowest (1) value of performance enhancement coefficient is found at the case which $Re=31,059$ and pitch length is 50 mm and which the case where circular smooth tube was used for all range of Re numbers.

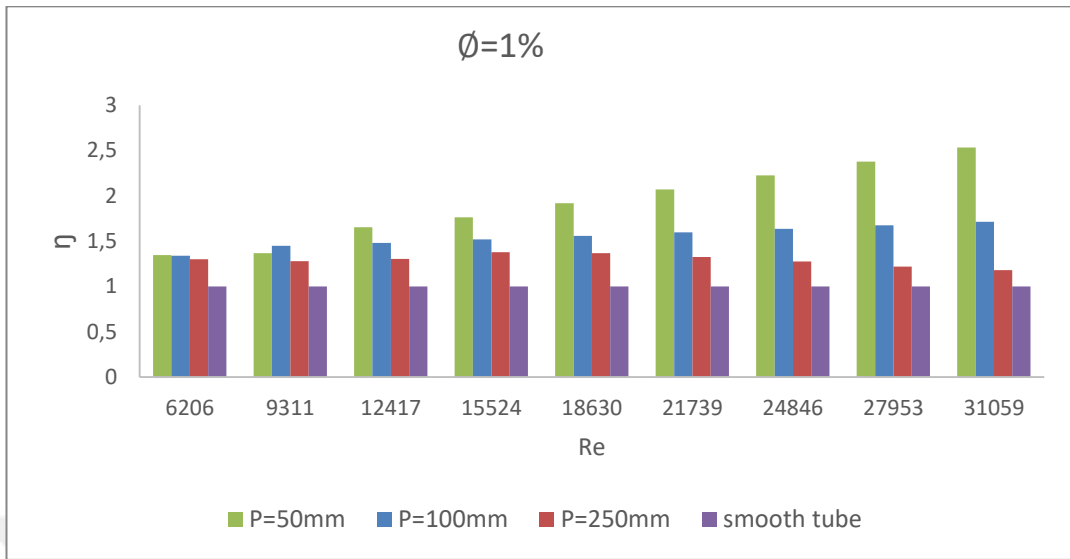


Figure 4.51. The effect of performance evaluation analysis and Reynolds number for Nano fluid with volume concentration at $\phi=1\%$

4.4.6.2 η with volume fraction $\phi=2\%$

Fig. 4.52 presents the relation between η and Re numbers for different twisted tubes. The maximum value of η (2.642) is achieved during $p=50$ mm twisted tube used case at $Re=34,699$. The minimum value of η (1) is found at circular smooth tube used cases.

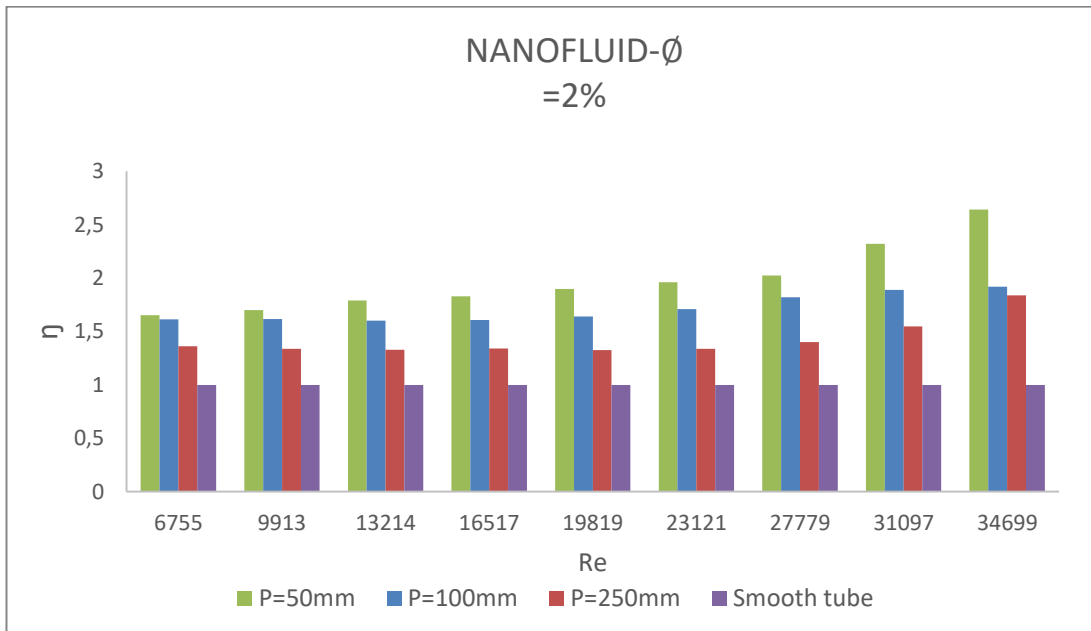


Figure 4.52. The effect of performance evaluation analysis and Reynolds number into the nano fluid with volume fraction at $\phi=2\%$ with modified different pitch ratios.

4.4.6.3 η with volume fraction $\phi=3\%$

The variation between performance evaluation analysis and Reynolds number for Nano fluid with volume concentration at $\phi=3\%$ is presented in Fig. 4.53. Highest η values found as 2.764 for $Re=36,494$ and $p=50\text{ mm}$. The lowest η values also found at which the case circular smooth tube was used.

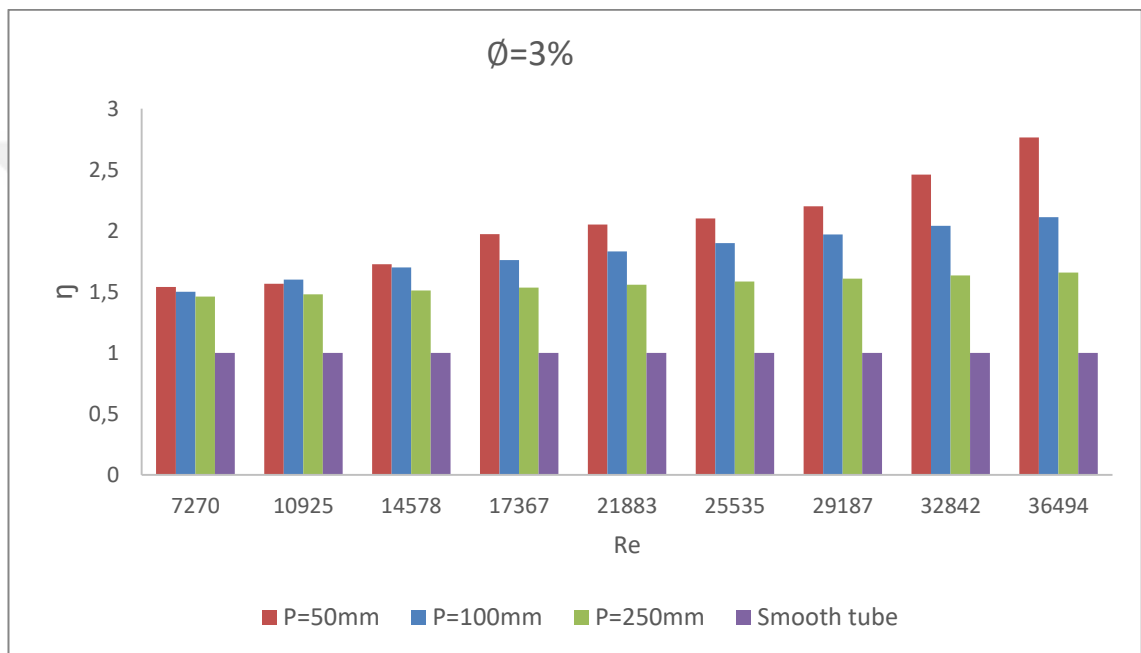


Figure 4.53. The effect of performance evaluation analysis and Reynolds number for Nano fluid with volume concentration at $\phi=3\%$ with modified different pitch ratios

4.4.6.4 η with volume fraction $\phi=4\%$

The relation between η and Re numbers is given in fig. 4.54 for at $\phi=4\%$ cases fluid for all investigated twisted tubes. The maximum value of η (3.624) is found at $Re=35,613$ and pitch length of 50 mm. The lowest η value is also obtained while circular smooth tube was used.

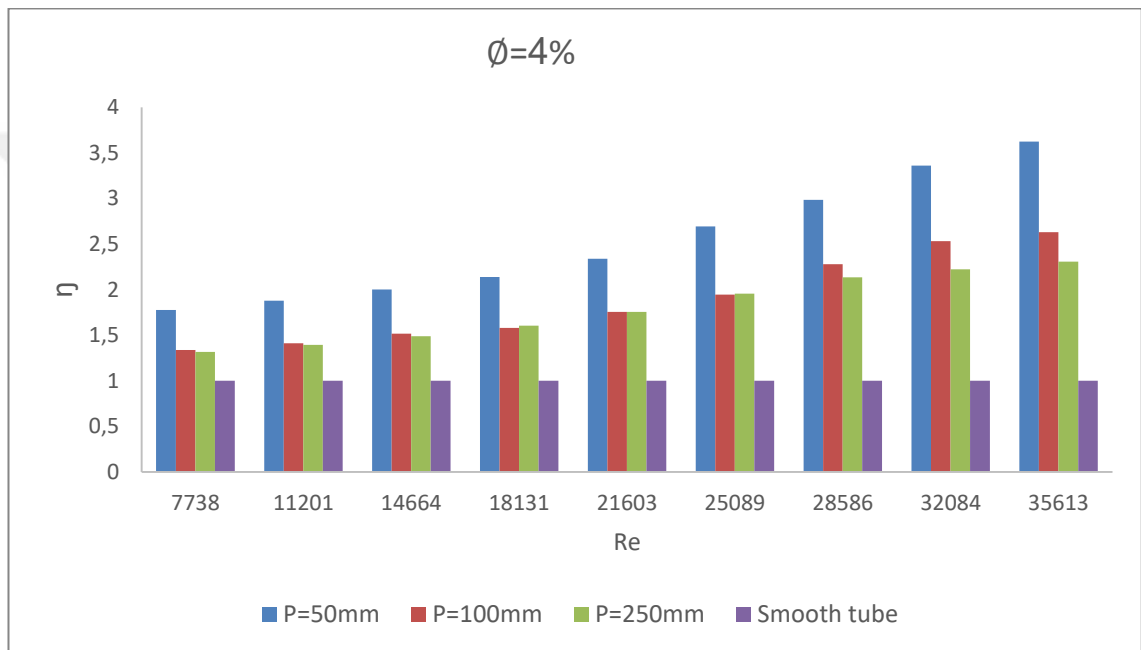


Figure 4.54. The effect of performance evaluation analysis and Reynolds number for Nano fluid with volume concentration at $\phi=4\%$ with modified different pitch ratios

CHAPTER 5

CONCLUSION AND RECOMMENDATIONS

5.1 The conclusion of this research

Main conclusions are as follows;

1. The results shows that the using CuO-water nanofluids through the twisted tubes can be used for improving the heat transfer.
2. The surface temperature decrease was directly related to the increase in the Reynolds number, and twisted tubes when the ratio of pitch diameter was increased, likewise the concentrations of nanofluids (0,1,2,3,4%) will be increase.
3. The increase in pitch diameter of the twisted tubes was directly drive to cause increase in Nusselt number.
4. The maximum coefficient of the performance enhancement obtained as a value of 2.456 in the twisted tube has pitch length of 50mm for Reynolds number of 34,024.
5. The increase in the pitch diameter of the twisted tubes drive directly to increase in the friction factor. Friction factor decrease while the increade of Reynolds number as expected for all cases.
6. Highest coefficient of performance enhancement value is found as 2.4045 for the case where the Reynolds number is 35,613, the volumetric ratio was $\phi=4\%$.

5.2 The Recommendations

1. The Information about thermo-physical properties for different kinds with important fluids like glycol, ethylene, water and oil of engine, is very seldom, nanofluid heat transfer should be tested on a big scale. These have a higher value of Pr (Prandtl number) as well as less (k) thermal conductivity
2. Nanofluids can also be analysed in particulars relating to convection heat transfer and the thermofluid analyses by using a two-phase method
3. For the integration of high numbers of twisted inside the tube in which suggest using more than 40,000 Reynolds numbers to obtain more result to present for industrial design.
4. With another twisted tube configurations was used with different types of nanoparticles may advance the heat transfer performance well.

Therefore, this matters can be intended to the future researchers suggest as follow:

- a) Apply performance of heat transfer with a different type of tube uses, and with a periodic boundary layer status.
- b) Apply the performance of thermal and hydraulic with a different pitch length and pitch diameter ratios.
- c) Apply this study with a different volumetric concentration ratio and investigate the change in the values of physical properties (Re, Nu, F, pressure drop, density, viscosity, and surface temperature)

REFERENCES

1. Bergles.A., E., 1981. Application of heat transfer Augmentation.
2. Nageswaran Tamil Alagan et al., 2017 Högskolan Väst · Department of Engineering Science- https://www.researchgate.net/profile/Nageswaran_Tamil_Alagan, https://www.researchgate.net/figure/Phase-change-heat-transfer-PCHT-enhancement-methods-with-active-and-passive-techniques_fig1_331092926
3. Adrian Bejan et al. / J.A. Jones Distinguished Professor of Mechanical Engineering, Duke University International Journal of Heat and Mass Transfer 40 (4), 799-816
4. Pirbastami, S., 2015. CFD Simulation of Heat Enhancement in Internally Helical Grooved Tubes. University Of Nevada, MSc/Thesis, Las Vegas, 89P, Manglik, R., 2003. Heat Transfer Enhancement.pp. 1029. *In: Heat transfer handbook*). University of Cincinnati, Ohio.
5. Arthur, B. ,2013. Augmentation of Heat Transfer, Single Phase. (web pag:www.thermopedia.com/content/575) , <https://hrsasia.co.in/twisted-tube-heat-exchanger.aspx>
6. Naik, M., Janardana, G., Sundar, L., 2013. Experimental investigation of heat transfer and friction factor with water–propylene glycol based CuO nanofluid in a tube with twisted tape inserts. **International Communications in Heat and Mass Transfer**, **46**:13–21.
7. Lee S, Choi SUS, Li S, Eastman JA. Measuring thermal conductivity of fluids containing oxide- nanoparticles. ASME J Heat Transfer 1999;121:280–9.
8. Xuan Y, Li Q., Nikam, P Heat transfer enhancement of nanofluids. Int J Heat Fluid Flow 2000;21:58–64.
9. Singh V. ,Gupta, M , A Review Heat transfer augmentation in a tube using nanofluids under constant heat flux boundary condition: Department of Mechanical Engineering, Guru Jambheshwar University of Science and Technology, Hisar 125001, Haryana, India.
10. Patel ,V. , Chitrapu, Y. Nanotechnology and fluid mechanic 2014
11. Jaiwant, D., 2014.nanofluids. (Web page: <https://www.slideshare.net/jalisantosh/nanofluids>),
12. Leong, K. Y., et al. "Performance investigation of an automotive car radiator

- operated with nanofluid-based coolants (nanofluid as a coolant in a radiator)." *Applied Thermal Engineering* 30.17 (2010): 2685-2692.
13. Swain ,M , Li, Y., Zhou, J., Tung, S, preparation and comparison of Al₂O₃-water nanofluid with base fluid, gandhi institute for technology (gift), khurda, bhubaneswar
 14. Xuan, Y., Li, Q., 2000. Heat Transfer Enhancement of Nanofluids. **International Journal of Heat and Fluid Flow** 21, 58-64 , https://www.researchgate.net/figure/Practical-applications-of-nanofluids_fig3_310774247
 15. Vajjha, R., Das, D., 2011, A Critical Review on Convective Heat Transfer Correlations of Nanofluids, **Renewable and Sustainable Energy Reviews** 15, 3271–3277.
 16. Fotukian, S., Esfahany Zeinali Heris et al, M., 2010 Experimental Study of Turbulent Convective Heat Transfer and Pressure Drop of Dilute Cu₂O/Water Nanofluid Inside a Circular Tube, **International Communications in Heat and Mass Transfer** 37, 214–219
 17. Pak B., Cho Y. ,1998, Hydrodynamic and Heat Transfer Study of Dispersed Fluids with Submicron Metallic Oxide Particle, **Experimental Heat Transfer** 11: 151-170
 18. Qiang, L., Yimin X., 2002. Convective Heat Transfer and Flow Characteristics of Cu-Water Nanofluid, **Science in China (Series E)** 45 (4).
 19. Namburu, P., Das, D., Tanguturi, K., Vajjha, R., 2009. Numerical Study of Turbulent Flow and Heat Transfer Characteristics of Nanofluids Considering Variable Properties. **International Journal of Thermal Sciences** 48, 290–302.
 20. Gunes, S., Ozceyhan, V., Buyukalaca, O., 2010. Heat Transfer Enhancement In A Tube With Equilateral Triangle Cross Sectioned Coiled Wire Inserts. **Experimental Thermal and Fluid Science**, 34, 684–691.
 21. Sarkar J., R., Das, D., Kulkarni ,D. ,2010. Development of New Correlations for Convective Heat Transfer and Friction Factor in Turbulent Regime for Nano Fluids, **International Journal of Heat and Mass Transfer** 53, 4607–4618.

22. Duangthongsuk, W., Wongwises, S., 2010. Experimental Study On the Heat Transfer Performance and Pressure Drop of Tio₂-Water Nanofluids Flowing Under a Turbulent Flow, **International Journal of Heat and Mass Transfer**, **53**.
23. Kannadasan, N., Ramanathan, K., Suresh, S., 2012. Comparison of Heat Transfer and Pressure Drop in Horizontal and Vertical Helically Coiled Heat Exchanger with CuO/Water Based Nanofluids, **Experimental Thermal and Fluid Science** **42**, 64–70
24. Dawood, H., Mohammed, H., Munisamy, K., 2014. Heat Transfer Augmentation Using Nanofluids in an Elliptic Annulus with Constant Heat Flux Boundary Condition, **Case Studies in Thermal Engineering**, **4**, 32–41.
25. Vajjha, R., Das, D., Ray, D., 2015. Development of New Correlations For The Nusselt Number And The Friction Factor Under Turbulent Flow Of Nanofluids In Flat Tubes. **International Journal of Heat and Mass Transfer** **80**, 353–367.
26. Abd, A., Al-Jabair, S., Sultan, K., 2012, Experimental Investigation of Heat Transfer and Flow of Nano Fluids in Horizontal Circular Tube. **World Academy of Science, Engineering and Technology**, **6** (1).
27. Vahidinia, F., Rahmdel, M., 2015. Turbulent Mixed Convection of a Nanofluid in a Horizontal Circular Tube with Non-Uniform Wall Heat Flux Using a Two-Phase Approach. **Trans. Phenom. Nano Micro Scales**, **3(2)**: 106-117.
28. Zarringhalam, M., Karimipour, A., Toghraie, D., 2016. Experimental Study Of The Effect Of Solid Volume Fraction And Reynolds Number On Heat Transfer Coefficient and Pressure Drop Of CuO–Water Nanofluid, **Experimental Thermal and Fluid Science**, **76**, 342–351
29. Abdolbaqi, M., Mamat, R., Sidik, N., Azmi, W., Selvakumar, P., 2017. Experimental Investigation and Development of New Correlations for Heat Transfer Enhancement and Friction Factor of Bioglycol/Water Based Tio₂ Nanofluids in Flat Tubes. **International Journal of Heat and Mass Transfer** **108**, 1026–1035.
30. Kumar, P., Judd, R., 1970. Heat Transfer with Coiled Wire Turbulence

Promoters. **The Canadian Journal Chemical Engineering, 48.**

31. Cengel, Y.A., Ghajar, A.J., 2015. Heat And Mass Transfer Fundamentals And Application. Mc Graw Hill Education
32. Garcia, A., Vicente, P., Viedma A., 2005. Experimental Study Of Heat Transfer Enhancement With Wire Coil Inserts In Laminar-Transition-Turbulent Regimes At Different Prandtl Numbers. **International Journal of Heat and Mass Transfer, 48**, 4640–4651
33. Eiamsa-ard, S., Thianpong, C., Promvonge, P., Experimental Investigation of Heat Transfer and Flow Friction in a Circular Tube Fitted with Regularly Spaced Twisted Tape Elements.
34. Naphon, P., Sriromruln, P., 2006. Single-Phase Heat Transfer And Pressure Drop In The Micro-Fin Tubes With Coiled Wire Insert. **International Communications in Heat and Mass Transfer 33**, 176– 183.
35. M., Salimpour, M., Pazouki, V., 2008. Pressure Drop Increase of Forced Convective Condensation Inside Horizontal Coiled Wire Inserted Tubes. **International Communications in Heat and Mass Transfer 35**, 1220–1226.
36. Promvonge, P., 2008. Thermal Augmentation in Circular Tube with Twisted Tape and Wire Coil Turbulators. **Energy Conversion and Management 49**, 2949-2955.
37. Akhavan-Behabadi, M., Mohseni, S., Najafi, H., Ramazanzadeh, H., 2009. Heat Transfer and Pressure Drop Characteristics of Forced Convective Evaporation in Horizontal Tubes with Coiled Wire Inserts. **International Communications in Heat and Mass Transfer 36**, 1089-1095.
38. Pak, B. C., & Cho, Y. I., 1998. Hydrodynamic and heat transfer study of dispersed fluids with submicron metallic oxide particles. **Experimental Heat Transfer an International Journal, 11**(2): 151-170.
39. Akhavan-Behabadi, M., Kumar, R., Salimpour, N., Azimi, R., 2010. Pressure Drop and Heat Transfer Augmentation Due to Coiled Wire Inserts During Laminar Flow of Oil Inside a Horizontal Tube. **International Journal of Thermal Sciences, 49**, 373–379.
40. Eiamsa-ard, S., Koolnapadol, N., Promvonge, P., 2012. Heat Transfer Behavior

- in a Square Duct with Tandem Wire Coil Element Insert. **Chinese Journal of Chemical Engineering**, 20(5):863-869
41. Yang San, J., Chieh Huang, W., AnChen, C., 2015. Experimental Investigation On Heat Transfer And Fluid Friction Correlations For Circular Tubes With Coiled-Wire Inserts. **International Communications in Heat and Mass Transfer**, 65:8–14.
 42. Keklikcioglu, O., Ozceyhan, V., 2016. Experimental Investigation On Heat Transfer Enhancement Of A Tube With Coiled-Wire Inserts Installed With A Separation From The Tube Wall. **International Communications in Heat and Mass Transfer xxx - ICHMT-03496**
 43. Sharafeldean, M., Berbish, N., Moawed, M., Ali, R., 2016. Experimental Investigation of Heat Transfer and Pressure Drop of Turbulent Flow Inside Tube with Inserted Helical Coils. **Heat Mass Transfer DOI 10.1007/s00231-016-1897-z**
 44. Sharma, K., Sundar, L., Sarma, P., 2009. Estimation of Heat Transfer Coefficient and Friction Factor in The Transition Flow with Low Volume Concentration of Al₂O₃ Nano Fluid Flowing in A Circular Tube and with Twisted Tape Insert. **International Communications in Heat and Mass Transfer**, 36, 503–507.
 45. Chandrasekar, M., Suresh, S., Bose, A., 2010. Experimental Studies On Heat Transfer And Friction Factor Characteristics Of Al₂O₃/Water Nano Fluid In A Circular Pipe Under Laminar Flow With Wire Coil Inserts. **Experimental Thermal and Fluid Science** 34, 122–130.
 46. Pathipakka, G., Sivashanmugam, P., 2010. Heat Transfer Behaviour Of Nano Fluids In A Uniformly Heated Circular Tube Fitted With Helical Inserts In Laminar Flow. **Superlattices and Microstructures**, 47, 349-360.
 47. Suresh, S., Chandrasekar, M., Sekhar, S., 2011. Experimental Studies On Heat Transfer And Friction Factor Characteristics Of CuO/Water Nanofluid Under Turbulent Flow In A Helically Dimpled Tube. **Experimental Thermal and Fluid Science**, 35, 542–549.
 48. Eesa, K., Eiamsa-ard, S., 2011. Enhancement Of Heat Transfer Using

- Cuo/Water Nanofluid And Twisted Tape With Alternate Axis. **International Communications in Heat and Mass Transfer**, **38**, 742–748.
49. ANSYS Meshing Users Guide, 2013..
 50. Kannadasan, N., Ramanathan, K., Suresh, S., 2012. Comparison Of Heat Transfer And Pressure Drop In Horizontal And Vertical Helically Coiled Heat Exchanger With Cuo/Water Based Nano Fluids. **Experimental Thermal and Fluid Science**, **42**:64–70.
 51. Rashidi, S., Zade, N. M., Esfahani, J. A., 2017. Thermo-Fluid Performance And Entropy Generation Analysis For A New Eccentric Helical Screw Tape Insert In A 3D Tube. **Chemical Engineering and Processing S0255-2701** (16) 30605-5
 52. Sharma E., Hashemi, S., 2012. An Empirical Study On Heat Transfer And Pressure Drop Characteristics Of Cuo–Base Oil Nanofluid Flow In A Horizontal Helically Coiled Tube Under Constant Heat Flux. **International Communications in Heat and Mass Transfer**, **39**, 144–151
 53. Demir, M., Akhavan-Behabadi, M., Nasr, M., 2012. Experimental Study On Heat Transfer And Pressure Drop Of Nanofluid Flow In A Horizontal Coiled Wire Inserted Tube Under Constant Heat Flux. **Experimental Thermal and Fluid Science**, **36**: 158–168.
 54. R.L. Hamilton, O.K. Crosser, "Thermal conductivity of heterogeneous two component system", *Industrial and Engineering Chemistry Fundamentals*, 1962; 1: 187-191. <https://doi.org/10.1021/i160003a005>.
 55. Praveen K. Namburu , Devdatta P. Kulkarni, "Viscosity of copper oxide nanoparticles dispersed in ethylene glycol and water mixture", Department of Mechanical Engineering, University of Alaska, Fairbanks, P.O. Box 755905, Fairbanks, AK 99775-5905, USA
 56. Naik, M., Jacaranda, G., Sundar, L., 2013. Experimental Investigation Of Heat Transfer And Friction Factor With Water–Propylene Glycol Based Cuo Nanofluid In A Tube With Twisted Tape Inserts. **International Communications in Heat and Mass Transfer**, **46**:13–21.

